Combatting AMR: a molecular approach to the discovery of potent and non-toxic rhenium complexes active against *C. albicans*-MRSA co-infection

Sara Nasiri Sovari,[a†] Natasa Radakovic,[b†] Paul Roch,[a] Aurélien Crochet,[a] Aleksandar Pavic*[b] and Fabio Zobi*[a]

a. Department of Chemistry, Fribourg University, Chemin Du Musée 9, 1700, Fribourg, Switzerland.

b. Institute of Molecular Genetics and Genetic Engineering, University of Belgrade, Vojvode Stepe 444a, 11042 Belgrade, Serbia.

† Equally contributed

* Correspondence: sasapavic@imgge.bg.ac.rs and fabio.zobi@unifr.ch

Abstract.

Antimicrobial resistance (AMR) is a major emerging threat to public health, causing serious issues in the successful prevention and treatment of persistent diseases. While the problem escalates, lack of financial incentive has lead major pharmaceutical companies to interrupt their antibiotic drug discovery programs. The World Health Organisation (WHO) has called for novel solutions outside the traditional development pathway, with emphasis on new classes of active compounds with non-classical mechanisms of action. Metal complexes are an untapped source of antibiotic potential owing to unique modes of action and a wider range of three-dimensional geometries as compared to purely organic compounds. In this study, we present the antimicrobial and antifungal efficacy of a family of rhenium tricarbonyl diimine complexes with varying ligands, charge and lipophilicity. Our study allowed the identification of potent and non-toxic complexes active *in vivo* against *S. aureus* infections at MIC doses as low as 300 ng/mL, as well as against *C. albicans*-MRSA mixed co-infection. The compounds are capable of suppressing the *C. albicans* morphogenetic yeast-to-hyphal transition, eradicating fungal-*S. aureus* co-infection, while showing no sign of cardio-, hepato-, hematotoxiciy or teratogenicity.

Introduction

The rise of antimicrobial resistance (AMR) and the lack of effective drugs to combat resistant strains have become major health threats to humankind.[1, 2] AMR emerges much faster than new antimicrobials discovery, and usually develops a few years after a novel drug is introduced to the clinic. Accordingly, infectious diseases continue to be the leading cause of premature death in humans,[3] especially in developing countries.[4] It has been estimated that more than 700.000 people die each year globally due to AMR infections, with 1900 deaths occurring every day.[5] Unless new effective treatments are developed, the UN Ad hoc Interagency Coordinating Group (IACG) on Antimicrobial Resistance warned of the risk of reaching 10 million of deaths each year by 2050.[5] This is more than the present death toll due to cancer, and the WHO has called for novel therapeutic solution in particular drugs with new mechanisms of action.[6, 7] Despite such disturbing prognosis and a critical demand for effective drugs, lack of financial incentive has resulted in large pharmaceutical companies leaving the market in favour of pursuing more profitable lines of drug development.[8] Thus, the number of newly approved antibiotics and antifungals has continued to decline since the 1980s.[9]

As a result of the current antimicrobial crisis, both bacteria and fungi have become increasingly resistant to all available drugs, some of which have developed multidrug resistance ("superbugs") and pose an ever increasing challenge in current clinical practice. Among them, *Staphylococcus aureus* is the leading cause of hospital- and community-acquired infections. The bacterium is responsible for various diseases, ranging from transient skin infections[10] to serious acute and chronic infections including endocarditis, pneumonia, toxic shock syndrome and life-threatening sepsis.[11] Only in the United States, this pathogen causes nearly half a million hospitalizations and 50.000 deaths each year.[12] The methicillin-resistant *Staphylococcus aureus* (MRSA) is one of two the most prevalent superbugs in the U.S., and, owing to its resistance to numerous antibiotics (penicillins, cephalosporins, aminoglycosides, tetracyclines, macrolides, quinophthalones, and sulfonamides), provokes difficult-to-treat infections with high morbidity and mortality rates.[13] According to the Center for Disease Control and Prevention (CDC), there were ca. 120.000 cases of bloodstream infections and almost 20.000 deaths in 2017.[14] Currently, the clinical therapies for MRSA infections rely on the use of vancomycin and daptomycin as the first-line antibiotics, with linezolid serving as the drug of last resort.[13] However, strains resistant to each of these medicines have already emerged,[15] highlighting the urgent need to develop novel therapeutic options to combat MRSA infection. Therefore, the WHO included MRSA into the global list of antibiotic-resistant pathogens with high priority in 2017.

In addition to bacterial superbugs, several epidemiological reports stressed a rapid emergence of drug-resistant fungal infections in the last three decades.[16] The latest studies estimate that nearly a billion people are affected by fungal infections, with more than 1.6 million death cases per year, similar to

that of tuberculosis and >3-fold higher than malaria.[17] Infections caused by *Candida* species (candidiasis and candiduria), are the most prevalent fungal infections, with 10's of millions of mucosal candidiasis and ~700.000 invasive candidiasis cases. Invasive candidiasis is a particularly life-threatening infection, whose increased prevalence is closely associated with epidemic HIV infection, emergence of malignancies, solid organ transplantation and diabetes.[18, 19] Out of more than 20 different *Candida* species known to cause human infections, *C. albicans* is the most prevalent pathogen, causing superficial, mucosal, deep-seated and systemic infections.[20] Moreover, invasive candidasis caused by *C. albicans* represents the fourth leading cause of all bloodstream infections worldwide, with the global burden of approximately 750.000 cases annually and disturbingly high mortality rate of 40-75%, surpassing thus many bacterial pathogens.[17]

Such worrisome epidemiological landscape of invasive candidiasis is attributed in part to limitations in the available antifungal drugs repertoire and the rapid emergence of resistance to existing ones. Unfortunately, only four classes of antifungal agents are available in current clinical practice (polyenes, azoles, pyrimidines, and echinocandines), the last of which has been discovered thirty years ago.[21, 22] However, all clinical antifungal agents possess significant therapeutic limitations, ranging from severe systemic toxicity (polyenes), kidney and liver toxicity (azoles) to restricted routes of administration (echinocandines). The emergence of multidrug-resistant clinical strains (against two or even three classes of antifungals) represents currently one of the greatest public concern.

Particularly difficult to eradicate in the hospital settings are co-infections caused with *C. albicans* and *S. aureus*. *C. albicans* frequently co-exist within polymicrobial communities with both methicillin-sensitive and methicillin-resistant *S. aureus*, with 27% of all nosocomial *C. albicans* bloodstream infections being associated with *S. aureus*, with exceptionally high mortality rate.[23, 24] These two pathogens establish a symbiotic relationship causing severe superficial or systemic infections (chronic wounds, cystic fibrosis, oral thrush, urinary tract and internal medical devices).[25] Close contact and interactions between these pathogens lead to increased virulence, resistance to many clinical drugs (multidrug resistant infections) and successful evasion of host immunity.[26, 27] As a result, these co-infections mediate markedly increased mortality compared to those of monomicrobial infections, which is referred to as "lethal synergism".[28] Moreover, several studies have revealed that *C. albicans* facilitates the invasion across the mucosal barriers of *S. aureus* attached to penetrating hyphae, leading to life-threating systemic infection in infected patients.[24] Finding effective therapies targeting such polymicrobial infections is even harder considering their complexity and lethal synergism.

In light of the dire need for new treatments, metal complexes have emerged as a promising candidates in the battle against pathogenic microorganisms,[29-33] offering hope especially against multidrug resistant and polymicrobial infections. Contrary to organic molecules, a wider range of 3D structures, and distinctively unique mechanisms of action characterize metal complexes. Rhenium tricarbonyl

diimine complexes have been increasingly evaluated over the last two decades for their potential application in medicine. The molecules are particularly attractive as anticancer agents[34-37] and cytoprotective CO releasing molecules,[38] but at the same time, they are progressively recognized, among others metals,[29, 39] as valuable antimicrobial drugs.[30, 31, 40-42] In 2013, a series of trimetallic complexes containing a *fac*-tricarbonyl rhenium unit was described by Metzler-Nolte, Bandow *et al.*[40] The antimicrobial potency of the complexes against MRSA is remarkable (MIC = 2 μM) and the rhenium unit was shown to be critical for the antibacterial properties of the molecules.[43] The authors introduced later a series of N-heterocyclic carbene diimine complexes of the metal ion showing high activity against Gram-positive strains, including MRSA, with MIC values of 0.7–2 μM.[41] Frei and coworkers presented the antibacterial activity of rhenium bisquinoline species, which can be photo-actived against drug-resistant *S. aureus* and *E. coli* with similarly low MIC values.[42]

Our groups are also interested in the chemistry of 18- and 17-electron *fac*-$[Re^{I}(CO)_3]^+$ and *cis*-$[Re^{II}(CO)_2]^{2+}$ species for their potential use in medicinal chemistry, as anticancer,[44-46] CO-releasing and antibacterial agents.[47-49] Recently, we reported a study on the antimicrobial properties of a series of 3-arylcoumarin rhenium complexes and found that about half of the species investigated exhibit potent *in vitro* and *in vivo* activity against MRSA with MICs in the nanomolar range (ca. 350–700 nM *in vivo*).[49] Remarkably, the complexes with anti-staphylococcal/MRSA activity were able to increase infected fish rate survival up to 100%. The mechanism of action these agents remains largely unknown. The trimetallic complexes of Metzler-Nolte and Bandow target the cytoplasmic membrane and appear to act by affecting membrane architecture and disrupting essential cellular processes taking place at the membrane such as respiration and cell wall biosynthesis and integrity.[40] Conversely, the coumarin derivatives have no effect on the bacterial cell membrane potential.[49] The bisquinoline complexes of Frei act *via* two distinct mechanisms,[42] one associated with ROS production possibly leading to destabilisation of Fe-S cluster and increased aminoglycoside uptake, while the mode of action of N-heterocyclic carbene diimine complexes remains undetermined so far.[41]

In the effort of continuing our investigation and discovery of new rhenium-based antimicrobial therapeutic agents, and with the aim of gaining a better understanding about the structure-activity relationship of the complexes, we designed and synthesized a family of *fac*-$[Re(CO)_3]^+$ diimine (NN) complexes with different charge, ligands and NN substituents. Metal species and ligands were tested for their antimicrobial activity against a panel of clinically relevant *Candida* and *S. aureus* strains and selected species were further evaluated *in vivo* using the zebrafish infection models. Our study allowed the identification of potent and non-toxic rhenium complexes active *in vivo* against antimicrobial infections and *C. albicans*-MRSA mixed co-infection. The compounds are capable of suppressing the *C. albicans* morphogenetic yeast-to-hyphal transition, eradicating fungal-*S. aureus* co-infection, while

showing no sign of cardio-, hepato-, hematotoxiciy or teratogenicity at concentrations >3x the effective dose.

Results and discussion

Data analysis and molecular design.

The starting point of our study was a literature search and an extensive analysis of the molecular structures of the different rhenium complexes tested for their antimicrobial properties. To date, the structures of 48 mononuclear rhenium complexes have been reported in literature within this context.[40-43, 49-52] To the total number of tested complexes one should add the 77 rhenium species reported by Frei *et al.*, of which 7 were found to have antimicrobial activity, with only one of these being both non-toxic and active against microbes *in vitro*.[29] However, the structures of these compounds were not reported in the publication and could not be considered here. Before discussing the results of this analysis, we point out that the same should not be interpreted rigorously, as the number of complexes of each ligand type (LT) is limited and not statistically sufficient to estimate the population parameters using the appropriate sample statistics. Furthermore, we limited the examination to a microorganism common to all (namely MRSA), but the same complexes might show higher or lower potency if tested against other species or strains. The analysis was intended as an initial guide to identify possible common parameters for the selection of the LT in our molecular design.

What transpired from our analysis is that complexes of LT4-7 show on average the lowest MIC values against MRSA (Fig. 1). Although not a common feature for all LTs, it is also evident that the most potent complexes of LT4-7 are cationic in nature. After careful consideration, we decided to select for our study rhenium tricarbonyl diimine complexes of LT5 and 6. From a purely numeric standpoint, one may be perhaps inclined to focus on complexes of LT7, however, these species, described by Metzler-Nolte, Bandow *et al.*, are all closely related and all have as R a peptide nucleic acid backbone with an alkyne side chain, substituted with either aromatic rings, cymantrene, ferrocene, ruthenocene or combinations of those. The corresponding underivatized Re complex (i.e. R = H for LT7) is the only inactive molecule of the series.[43] Similarly, we excluded LT4 because the chelating coordination mode of the ligand would invariably give cationic complexes of the *fac*-$[Re(CO)_3]^+$ core, and we were interested in exploring also charge variation of the first coordination sphere of metal by the appropriate selection of a monodentate ligand X in *fac*-$[Re(CO)_3LT\#X]^n$ type-complexes.

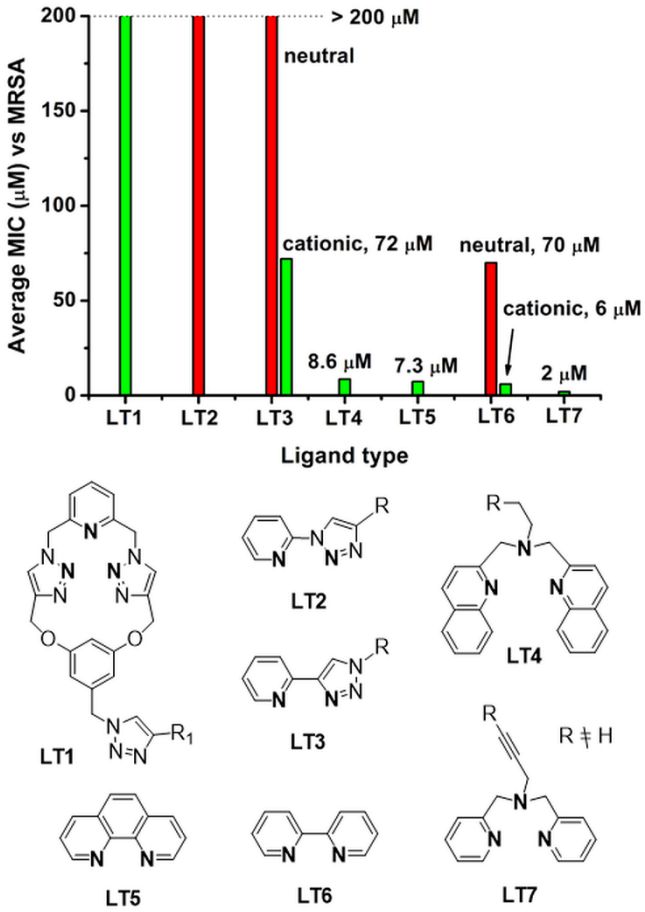

Fig. 1. Average minimum inhibitory concentration of published *fac*-$[Re(CO)_3]^+$ monomeric complexes against methicillin-resistant *S. aureus* (MRSA) as a function of ligand type (LT) and overall charge of the complex (red and green bar for neutral and cationic species respectively). Atoms bound to the Re atoms are bold. See text for details.

Synthesis and Characterization of ReNN#X Complexes.

Based on the above considerations, we prepared 57 *fac*-$[Re(CO)_3]^+$ diimine (NN) complexes of bipyridine and phenenthroline with different monodentate ligands as shown in Fig. 2. Some of the pyridine species have already been reported. Most of them were studied for their photophysical[53-56] or catalytic[57] properties, only a few have been evaluated in a biological context[58, 59] and none as antimicrobial agents. Based on our previous findings,[49] we decided to include two 3-arylcoumarin monodentate ligands (L1 and L2, Fig. 2) which were prepared according to synthetic pathways adapted from our previous study in 95 and 75% yield, respectively (Scheme S1).[49] Molecules were purified by normal phase column chromatography, fully characterized by ^{1}H NMR and ^{13}C NMR spectroscopy, mass spectrometry, IR spectroscopy (ESI), and single-crystal X-ray structure analyses (Scheme S1 and Table

S1). The preparation of rhenium complexes, ReNN#X (where # = 1-13, Fig. 2) was accomplished *via* standard synthetic protocols normally used in the preparation of such type of complexes. ReNN#Br species were obtained by the reaction of $Re(CO)_5Br$ with NN# in refluxing toluene and served as well as starting materials for the following steps.

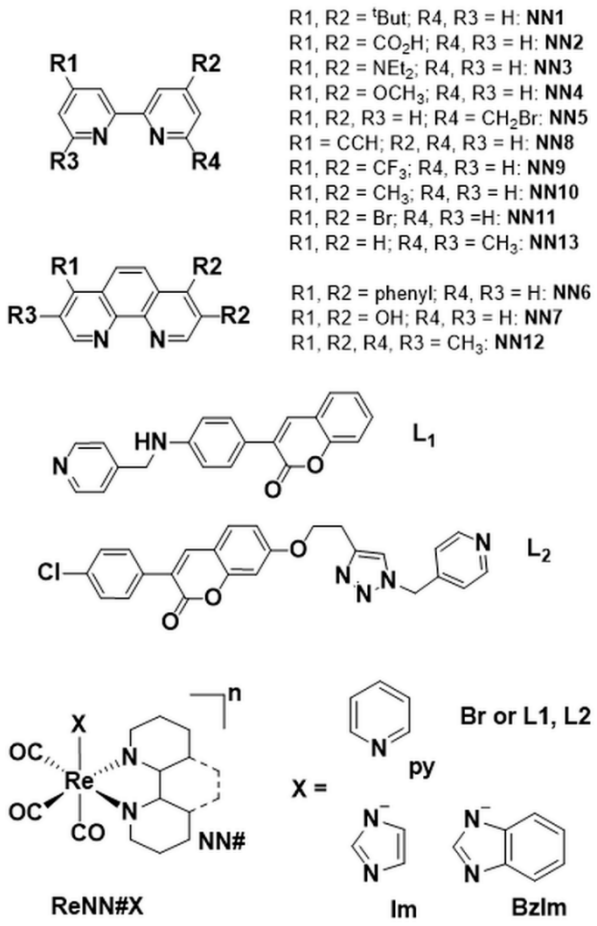

Fig. 2. Structures and associated codes of NN#, X and ReNN#X complexes investigated in this study.

The complexation of 3-arylcoumarin monodentate ligands (L1 and L2) to *fac*-$[Re(CO)_3NN\#]$ was carried *via* the intermediate *fac*-$[Re(CO)_3NN\#(CF_3SO_3)]$ molecule, isolated from treatment of ReNN#Br with trifluoromethanesulfonic acid. These compounds were isolated as either $CF_3SO_3^-$ or PF_6^- salts. For all other ReNN#X complexes, ReNN#Br was treated $AgCF_3SO_3$ in the presence of Et_3N and X, and the desired complexes isolated as either neutral species (for X = Im or BzIm) or as $CF_3SO_3^-$ salts (for X = py) following purification on alumina. The neutral charge of the Im and BzIm complexes was confirmed by the lack of ^{19}F NMR signals, the shift of the CO frequencies, which are consistent with what previously reported,[60] and crystallographically for ReNN#BzIm (# = 10 and 13, Fig. 4). ReNN#X complexes were also characterized by standard techniques including single-crystal X-ray structure analysis for ReNN#py (# = 9, 10, 12 and 13, Fig. 3) and ReNN#X (X = BzIm for # = 10 and 13 and X = L1, #10, Fig. 4).

Spectroscopically the compounds show all typical signals associated with the species (ESI). In coordinating solvents (acetonitrile, methanol, DMSO or a mixture of water and DMSO), we found no evidence of ligand displacement or solvent exchange for these species over a three-day period.

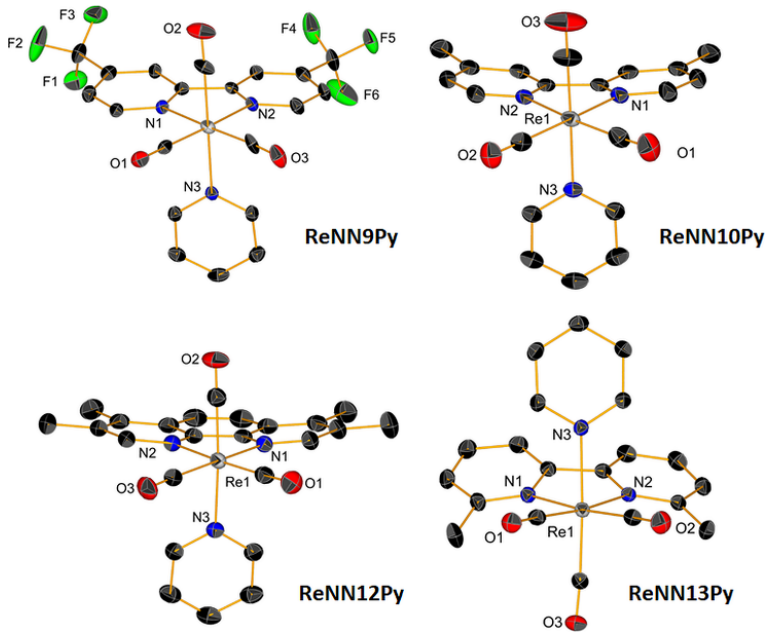

Fig. 3. Ortep representation of ReNN#py (# = 9, 10, 12 and 13). Thermal ellipsoids set at a 30% probability level. Hydrogen atoms, as well as solvent and counter ion are omitted for clarity.

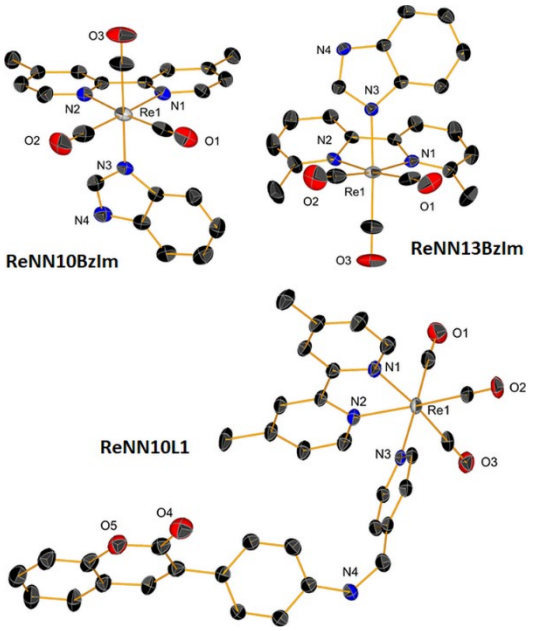

Fig. 4. Ortep representation of ReNN#BzIm (# = 10and 13) and ReNN10L1 . Thermal ellipsoids set at a 30% probability level. Hydrogen atoms, as well as solvent and counter ion (for ReNN10L1) are omitted for clarity.

In our approach, the different ReNN#X complexes served to evaluate the following variables: 1) analysis of ReNN#X vs NN#, whether there is an advantage in using complexes of the *fac*-$[Re(CO)_3]^+$ over the organic NN# molecules and whether the efficacy of NN# is associated with the activity of the corresponding Re complex; 2) analysis of ReNN#Br vs ReNN#(Bz)Im whether the ligand X is responsible for modulating the activity of neutral complexes; 3) analysis of $[ReNN\#X]^0$ (X= Br, Im or BzIm) vs $[ReNN\#L]^+$ (L= py, L1 or L2) whether the overall charge of the complex is an important factor for the antimicrobial efficacy of these complexes. We considered that this rational combinatorial approach might allow us to identify common parameters of the most active species in order to provide, at very least, new data for the future design of these antimicrobial agents.

Antimicrobial and cytotoxic properties

The antimicrobial activity of 57 ReNN#X complexes (26 neutral, 31 cationic) and their corresponding 13 NN# ligands was determined against, two *S. aureus* strains (Table 1) including methicillin-resistant *S. aureus* (MRSA 43300), and methicillin-sensitive *S. aureus* (MSSA 25923), and five *Candida* spp., including *C. albicans*, *C. parapsilosis*, *C. krusei* , *C. glabrata*, and *C. auris* (Table 2). The species of these two genera are responsible for the majority of hospital-acquired infections and are challenging to treat, especially their co-infections.[28] In addition, the therapeutic index (Ti), as a measure of the selective activity against pathogenic microorganism in comparison to the host effect, was determined by using the zebrafish (*Danio rerio*) model, as the preclinical animal model for toxicity assessment (Table 1 and 2). Moreover, the selective haemolytic toxicity of the species with favourable antimicrobial activity was determined by investigating their haemolytic potential *in vitro*. We had originally planned to test all 78 complex combinations of NN# and X ligands. However, given solubility and purification problems of derivatives of NN2, NN7, NN8 and NN11 (and consequently problems related to accurate concentrations determination), we omitted complexes of specific ligands X with those NN ligands.

Before moving to a detailed discussion of the data, we should mention that we define here compounds with excellent and very good antimicrobial activity as those species having MICs values ≤ 1.5 μM and ≤ 3.1 μM, respectively. A second stringent, and more important, criterion that guided our selection for *in vivo* studies (*vide infra*) is the therapeutic index (Ti) of the complexes (defined as the LC_{50}/MIC ratio). A value 9 ≤ Ti ≤ 20 is considered as indicative of a compound with a very good therapeutic profile, while a Ti ≥ 20 value as indicating an excellent *in vivo* profile. Only compound with Ti ≥ 9 (antibacterial) or Ti ≥ 3 (antifungal) were considered for the evaluation of their *in vivo* antimicrobial efficacy.

Table 1. *In vivo* toxicity (LC_{50}, μM), *in vitro* minimum inhibitory concentration[a] (MIC, μM), therapeutic index (Ti)[b] of ReNN#X complexes[c] against *S. aureus* strains. Only compounds with MIC ≤ 50 μM are tabulated.

Complex	Zebrafish LC_{50}	*S. aureus* MRSA43300	*S. aureus* ATCC25923
ReNN1Im	>60	25	25
ReNN3Im	7.1	3.1	3.1
ReNN4Im	>60	25	50
ReNN5Im	27.4	12.5	12.5
ReNN13Im	>60	25	25
ReNN1BzIm	17.9	12.5	12.5
ReNN6BzIm	**>60**	**6.2 (9.7)**	**12.5 (5)**
ReNN10BzIm	**>60**	**6.2 (9.7)**	**6.2 (9.7)**
ReNN1Py	>60	12.5 (5)	12.5 (5)
ReNN3Py	**18.7**	**0.8 (23.9)**	**0.8 (23.9)**
ReNN4Py	>60	25	12.5 (5)
ReNN5Py	**38.9**	**3.1 (12.6)**	**3.1 (12.6)**
ReNN6Py	**18.7**	**0.4 (47.4)**	**0.6 (31.2)**
ReNN12Py	41.5	12.5	12.5
ReNN1L1	**7.1**	**0.8 (9.1)**	**3.1**
ReNN3L1	48.6	25	12.5
ReNN4L1	30.3	6.2 (5)	6.2 (5)
ReNN6L1	>60	50	6.2 (9.7)
ReNN9L1	56.2	12.5 (5)	6.2 (9)
ReNN10L1	**>60**	**3.1 (19.2)**	**6.2 (9.7)**
ReNN11L1	>60	25	12.5 (5)
ReNN12L1	14.1	3.1 (5)	6.2
ReNN13L1	7.1	1.6 (5)	3.1
ReNN1L2	7.1	12.5	25
ReNN4L2	7.1	6.2	12.5
ReNN9L2	**>60**	**1.6 (38.6)**	**6.2 (9.7)**
ReNN11L2	>60	6.2 (5)	25
ReNN13L2	7.1	12.5	12.5
Linezolid	>60	5.9 (10.1)	5.9 (10.1)

[a]MIC values of ≤ 3.1 uM are regarded as indication of good antimicrobial activity. [b]Values in (brackets) are therapeutic index (Ti) values. Only Ti ≥ 5 are shown. [c]Bold **complexes** were considered to be most promising for *in vivo* studies.

The results of the *in vitro* antimicrobial activity screening (Table 1 and 2) revealed that while the majority (10 out of 13, ESI) of tested NN# molecules had neither antibacterial nor antifungal activity at the doses ≤ 50 μM, the corresponding *fac*-$[Re(CO)_3]^+$ complexes showed:

i) **mono- or dual activity** when coordinated to completely **inactive** NN# ligands – i.e. $[Re(CO)_3NN\#X]$ species (# = 4, 8, 9, 10, 11) were active against *S. aureus*, and $[Re(CO)_3NN\#X]$ species (# = 1, 5, 13) were effective against both *S. aureus* and *Candida* spp.;

ii) **markedly higher activity** against *S. aureus* and/or *Candida* species when coordinated to **active** NN# ligands – e.g. $[Re(CO)_3NN3X]$ species were respectively up to 8- and 64-times more active on *Candida*

and *S. aureus* than NN3. Likewise, [Re(CO)$_3$NN12X] species displayed up to 8-fold higher antibacterial activity compared to the NN12 ligand;

iii) **reduced or no antifungal activity** contrary to the **active** respective ligands – i.e. [ReNN#X] vs. NN# with # = 10 or 12.

Besides these general findings, the *in vivo* toxicity analysis of ReNN#X vs. NN# ligands (based on LC_{50} values determined in the zebrafish assay) revealed significantly lower toxicity of almost all complexes compared to the respective ligands, ranging from 2.7-fold (i.e. [ReNN3X] derivatives) to 39-fold (i.e. [ReNN6X] derivatives). This is particularly true for complexes with X = pyridine, imidazole or Br, where no toxic effects occurred *in vivo* at doses ≤ 60 μM. The only two ligands active against the tested microbes (NN6; bathophenanthroline and NN12; 3,4,7,8-tetramethyl-1,10-phenanthroline), appeared highly toxic, causing cardiotoxic, hepatotoxic and teratogenic abnormalities. Taken together, the data clearly show that the complexation of NN ligands to the *fac*-[Re(CO)$_3$]$^+$ core resulted in more active and markedly less toxic molecules.

Table 2. *In vitro* minimum inhibitory concentration[a] (MIC, μM) and therapeutic index (Ti)[b] of ReNN#X complexes[c] against *Candida* strains. Only compounds with MIC ≤ 50 μM are tabulated.

Complex	C. albicans SC5314	C. parapsilosis ATCC22019	*C. krusei* ATCC6258	*C. auris* strain *8*
ReNN3Im	3.1 (2.3)	12.5	25	25
ReNN5Im	50	25	12.5 (2.2)	50
ReNN6Im	6.2	-	-	25
ReNN1BzIm	25	12.5	25	25
ReNN6BzIm	**12.5 (4.8)**	**12.5 (4.8)**	25 (2.4)	**12.5 (4.8)**
ReNN10BzIm	50	25 (2.4)	25 (2.4)	50
ReNN3Py	**6.2 (3)**	**3.1 (6)**	25	-
ReNN5Py	12.5 (3)	12.5 (3)	25	-
ReNN6Py	**6.2 (3)**	12.5	12.5	50
ReNN1L1	3.1 (2.3)	6.2	-	-
ReNN12L1	6.2 (2.3)	>50 (50)	-	-
ReNN13L1	6.2	3.1 (2.3)	12.5	
ReNN1L2	6.2	-	-	12.5
ReNN4L2	12.5	12.5	12.5	-

[a]MIC values of ≤ 3.1 uM are regarded as indication of good antimicrobial activity. [b]Values in (brackets) are therapeutic index (Ti) values. Only Ti > 2 are shown. [c]Bold **complexes** were considered to be most promising for *in vivo* studies. *C. glabrata* ATCC2001 data are not shown here; see ESI.

According to the criterion that active species are those with the MIC values ≤ 50 μM, we found that a much higher proportion of Re(I) tricarbonyl complexes was active against *S. aureus* (60%) than against *C. albicans* (39%) ($P < 0.01$, χ^2 test) whereas active complexes had lower MIC values against the tested

bacteria than fungi, and consequently higher Ti values (ESI). Herein, we only tabulated data of compounds with MICs ≤ 50 μM (a complete list is in ESI). Among the Re complexes displaying dual activity against both pathogens (78%, 21 out of 57), 19% of them (11 out of 57) provoked no toxic response *in vivo* at both effective (MIC) doses (Table 1).

Several Re complexes show excellent to very good activity against both methicillin-resistant and methicillin-sensitive *S. aureus,* where the species containing the coumarin L1 or the pyridine ligand demonstrated the highest potency. While the majority of the active L1 complexes showed 4 < Ti < 5, some pyridine species had Ti > 20, demonstrating thus an excellent therapeutic profile. Among these, complexes ReNN6Py and ReNN3Py exhibited the highest potency against MRSA (Ti = 47 and 24, respectively), being active in the nanomolar range with MIC values as low as 400 nM (330 and 635 ng/mL, respectively, Table 1 and Fig. 5). The complexes display up to 15-times greater activity than linezolid (Table 1) and a 2-fold greater activity than vancomycin. Vancomycin is the antibiotic of choice against staphylococcal infections, while linezolid represents the only superior alternative for the treatment of nosocomial pneumonia caused by vancomycin-resistant MRSA in the USA and Europe.[61]

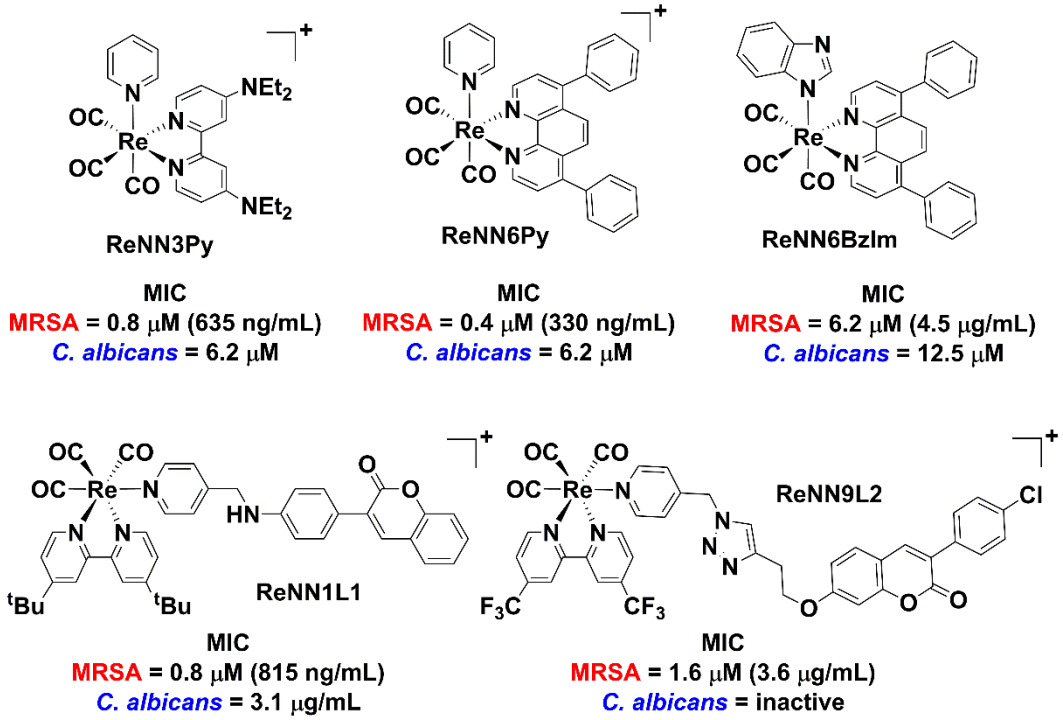

Fig. 5. Structures of the most effective antimicrobial agents identified in this study.

In addition to the anti-staphylococcal activity, complexes ReNN3Py and ReNN6Py were also active against *C. albicans* SC5314, with MICs of 6.2 μM (4 μg/mL). This finding is of particular importance, since MRSA and *C. albicans* are frequently co-associated with superficial and systemic infections and co-operate to resist antimicrobial drugs, causing high morbidity and mortality rates.[28] In comparison

to other rhenium tricarbonyl antimicrobial species tested against MRSA strains, the MIC values of complexes ReNN3Py, ReNN1L1, and ReNN9L2 are similar to those of the most active species reported so far,[41, 43] while ReNN6Py, to our knowledge, is the most potent Re complex reported to date and one of the most effective metal-based species.[39, 48, 62-65] In addition to these highly active complexes, it is worth mentioning compounds ReNN1L1, ReNN13L1, ReNN9L2 (MICs = 1.56 μM) and ReNN10L1 (3.12 μM) which displayed up to a 4-fold higher potency than linezolid against MRSA.

Alongside active effective concentrations, of particular importance is the fact that ReNN3Py, ReNN6Py, ReNN1L1, ReNN10L1 and ReNN9L2 exhibit no toxicity *in vivo*, with an excellent Ti (>45 for ReNN6Py and >38 for ReNN9L2, Table 1), making them very valuable candidates for further animal studies and potential clinical application to combat staphylococcal infections. It is also important to note that many Re(I) tricarbonyl complexes tested in this study, including the most potent derivatives, showed higher activity and a much better safety profile than silver(I) sulfadiazine (Table 1), a topical antibiotic used for more than 40 years to prevent infection in burns.[66] Accordingly, this finding also indicates possible applications of Re(I) tricarbonyl complexes in skin infections treatments. Moreover, *in vitro* analysis of the haemolytic properties of the complexes active against MRSA and/or *C. albicans* SC5314 (MICs ≤ 6.25 μM) revealed that none of the tested species induced haemolysis of red blood cells at 3 × MIC dose, additionally confirming their safety profile. Altogether, these data suggest a microbe-specific mechanism of activity without adverse effect on the host (zebrafish and human) cells.

Hepatotoxicity assessment of the most potent antimicrobial complexes.

Hepatotoxicity represents the most common adverse effect of antimicrobial drugs and a major challenge in clinical medicine, particularly for azole-based antifungals, limiting their long-term use for polymicrobial and severe fungal infections treatment. In addition, liver injury remains a leading cause of drugs failure in clinical trials and post-approval withdrawals.[67] Therefore, we addressed this issue by studying whether the most active Re complexes provoke liver damages at (sub)therapeutic doses using the embryos of the transgenic *Tg*(*fabp10*:EGFP) zebrafish line with fluorescently labelled liver. The zebrafish model of liver toxicity is a proven accurate animal model for assessing drug-induced liver injury.[68, 69] Herein, 72-hpf (hours post fertilization) old embryos were exposed do ½ × MIC, 1 × MIC and 2 × MIC doses of selected complexes (up to 120 hpf) and assessed for various signs of hepatotoxicity including the liver area index, liver fluorescence and necrosis, as well as the yolk consumption, proven to accurately represent liver damages.[69, 70] Notably, we found that none of the most active complexes (ReNN3Py, ReNN6Py, ReNN1L1, ReNN9L2 and ReNN6BzIm) caused any sign of the hepatotoxicity in the embryos exposed at their respective 1 × MIC doses on *C. albicans* and MRSA (Fig. 6). Moreover, ReNN3Py, ReNN6Py and ReNN1L1 did not provoke unwanted effects even at doses corresponding to

8 - 32 × MIC on MRSA (Fig. 6A) or 2 × MIC on *C. albicans*. The same is true for ReNN9L2 at the dose corresponding 17 × MIC on MRSA. ReNN6BzIm, on the other hand, appeared to be cardio- and hepatotoxic at the doses ≥ 25 µM (corresponding to ≥ 4 × MIC on MRSA and ≥ 2 × MIC on *C. albicans*). Accordingly, these results suggest possible use of selected complexes at a much higher dose. On the contrary, under similar conditions, tetracycline, an antibiotic used against wide spectrum of bacteria including MRSA, causes liver necrosis when applied at higher doses.[49] Similarly, itraconazole, an FDA-approved azole, induced severe liver failure (markedly reduced liver size, liver area index and yolk consumption) and pericardial edema already at ½ × MIC (0.2 µM, Fig. 6). Inner organs toxicity of itraconazole, particularly hepatotoxicity, is a major issue limiting its long-term clinical use in treating fungal infections and in some cases requires treatment discontinuation,[71] especially in the cases where higher drug doses are required.

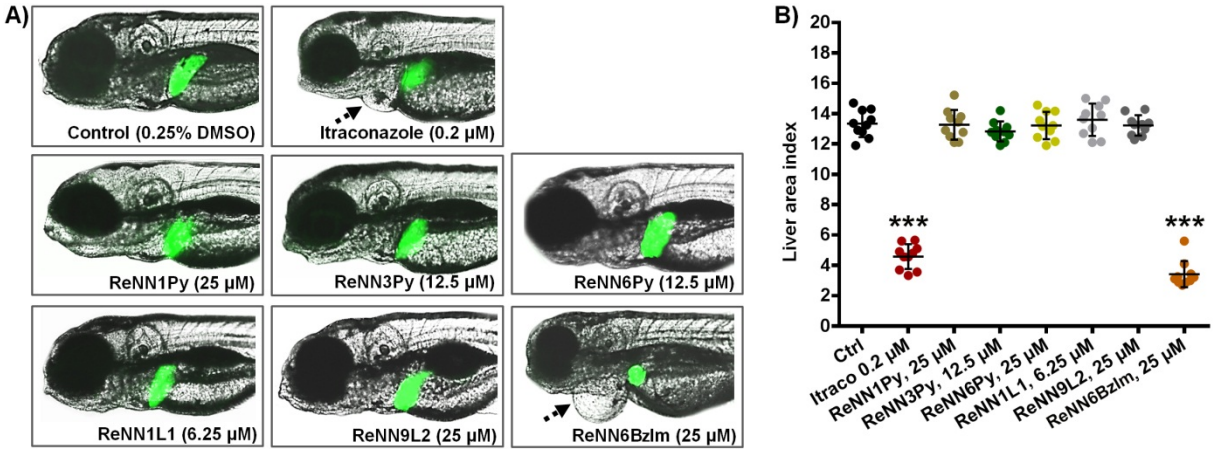

Fig. 6. Hepatotoxicity of selected active antimicrobial Re(I) tricarbonyl complexes assessed *in vivo* in transgenic *Tg(-2.8fabp10a:EGFP)* zebrafish embryos with fluorescently labelled liver (n = 10) according to (A) the liver fluoresce and (B) the liver area index. Hepatotoxicity endpoints analysed in the zebrafish embryos treated with the selected complexes were compared to those in the control (DMSO-treated) group and the group treated with itraconazole, a clinically approved antifungal drug. With the exception of ReNN6BzIm, none of the tested complexes provoked signs of liver toxicity in embryos exposed to the doses corresponding to 8-32 × MIC on MRSA and 2 × MIC on *C. albicans*. Dashed arrow indicates the development of pericardial edema.

Antimicrobial activity *in vivo*

Re(I) tricarbonyl complexes are highly effective against MRSA infection

Having established the antimicrobial potency and hepatotoxic concentrations of selected ReNN#X species, we investigated the efficacy of the most active complexes (ReNN3Py, ReNN6Py, ReNN6BzIm, ReNN9L2, Fig. 5) against each pathogen (MRSA and *C. albicans*) *in vivo* using the zebrafish infection

models. Various pathogenicity studies on human-associated microorganisms have been performed in the zebrafish infection models, giving insight into the differences in the virulence between clinical strains, and offering a unique opportunity to develop new drugs and evaluate their antimicrobial efficacy *in vivo*.[72-74] We first employed the zebrafish-*S. aureus* ATCC43300 model of infection by injecting 1500-1600 fluorescently labelled bacterial cells into the bloodstream (the circulation valley) of 34-hpf old embryos aiming to establish fast systemic infection. Infected embryos were exposed to ½ x MIC, 1 x MIC and 2 x MIC doses of each tested complex, and inspected for survival over a period of 4 days post infection (dpi) and bacterial cell occurrence (fluorescence) as measures of the antibacterial efficacy. The activity of the selected complexes was compared to that of linezolid, as previously reported.[49]

We found that the applied Re(I) complexes successfully rescued zebrafish embryos from lethal MRSA infection during a 4-days treatment, with the protective effect being evident already at 24-48 hpi and ½ x MIC dose ($P < 0.05$, log-rank test, Fig. 7). While untreated embryos developed large pericardial edema by 48 hpi with strong red fluorescence originating from labelled *S. aureus*, and progressively died by 4 dpi (mortality rate of 55%), fish treated with selected ReNN#X complexes had markedly reduced bacterial load (based on fluorescence signal), no signs of cardiotoxicity (Fig. 7A) and all survived by 4 dpi (Fig. 7B). Based on the survival rate of infected embryos by 4 dpi, ReNN6Py and ReNN9L2 appeared to be the most effective compounds, increasing the infected embryos survival rate to 100% even at the dose of ½ × MIC, compared to that in untreated group. Moreover, at 48 h post treatment, with doses of 1 × MIC and 2 × MIC, no detectable fluorescence of labelled *S. aureus* cells was observed within the body of the infected animals, suggesting effective MRSA infection eradication (Fig. 7A). On the other side, although ReNN6BzIm was effective at each administered dose, this complex was slightly cardiotoxic since it provoked pericardial edema in the surviving embryos at 2 × MIC dose by 4 dpi (data not shown). Taken together, the data obtained in this infection assay indicate that complexes ReNN6Py, ReNN3Py and ReNN9L2 are efficient and safe agents against MRSA infection *in vivo*. Moreover, the dose-dependent rescuing effect of these three complexes is higher than the effect of linezolid on MRSA-infected zebrafish embryos, as already observed with similar complexes in a previous study.[49]

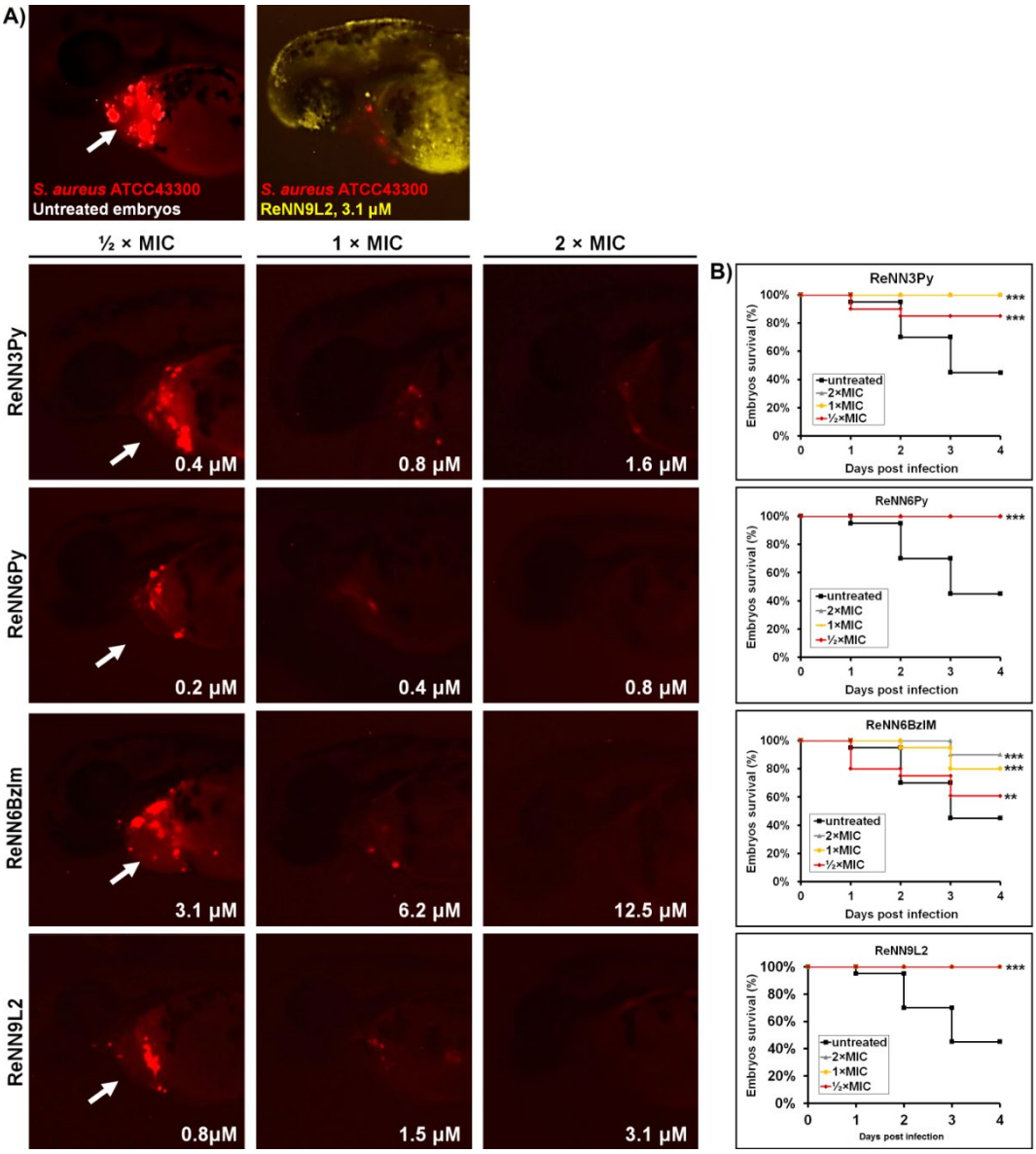

Fig. 7. Re(I) tricarbonyl complexes are effective *in vivo* against lethal MRSA infection. The complexes ReNN3Py, ReNN6Py, ReNN6BzIm and ReNN9L2 successfully rescued zebrafish embryos from the lethal MRSA-infection. Wild (AB) zebrafish embryos were infected with 1500-1600 fluorescently labelled cells of *S. aureus* ATCC43300 (MRSA) into the circulation valley and treated with different doses of the tested complexes during a course of 4 days. Morphology of infected embryos at 1 day post infection (dpi) without treatment and upon treatment with selected complexes is shown (A). The antibacterial efficacy of the applied complexes was assessed by monitoring fluorescence of bacterial cells burden (white arrows on red fluorescence in the panel A) and the survival of MRSA-infected embryos (Kaplan-Meier survival curves, B) during a course of 4-days treatment (n = 20). Signs of multiplied infection in untreated embryos were visible already at 24 h after bacterial cells injection (white arrows), while infection burden was markedly supressed upon the applied treatments, especially at the MIC doses of complexes. Owing to the autofluorescence of ReNN9L2 (originating from the coumarin ligand L2), its presence and distribution through the body of infected embryos (yellow fluorescence, top right A panel) was observable within circulation (Cuvier ductus). Significance in the survival rates between treated and untreated embryos is indicated with asterisks (*P < 0.05; **P < 0.01; ***P < 0.001).

Re(I) tricarbonyl complexes successfully inhibit *C. albicans* filamentation and infection progress

In order to evaluate the *in vivo* antifungal efficacy of selected complexes, we used the zebrafish model of disseminated candidiasis. This model provides a unique opportunity to dissect host and pathogen interaction, as well as the effect of applied therapies on the yeast-to-hyphae transition and eradication of the fungal infection.[75-77] The therapeutic efficacy of ReNN3Py, ReNN6Py and ReNN6BzIm was appraised by assessing the survival rate of *C. albicans*-infected embryos and the potential inhibitory effect of the compounds on fungal filamentation.

Microinjection of 52-68 GFP-labelled cells of *C. albicans* SC5314 (M137 strain)[78] through the otic vesicle into the hindbrain of the fish, resulted in 60% mortality rate of embryos by 4 days post infection (dpi), with the majority of infected embryos dying within the first 2 dpi. On the other hand, the survival rate of *C. albicans*-infected zebrafish was markedly increased by 4 dpi ($p < 0.001$, log-rank test, Fig. 8) by treatment of the infected organisms with the Re complexes. During 48 hours post treatments (hpt), the survival rate of infected embryos was significantly higher already at ½ x MIC doses compared to the survival of untreated embryos (75-100 % vs. 55%, $p<0.001$, log-rank test, Fig. 8). According to the Kaplan-Meier curve, ReNN6Py was the most effective complex, rescuing all infected embryos from lethal candidiasis at each applied dose (survival rate = 100% at ½ x MIC, 2.5 μg/mL = 3.1 μM). A similar therapeutic effect was achieved in the treatment with 1 × MIC dose of ReNN3Py (5 μg /mL = 6.2 μM) while the embryos survival at ½ × MIC dose was slightly lower (85% vs. 40% in untreated group, $p < 0.001$, log-rank assay. Fig. 8). ReNN6BzIm showed lower protective effect of against *C. albicans* infection than ReNN6Py and ReNN3Py, with similar survival rate at 1 × MIC and ½ × MIC doses (80% and 75%, respectively), but signs of cardiotoxicity were observed in 20-30% of embryos exposed to the highest dose of this complex (Fig. 8).

In addition to the remarkable antifungal effect against lethal *C. albicans* SC5314 infection, we found that ReNN3Py and ReNN6Py equally inhibited fungal filamentation *in vivo* in a dose-dependent manner. ReNN6BzIm has a similar effect but at higher doses. The yeast-to-hyphae transition represents the major virulence trait associated with *C. albicans* infection, enabling the fungus to penetrate epithelial barriers, invade inner tissues, causing inner organs damages and biofilms formation.[79] Brothers[80] and Seman[81] clearly demonstrated that filamentation is crucial for *C. albicans* virulence in zebrafish as a host, whereas the filamentation-deficient strains are only weakly pathogenic *in vivo*. In line with these studies, Pavic *et al*. showed that the survival of *C. albicans*-infected embryos is in strong correlation with the level of fungus filamentation, and that by blocking hyphal formation with Ag(I) complexes it is possible to rescue embryos from the lethal infection.[76] In this study, we found that *C. albicans* filamentation was completely supressed in the fungus-infected hindbrain already at ½ × MIC dose of ReNN6Py and ReNN6BzIm, as well as at 1 × MIC dose of ReNN3Py. In comparison to the control

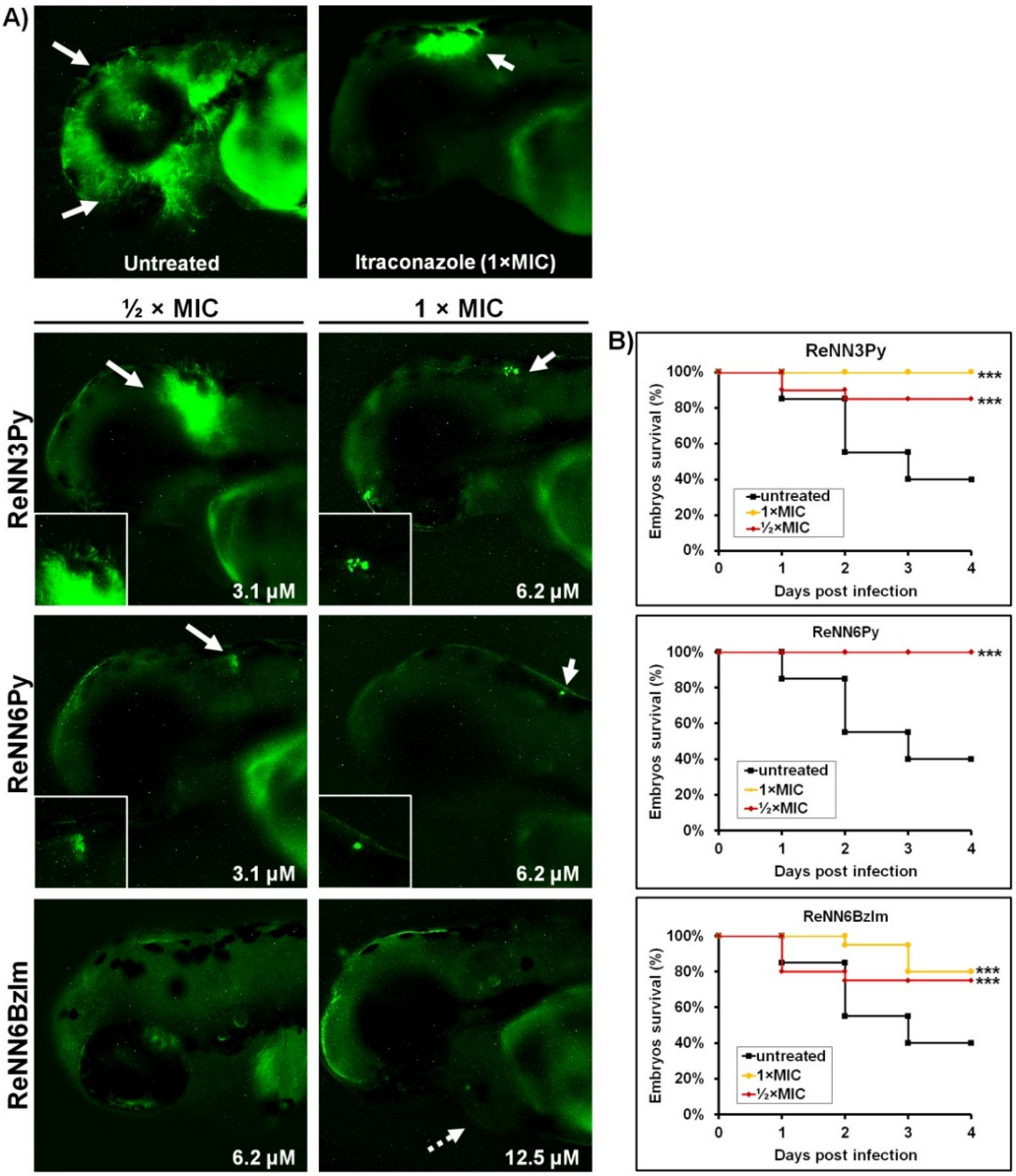

Fig. 8. Re(I) tricarbonyl complexes are effective *in vivo* against lethal disseminated candidiasis. The antifungal efficacy of complexes ReNN3Py, ReNN6Py and ReNN6BzIm was assessed in the zebrafish-*C. albicans* infection model. Wild type (AB) embryos were microinjected with 55 – 70 GFP-expressing *C. albicans* cells into the hindbrain through the otic vesicle, and treated with the different doses of the selected complexes. Antifungal efficacy was assessed by monitoring fungal filamentation and the survival of infected embryos during 4 dpi. Fluorescent microscopy (A) and the Kaplan-Meier survival curve of untreated and treated *C. albicans*-infected embryos at 1 dpi and 4 dpi (B), respectively, are shown. All tested complexes successfully prevented *C. albicans* filamentation within the hindbrain (boxed) and rescued embryos from lethal infection. Appearance of weak pericardial edema at 1 × MIC of ReNN6BzIm occurred (dashed arrow). Significance in the survival rates between treated and untreated embryos is indicated with asterisks (*P < 0.05; **P < 0.01; ***P < 0.001).

(untreated) group, much shorter and less dense hyphae occurred upon treatment with ½ × MIC dose of ReNN6Py or the antifungal drug itraconazole (Fig. 8). Moreover, in ca. 50-60% of untreated embryos, *C. albicans* filamented a few hours post infection and formed a robust network of hyphae by 48 hpi, which penetrated the head epithelium and other epithelial barriers within the body, resulting in infection dissemination and/or the embryos death (Fig. 8). The Re complexes effectively prevented such occurrence. To the best of our knowledge this is the first *in vivo* study providing evidence that Re(I) tricarbonyl species are efficient antifungal agents in protecting infected animals from lethal candidal infection.

Re(I) tricarbonyl complexes are effective antimicrobial agents in *C. albicans*-MRSA co-infection

Since ReNN3Py, ReNN6Py and ReNN6BzIm demonstrated both anti-*Candida* and anti-MRSA activity *in vitro* and *in vivo,* we have evaluated whether the pyridine derivatives are also effective against mixed *C. albicans*-MRSA infection by determining the dose-dependent pathogens survival (colony forming unit – CFU) and fungal filamentation following treatments. *C. albicans* and *Staphylococcus* species are part of the commensal microbial flora, but can cause serious hospital-acquired infections, with an exceptional ability to inhabit diverse niches in humans, especially in immunocompromised patients. Both *C. albicans* and *Staphylococcus* are pathogens frequently co-associated with superficial and systemic infections, where their mutual interactions lead to increased virulence, drug tolerance and immune evasion in both species.[28] Remarkably, *C. albicans* and *S. aureus* together establish difficult-to-treat polymicrobial diseases, including cystic fibrosis, denture stomatitis, periodontitis, urinary tract and burn wound infections, as well as infections of medical devices such as central venous catheters.[28] The complexity of these polymicrobial infections poses an additional challenge to find efficient treatment strategies.

As shown in Fig. 9, both Re(I) tricarbonyl complexes have potent antimicrobial activity against *C. albicans*-MRSA co-infection. Effective doses against mixed infection (12.5 µM for ReNN3Py and 6.25 µM for ReNN6Py) are in a line with MICs measured against *Candida* (Table 2). Based on CFU values, obtained after the plating on YPD and BHI media, ReNN6Py appeared to be much more effective than ReNN3Py, since neither viable fungal nor bacterial cells (0 CFU) were recorded in the treatment with 12.5 µM of ReNN6Py. A load of 9.3×10^4 *C. albicans* cells/mL and no bacterial cells were recorded at the same dose of ReNN3Py. Untreated (control) samples had 9.3×10^7 *C. albicans* cells/mL and 5×10^9 *S. aureus* cells/mL, indicating a remarkable potency of the complexes.

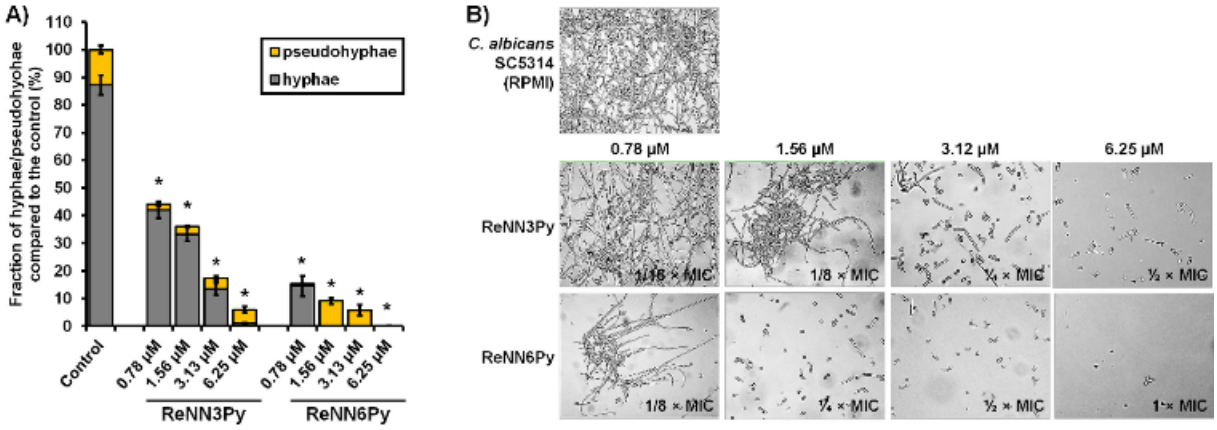

Fig. 9. Re(I) tricarbonyl complexes are highly effective against *C. albicans*-MRSA co-infection. The treatments of both pathogens within mixed infection with the complexes ReNN3Py and ReNN6Py resulted in an effective suppression of fungal growth, filamentation and hyphal elongation during 48 h exposure. The applied complexes exerted different dose-dependent effects on the ability of *C. albicans* to form hyphae and pseudohyphae (A), as well as on hyphal length (B). ReNN6Py appeared to be more active than ReNN3Py. Compared to the filamentation of untreated *C. albicans* cells, the filamentation was inhibited at doses > 0.78 µM of ReNN6Py and > 3.13 µM of ReNN3Py.

It is important to emphasize that, based on MIC values in mixed versus mono-infection, none of the tested pathogens showed lower sensitivity to the applied complexes when co-cultured and grown together. This is a very important finding since lower efficacy of clinical antibiotics (e.g. vancomycin) against *S. aureus* was documented when the bacterium grew together with *C. albicans*, requiring higher drugs concentrations and longer duration of combination therapy to eliminate the infection.[24] ReNN6Py and ReNN3Py successfully eliminated *S. aureus* (0 CFU) at quite low doses of 0.78 µM (660 ng/mL) and 1.56 µM (1.3 µg/mL), respectively. To the best of our knowledge, ReNN6Py and ReNN3Py are the first examples of metal complexes effective against mixed *S. aureus*-*C. albicans* infection. The use of a single agent with dual activity may offer some advantages over combination (antibiotic-antifungals) therapy.

In addition, we examined the effect of ReNN3Py and ReNN6Py on the yeast-to-hyphal transition when *C. albicans* grew together with *S. aureus* MRSA. This morphogenetic switch represents an important virulence trait of *C. albicans* for biofilm formation, dissemination, and resistance to antifungal drug treatment.[82] We found that both complexes effectively suppressed fungal filamentation at sub-MIC doses (Fig. 9A), while simultaneously killing MRSA (Fig. 9B). ReNN6Py appears more potent than

ReNN3Py and markedly reduced hyphal growth at 1/8 x MIC (0.78 μM) compared to the length of untreated hyphae, while the filamentation was almost completely inhibited at ¼ x MIC dose (1.56 μM). ReNN3Py exerted comparable activity at 6.25 μM (½ x MIC) and 1.56 μM (1/8 x MIC dose) doses, respectively (Fig. 9B). In contrast, untreated *C. albicans* formed long hyphae (filaments) and established a very dense mass. This anti-virulence activity finding, together with the dual antimicrobial activity of the complexes, is of particular importance in preventing the life-threating outcome of *C. albicans*-*S. aureus* co-infection, since invading and aggressive hyphae enable the fungus to penetrate epithelial barriers and disseminate into the bloodstream causing systemic infection, allowing bacterial cells attached to the fungal filaments to use this route to spread within the body.[12, 83] This is particularly worrisome in patients with a debilitated or seriously compromised immune system. To the best of our knowledge, the anti-virulence potential of Re(I) complexes has never been reported, and an exact mechanism of their action remains to be explored. Interestingly, we did not find the same morphogenetic inhibitory effect of ReNN3Py and ReNN6Py on solid RPMI medium, indicating that the complexes in liquid RPMI act *via* distinctive mechanism(s) different from those operating in solid conditions. Such result is not surprising since transcriptome analysis studies have revealed that the set of filamentation-associated genes being upregulated in *C. albicans* grown in liquid medium differ from those upregulated in the same solid medium.[84]

Antimicrobial activity, *in vivo* toxicity and SAR analysis

As mentioned in the opening pages of this article, alongside the discovery of new potent antimicrobial complexes, we were interested in understanding if common structural parameters emerged from a structure–activity relationship (SAR) analysis of ReNN#X. Overall, we could not established a correlation between ReNN#X activity and properties of NN# (e.g. basicity or relative logP). However, all active and non-toxic complexes are those bearing 4 of the 5 most lipophilic NN# (NN6, 1, 9 and 3, logPs = 5.95, 4.76, 3.14 and 3.05 respectively). We believe that, at least in part, the ligand X is responsible for modulating the activity of neutral complexes, although the relatively small fraction of active neutral complexes (in particular for X = BzIm) are toxic *in vivo*. Interestingly, none of the bromo (i.e. X = Br) ReNN# derivatives exhibited any activity against the microorganisms (both bacteria and fungi), with MICs >50 μM (ESI). It is possible that ReNN#Br species exchange Br for water or other molecules in the medium or endogenous to the zebrafish, being thereby deactivated. Other metal-based antimicrobial complexes (e.g. CORM-3) are deactivated *via* this pathway (Ru-thiols binding).[85]

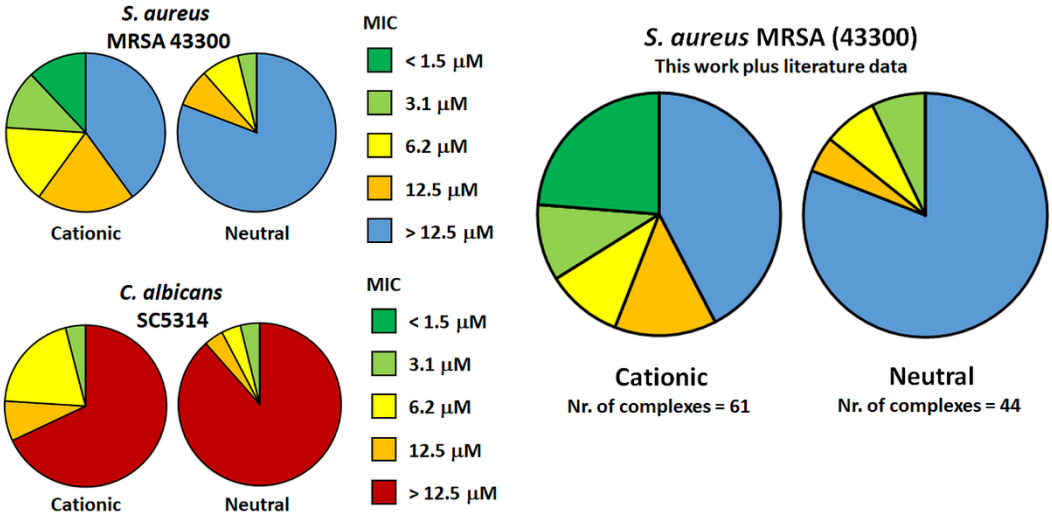

Fig. 10. Graphic representation of the numeric proportion of cationic (31 tested compounds) and neutral (26 tested compounds) ReNN#X complexes with corresponding MIC values against *S. aureus* MRSA 43300 (top left) and C. *albicans* SC5314 respectively (bottom left). Right: same representation against in *S. aureus* MRSA including all data available (this work and literature).

It appears to us that most crucial for the antimicrobial efficacy and low toxicity of the complexes is the overall charge of the same. The results of our study indicate that of the 57 Re species tested only 8 revealed very good to excellent activity (MICs ≤3.1, Table 1) against *S. aureus* strains, and of those 5 were both active and non-toxic (i.e. Tw ≥ 9). All active and non-toxic complexes are cationic in nature. Similarly, for *Candida* spp., only 8 compounds were active (MICs ≤6.2, Table 2), and of those, 2 were both active and non-toxic. Again, the last two complexes (i.e. ReNN3Py and ReNN6Py) are cationic in nature. Fig. 10 provides a graphic representation of the numeric proportion of cationic and neutral ReNN#X complexes with corresponding MIC values against *S. aureus* MRSA 43300 and *C. albicans* SC5314. As mentioned above, and as it may be concluded from the figure, cationic complexes show on average the lowest MICs. This is true for both bacteria and fungi. The mechanism of action of rhenium antimicrobial agents remains largely unknown, but we hypothesize that the positive charge of the complexes is important for their interaction with phosphatidylglycerol and cardiolipin anionic lipids.[86, 87]

Conclusions

In conclusion, we have employed a molecular approach to the discovery of potent and non-toxic rhenium tricarbonyl complexes active against MRSA-*C. albicans* co-infection. Within the family of complexes evaluated, we identified nontoxic species highly effective *in vivo* against MRSA infection

(with MIC < 330 ng/mL) and capable of successfully inhibiting *C. albicans* filamentation and infection progress at the same time. Two compounds, in particular (ReNN3Py and ReNN6Py) bearing the lipophilic 4,4'-tetraethyldiamine-bipyridine and bathophenanthroline diimine ligands, showed a remarkable therapeutic potential in combating MRSA-*C. albicans* co-infection, with the ability to suppress the morphogenetic yeast-to-hyphal transition of the fungus, as the major virulence trait associated with biofilm formation and drug resistance of this pathogen, and being responsible for systemic dissemination of both co-infection counterparts. The compounds show no sign of cardio-, hepato-, hematotoxicity or teratogenicity, suggesting a microbe-specific mechanism of activity without adverse effect to the host cells. The study and data are in line with the WHO and UN recommendation of a comprehensive overview of non-traditional antibacterial medicines, with a focus on non-classical approaches for the identification of molecules with different mechanisms of action outside the traditional development pathway. Within the specific class of metal complexes, SAR analysis tentatively suggests that cationic complexes bearing highly lipophilic bidentate ligands may serve as a blueprint for the further development of rhenium-based antimicrobial agents. Future efforts from our groups will be directed towards the elucidation of the mechanism of action of the complexes and the continuous development and discovery of new and highly potent antimicrobial agents to combat AMR.

Experimental Section

Detailed experimental procedures and molecules' characterization are in ESI.

Author contributions

S.N.S. (chemistry) and N.R. (biology) investigation, formal analysis, data curation, methodology, writing – original draft; P.R. (chemistry) preparation of ReNN#Br complexes; A.C. crystallography; A.P. writing – original draft, review & editing, conceptualization, supervision, validation, acquisition, resources, project administration; F.Z. writing – original draft, review & editing, conceptualization, supervision, validation, acquisition, resources, project administration.

Conflicts of interest

There are no conflicts to declare.

Acknowledgements

Financial support from the Fonds de recherche du Centenaire de l'Université de Fribourg (F.Z. and A.P., Project No. 818) and Ministry of Education, Science and Technological Development of the Republic of Serbia (A.P. and N.R., Project No. 451-03-9/2021-14/200042, 2021) is gratefully acknowledged. We are obliged to Dr A. Barac of the University Clinical Center of Serbia and Prof. Cornelia Lass-Floerl of the University of Innsbruck for providing the *C. auris* strain 8. We are also thankful to Prof. B. Hube, Leibniz Institute for Natural Product Research and Infection Biology, for providing GFP-labeled *Candida*.

Notes and references

1. M. A. Brockhurst, F. Harrison, J. W. Veening, E. Harrison, G. Blackwell, Z. Iqbal and C. Maclean, *Nat. Ecol. Evol.*, 2019, **3**, 515-517.
2. V. Cattoir and B. Felden, *J. Infect. Dis.*, 2019, **220**, 350-360.
3. L. Folgori, S. J. Ellis, J. A. Bielicki, P. T. Heath, M. Sharland and M. Balasegaram, *Lancet Glob. Health*, 2017, **5**, e1066-e1068.
4. K. K. Holmes, S. Bertozzi, B. R. Bloom, P. Jha, H. Gelband, L. M. DeMaria and S. Horton, in *Major Infectious Diseases*, eds. K. K. Holmes, S. Bertozzi, B. R. Bloom and P. Jha, International Bank for Reconstruction and Development/The World Bank, Washington (DC), 2017, DOI: 10.1596/978-1-4648-0524-0_ch1, ch. 1.
5. J. O'Neill, *AMR Rev.*, 2016, 1-84.
6. WHO, *Global shortage of innovative antibiotics fuels emergence and spread of drug-resistance*, 2021.
7. WHO, *2020 antibacterial agents in clinical and preclinical development: an overview and analysis*, 2021.
8. B. Plackett, *Nature*, 2020, **586**, S50-S52.
9. B. Spellberg and D. N. Gilbert, *Clin. Infect. Dis.*, 2014, **59**, S71-S75.
10. Q. Hu, H. Cheng, W. Yuan, F. Zeng, W. Shang, D. Tang, W. Xue, J. Fu, R. Zhou, J. Zhu, J. Yang, Z. Hu, J. Yuan, X. Zhang, Q. Rao, S. Li, Z. Chen, X. Hu, X. Wu and X. Rao, *J. Clin. Microbiol.*, 2015, **53**, 67-72.
11. S. Y. C. Tong, J. S. Davis, E. Eichenberger, T. L. Holland and V. G. Fowler, *Clin. Microbiol. Rev.*, 2015, **28**, 603-661.
12. L. M. Schlecht, B. M. Peters, B. P. Krom, J. A. Freiberg, G. M. Hänsch, S. G. Filler, M. A. Jabra-Rizk and M. E. Shirtliff, *Microbiol. SGM*, 2015, **161**, 168-181.
13. Y. Guo, G. Song, M. Sun, J. Wang and Y. Wang, *Front. Cell. Infect. Microbiol.*, 2020, **10**, 1-11.
14. A. P. Kourtis, K. Hatfield, J. Baggs, Y. Mu, I. See, E. Epson, J. Nadle, M. A. Kainer, G. Dumyati, S. Petit, S. M. Ray, D. Ham, C. Capers, H. Ewing, N. Coffin, L. C. McDonald, J. Jernigan and D. Cardo, *MMWR Morb. Mortal. Wkly Rep.*, 2019, **68**, 214-219.
15. F. C. Tenover, S. W. Sinner, R. E. Segal, V. Huang, S. S. Alexandre, J. E. McGowan and M. P. Weinstein, *Int. J. Antimicrob. Agents*, 2009, **33**, 564-568.
16. K. Kainz, M. A. Bauer, F. Madeo and D. Carmona-Gutierrez, *Microb. Cell*, 2020, **7**, 143-145.
17. F. Bongomin, S. Gago, R. O. Oladele and D. W. Denning, *J. Fungi*, 2017, **3**, 1-29.
18. M. A. Pfaller and D. J. Diekema, *Clin. Microbiol. Rev.*, 2007, **20**, 133-163.
19. J. A. Cortés and I. F. Corrales, in *Fungal Infection*, eds. E. Silva de Loreto and J. S. Moraes Tondolo, IntechOpen, London (UK), 2019, DOI: 10.5772/intechopen.81813, ch. 3.
20. T. P. McCarty, C. M. White and P. G. Pappas, *Infect. Dis. Clin.*, 2021, **35**, 389-413.
21. L. Ostrosky-Zeichner, A. Casadevall, J. N. Galgiani, F. C. Odds and J. H. Rex, *Nat. Rev. Drug Discov.*, 2010, **9**, 719-727.
22. S. G. Whaley, E. L. Berkow, J. M. Rybak, A. T. Nishimoto, K. S. Barker and P. D. Rogers, *Front. Microbiol.*, 2016, **7**, 2173.
23. S. A. Klotz, B. S. Chasin, B. Powell, N. K. Gaur and P. N. Lipke, *Diagn. Microbiol. Infect. Dis.*, 2007, **59**, 401-406.
24. M. M. Harriott and M. C. Noverr, *Antimicrob. Agents Chemother.*, 2009, **53**, 3914-3922.
25. H. H. Lara and J. L. Lopez-Ribot, *Pathogens (Basel, Switzerland)*, 2020, **9**, 1-14.
26. M. Haque, M. Sartelli, J. McKimm and M. Abu Bakar, *Infect. Drug Resist.*, 2018, **11**, 2321-2333.
27. E. F. Kong, C. Tsui, S. Kucharíková, D. Andes, P. Van Dijck and M. A. Jabra-Rizk, *mBio*, 2016, **7**, 1-12.
28. H. Carolus, K. Van Dyck and P. Van Dijck, *Front. Microbiol.*, 2019, **10**, 2162.
29. A. Frei, J. Zuegg, A. G. Elliott, M. Baker, S. Braese, C. Brown, F. Chen, G. D. C, G. Dujardin, N. Jung, A. P. King, A. M. Mansour, M. Massi, J. Moat, H. A. Mohamed, A. K. Renfrew, P. J.

Rutledge, P. J. Sadler, M. H. Todd, C. E. Willans, J. J. Wilson, M. A. Cooper and M. A. T. Blaskovich, *Chem. Sci.*, 2020, **11**, 2627-2639.
30. A. Frei, *Antibiotics*, 2020, **9**, 90.
31. M. Patra, G. Gasser and N. Metzler-Nolte, *Dalton Trans.*, 2012, **41**, 6350-6358.
32. F. Li, J. G. Collins and F. R. Keene, *Chem. Soc. Rev.*, 2015, **44**, 2529-2542.
33. M. A. Sierra, L. Casarrubios and M. de la Torre, *Chem. Eur. J.*, 2019, **25**, 7232-7242.
34. A. Leonidova and G. Gasser, *ACS Chem. Biol.*, 2014, **9**, 2180-2193.
35. P. Collery, D. Desmaele and V. Vijaykumar, *Curr. Pharm. Des.*, 2019, **25**, 1-17.
36. E. B. Bauer, A. A. Haase, R. M. Reich, D. C. Crans and F. E. Kühn, *Coord. Chem. Rev.*, 2019, **393**, 79-117.
37. C. C. Konkankit, S. C. Marker, K. M. Knopf and J. J. Wilson, *Dalton Trans.*, 2018, **47**, 9934-9974.
38. H. B. Suliman, F. Zobi and C. A. Piantadosi, *Antiox. Redox Sign.*, 2016, **24**, 345-360.
39. F. Chen, J. Moat, D. McFeely, G. Clarkson, I. J. Hands-Portman, J. P. Furner-Pardoe, F. Harrison, C. G. Dowson and P. J. Sadler, *J. Med. Chem.*, 2018, **61**, 7330-7344.
40. M. Wenzel, M. Patra, C. H. Senges, I. Ott, J. J. Stepanek, A. Pinto, P. Prochnow, C. Vuong, S. Langklotz, N. Metzler-Nolte and J. E. Bandow, *ACS Chem. Biol.*, 2013, **8**, 1442-1450.
41. D. Siegmund, N. Lorenz, Y. Gothe, C. Spies, B. Geissler, P. Prochnow, P. Nuernberger, J. E. Bandow and N. Metzler-Nolte, *Dalton Trans.*, 2017, **46**, 15269-15279.
42. A. Frei, M. Amado, M. A. Cooper and M. A. T. Blaskovich, *Chem. Eur. J.*, 2019, **26**, 2852-2858.
43. M. Patra, M. Wenzel, P. Prochnow, V. Pierroz, G. Gasser, J. E. Bandow and N. Metzler-Nolte, *Chem. Sci.*, 2015, **6**, 214-224.
44. J. Delasoie, P. Schiel, S. Vojnovic, J. Nikodinovic-Runic and F. Zobi, *Pharmaceutics*, 2020, **12**, 480.
45. J. Delasoie, A. Pavic, N. Voutier, S. Vojnovic, A. Crochet, J. Nikodinovic-Runic and F. Zobi, *Eur. J. Med. Chem.*, 2020, **204**, 112583.
46. J. Rossier, D. Hauser, E. Kottelat, B. Rothen-Rutishauser and F. Zobi, *Dalton Trans.*, 2017, **46**, 2159-2164.
47. J. Delasoie, N. Radakovic, A. Pavic and F. Zobi, *Appl. Sci.*, 2020, **10**.
48. S. Nasiri Sovari and F. Zobi, *Chemistry*, 2020, **2**, 418-452.
49. S. N. Sovari, S. Vojnovic, S. S. Bogojevic, A. Crochet, A. Pavic, J. Nikodinovic-Runic and F. Zobi, *Eur. J. Med. Chem.*, 2020, **205**, 112533.
50. R. G. Miller, M. Vazquez-Hernandez, P. Prochnow, J. E. Bandow and N. Metzler-Nolte, *Inorg. Chem.*, 2019, **58**, 9404-9413.
51. A. Noor, G. S. Huff, S. V. Kumar, J. E. M. Lewis, B. M. Paterson, C. Schieber, P. S. Donnelly, H. J. L. Brooks, K. C. Gordon, S. C. Moratti and J. D. Crowley, *Organometallics*, 2014, **33**, 7031-7043.
52. S. V. Kumar, W. K. C. Lo, H. J. L. Brooks, L. R. Hanton and J. D. Crowley, *Aust. J. Chem.*, 2016, **69**, 489-498.
53. L. Wallace and D. P. Rillema, *Inorg. Chem.*, 1993, **32**, 3836-3843.
54. F. L. Thorp-Greenwood, J. A. Platts and M. P. Coogan, *Polyhedron*, 2014, **67**, 505-512.
55. L. Sacksteder, A. P. Zipp, E. A. Brown, J. Streich, J. N. Demas and B. A. DeGraff, *Inorg. Chem.*, 1990, **29**, 4335-4340.
56. B. B. Hueholt, W. Xu, M. Sabat, B. A. DeGraff and J. N. Demas, *J. Fluoresc.*, 2007, **17**, 522-527.
57. J. M. Smieja, E. E. Benson, B. Kumar, K. A. Grice, C. S. Seu, A. J. M. Miller, J. M. Mayer and C. P. Kubiak, *PNAS*, 2012, **109**, 15646-15650.
58. A. M.-H. Yip, J. Shum, H.-W. Liu, H. Zhou, M. Jia, N. Niu, Y. Li, C. Yu and K. K.-W. Lo, *Chem. Eur. J.*, 2019, **25**, 8970-8974.
59. J. Yang, J.-X. Zhao, Q. Cao, L. Hao, D. Zhou, Z. Gan, L.-N. Ji and Z.-W. Mao, *ACS Appl. Mater. Interfaces*, 2017, **9**, 13900-13912.
60. E. Gómez, M. A. Huertos, J. Pérez, L. Riera and A. Menéndez-Velázquez, *Inorg. Chem.*, 2010, **49**, 9527-9534.
61. M. W. Pletz, O. Burkhardt and T. Welte, *Eur. J. Med. Res.*, 2010, **15**, 507-513.

62. P. Guntzel, C. Nagel, J. Weigelt, J. W. Betts, C. A. Pattrick, H. M. Southam, R. M. La Ragione, R. K. Poole and U. Schatzschneider, *Metallomics*, 2019, **11**, 2033-2042.
63. X. Li, K. Heimann, F. Li, J. M. Warner, F. Richard Keene and J. Grant Collins, *Dalton Trans.*, 2016, **45**, 4017-4029.
64. E. Kouris, S. Kalogiannis, F. Perdih, I. Turel and G. Psomas, *J. Inorg. Biochem.*, 2016, **163**, 18-27.
65. P. L. Lam, G. L. Lu, K. H. Choi, Z. Lin, S. H. L. Kok, K. K. H. Lee, K. H. Lam, H. Li, R. Gambari, Z. X. Bian, W. Y. Wong and C. H. Chui, *RSC Adv.*, 2016, **6**, 16736-16744.
66. T. Dai, Y. Y. Huang, S. K. Sharma, J. T. Hashmi, D. B. Kurup and M. R. Hamblin, *Recent Pat. Antiinfect. Drug Discov.*, 2010, **5**, 124-151.
67. P. A. Walker, S. Ryder, A. Lavado, C. Dilworth and R. J. Riley, *Arch. Toxicol.*, 2020, **94**, 2559-2585.
68. S. Katoch and V. Patial, *J. Appl. Toxicol.*, 2021, **41**, 33-51.
69. Y. Zhang, L. W. Han, Q. X. He, W. Y. Chen, C. Sun, X. Wang, X. Q. Chen, R. C. Wang, C. D. Hsiao and K. C. Liu, *J. Pharmacol. Toxicol. Met.*, 2017, **84**, 102-110.
70. J. H. He, S. Y. Guo, F. Zhu, J. J. Zhu, Y. X. Chen, C. J. Huang, J. M. Gao, Q. X. Dong, Y. X. Xuan and C. Q. Li, *J. Pharmacol. Toxicol. Met.*, 2013, **67**, 25-32.
71. I. Kyriakidis, A. Tragiannidis, S. Munchen and A. H. Groll, *Expert Opin. Drug Saf.*, 2017, **16**, 149-165.
72. M. C. Gomes and S. Mostowy, *Trends Microbiol.*, 2020, **28**, 10-18.
73. V. Torraca and S. Mostowy, *Trends Cell Biol.*, 2018, **28**, 143-156.
74. K. Stagaman, T. J. Sharpton and K. Guillemin, *Lab Animal*, 2020, **49**, 201-207.
75. E. M. Mallick, A. C. Bergeron, S. K. Jones, Z. R. Newman, K. M. Brothers, R. Creton, R. T. Wheeler and R. J. Bennett, *Front. Microbiol.*, 2016, **7**, 1-18.
76. N. L. Stevanović, B. Đ. Glišić, S. Vojnovic, H. Wadepohl, T. P. Andrejević, S. Ž. Đurić, N. D. Savić, J. Nikodinovic-Runic, M. I. Djuran and A. Pavic, *J. Mol. Struc.*, 2021, **1232**, 130006.
77. N. D. Savic, S. Vojnovic, B. D. Glisic, A. Crochet, A. Pavic, G. V. Janjic, M. Pekmezovic, I. M. Opsenica, K. M. Fromm, J. Nikodinovic-Runic and M. I. Djuran, *Eur. J. Med. Chem.*, 2018, **156**, 760-773.
78. C. Fradin, P. De Groot, D. MacCallum, M. Schaller, F. Klis, F. C. Odds and B. Hube, *Mol. Microbiol.*, 2005, **56**, 397-415.
79. F. L. Mayer, D. Wilson and B. Hube, *Virulence*, 2013, **4**, 119-128.
80. K. M. Brothers and R. T. Wheeler, *J. Vis. Exp.*, 2012, DOI: 10.3791/4051.
81. B. G. Seman, J. L. Moore, A. K. Scherer, B. A. Blair, S. Manandhar, J. M. Jones, R. T. Wheeler and G. S. Deepe, *Infect. Immun.*, 2018, **86**, e00415-00418.
82. T. Vila, J. A. Romo, C. G. Pierce, S. F. McHardy, S. P. Saville and J. L. Lopez-Ribot, *Virulence*, 2017, **8**, 150-158.
83. N. O. Ponde, L. Lortal, G. Ramage, J. R. Naglik and J. P. Richardson, *Crit. Rev. Microbiol.*, 2021, **47**, 91-111.
84. S. Thewes, G. P. Moran, B. B. Magee, M. Schaller, D. J. Sullivan and B. Hube, *BMC Microbiol.*, 2008, **8**, 187.
85. H. M. Southam, T. W. Smith, R. L. Lyon, C. Liao, C. R. Trevitt, L. A. Middlemiss, F. L. Cox, J. A. Chapman, S. F. El-Khamisy, M. Hippler, M. P. Williamson, P. J. F. Henderson and R. K. Poole, *Redox Biol.*, 2018, **18**, 114-123.
86. R. M. Epand and R. F. Epand, *Biochim. Biophys. Acta*, 2009, **1788**, 289-294.
87. R. M. Epand and R. F. Epand, *Mol. Biosyst.*, 2009, **5**, 580-587.

SUPPORTING INFORMATION FOR

Combatting AMR: a molecular approach to the discovery of potent and non-toxic rhenium complexes active against *C. albicans*-MRSA co-infection

Sara Nasiri Sovari,[a†] Natasa Radakovic,[b†] Paul Roch,[a] Aurélien Crochet,[a] Aleksandar Pavic*[b] and Fabio Zobi*[a]

a. Department of Chemistry, Fribourg University, Chemin Du Musée 9, 1700, Fribourg, Switzerland.

b. Institute of Molecular Genetics and Genetic Engineering, University of Belgrade, Vojvode Stepe 444a, 11042 Belgrade, Serbia.

† Equally contributed

* Correspondence: sasapavic@imgge.bg.ac.rs and fabio.zobi@unifr.ch

Table of contents

Experimental protocols

Materials and methods

All chemicals were purchased in reagent or analytical grade from commercial suppliers (Sigma-Aldrich, Alfa Aesar, TCI, Fluorochem), and used without further purification. Solvents were either used as received or dried over molecular sieves prior to use. Ligands L1 and L2 and *fac*-[$Re^{I}(CO)_3$(NN#)Br] complexes were synthesized based on the procedures previously reported by our team.[1] ^{1}H and ^{13}C NMR spectra were recorded on a Bruker Avance III 400 MHz using residual solvent peaks as internal references. The following abbreviations are used: singlet (s), doublet (d), doublet of doublets (dd), triplet (t), doublet of triplets (td), quintuplet (quint), sextuplet (sext), and multiplet (m). High-resolution mass spectrometry was performed on a Bruker FTMS 4.7-T Apex II (BRUKER DALTONICS GmbH, Switzerland). The following abbreviations are used: high-resolution mass spectrometry (HRMS), electrospray ionization (ESI). HPLC analyses were performed on a Merck-Hitachi L7000. The analytical separations were conducted on a Macherey–Nagel Nucleodur PolarTec column (5 µm particle size, 110 Å pore size, 250 × 3 mm). The preparative separations were conducted on a Macherey–Nagel Nucleodur C_{18} HTec column (5 µm particle size, 110 Å pore size, 250 × 21 mm). The flow rate was set to 0.5 mL/min for analytical separations and 5 mL/min for the preparative ones. The eluting bands were detected at 320 nm. Analytical thin-layer chromatography (TLC) was performed on commercial silica plates (Merck 60-F 254, 0.25 mm thickness); compounds were visualized by UV light (254 nm and 366 nm). Preparative flash chromatography was performed with Merck silica gel (Si 60, 63−200 mesh) and Merck Aluminum oxide 90 standardized. IR spectra were recorded on a PerkinElmer Spectrum 100 FT-IR spectrometer. The UV-Vis spectra were recorded on a Jasco V-730. Single crystal diffraction collections were done on Stoe IPDS2 diffractometer ($MoK\alpha_1$ (λ = 0.71073 Å)) equipped with a cryostat from Oxford Cryosystems. The structures were solved with the ShelXT structure solution program using Intrinsic Phasing and refined with the ShelXL refinement package using Least Squares minimisation. All the crystal structures have been deposited at the Cambridge Crystallographic Data Centre. CCDC numbers 2089503-2089510 contain the supplementary crystallographic data for this paper. These data can be obtained free of charge from the Cambridge Crystallographic Data Centre via www.ccdc.cam.ac.uk/structures.

Synthesis and characterization of compounds

Synthetic scheme of L1 and L2

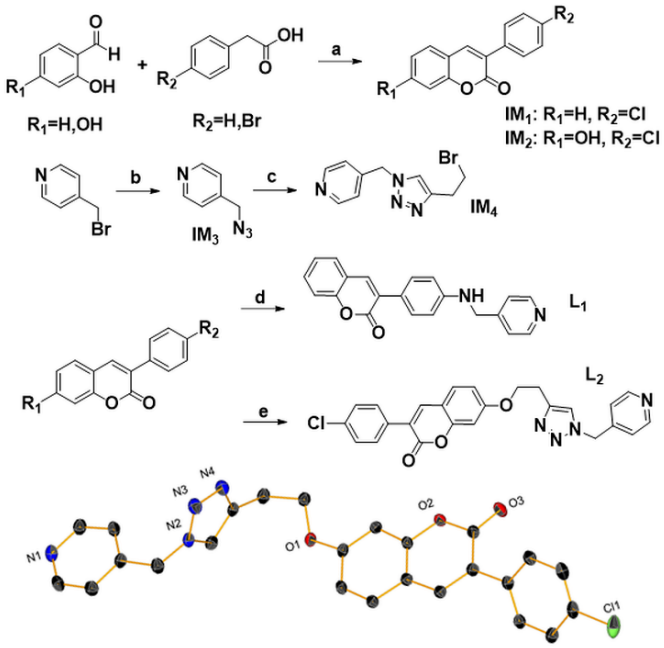

Scheme S1. Synthesis and chemical structures of 3-arylcoumarin ligands (L1-L2) including X-ray structure of L2. Conditions: (a) CH_3COOK, Ac_2O, at 120 ºC 10 h, under argon/ HCl 2N, MeOH, reflux, 4 h, 90-95%; (b) 4-(bromomethyl)pyridine.HCl, K_2CO_3, DMF, NaN_3, rt, 4 h, 90%; (c) IM_4, CuI , Et_3N (anhydrous), 4-bromo-1-butyne, acetonitrile, rt, overnight, under argon, 85%; (d) 4-picolylamine, $Pd_2(dba)_3$, xantphos, Cs_2CO_3, 1,4-dioxane, 100 ºC, overnight for L1, 95%; (e) IM_5, K_2CO_3, acetone, 60 ºC,10 h for L2, 75%.

General preparation of *fac*-[Re(CO)$_3$NN#X]PF$_6$/CF$_3$SO$_3$ complexes.

In order to prepare the final ReNN#X complexes, two methods were applied as follows:

Method a) *fac*-[Re(CO)$_3$NN#X]PF$_6$. The appropriate *fac*-[Re(CO)$_3$NN#Br] complex was suspended in DCM under argon and trifluoromethanesulfonic acid was added and the mixture stirred for 1 h at rt. Afterwards, *fac*-[Re(CO)$_3$NN#(CF$_3$SO$_3$)], was precipitated by slow addition of diethyl ether and then filtered and dried under vacuum, resulting in a solid yellow products. The next step was performed by adding the monodentate ligand to a solution of *fac*-[Re(CO)$_3$NN#(CF$_3$SO$_3$)] in MeOH, then the reaction mixture was refluxed under argon for 10 h. To obtain the final products, NH_4PF_6 (6.0 equiv.) was added to the solution. After precipitation of the final complex, the solution was filtered and the solid was washed with water to remove the excess NH_4PF_6.

Method b) *fac*-[Re(CO)$_3$NN#X]CF$_3$SO$_3$. To a solution of the appropriate *fac*-[Re(CO)$_3$NN#Br] complex (1.0 equiv.) in methanol under argon, $AgCF_3SO_3$ was added and refluxed for 8-12 h, then the solution was filtered to remove AgBr from the reaction mixture. The next step was performed by adding the monodentate ligand to a solution of *fac*-[Re(CO)$_3$NN#(CF$_3$SO$_3$)] in MeOH, then the reaction

mixture was refluxed under argon for 10 h, and finally filtered. The filtrate was evaporated and the yellow residue was purified over an alumina column using ethyl acetate: methanol (100:2-10%) as the mobile phase.

NN# ligand codes:

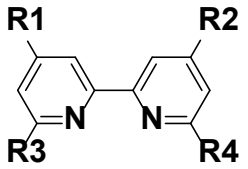

R1, R2 = ^{t}But; R4, R3 = H: **NN1**
R1, R2 = CO_2H; R4, R3 = H: **NN2**
R1, R2 = NEt_2; R4, R3 = H: **NN3**
R1, R2 = OCH_3; R4, R3 = H: **NN4**
R1, R2, R3 = H; R4 = CH_2Br: **NN5**
R1 = CCH; R2, R4, R3 = H: **NN8**
R1, R2 = CF_3; R4, R3 = H: **NN9**
R1, R2 = CH_3; R4, R3 = H: **NN10**
R1, R2 = Br; R4, R3 =H: **NN11**
R1, R2 = H; R4, R3 = CH_3: **NN13**

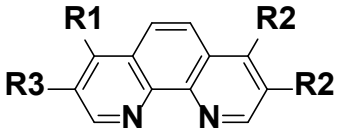

R1, R2 = phenyl; R4, R3 = H: **NN6**
R1, R2 = OH; R4, R3 = H: **NN7**
R1, R2, R4, R3 = CH_3: **NN12**

***fac*-[Re(CO)$_3$NN1L1]CF$_3$SO$_3$: (ReNN1L1).** Yellow solid, yield 86%, ESI-MS(m/z) calcd. for $C_{43}H_{40}F_3N_4O_8ReS$ (M^+) 867.26, found 867.20. IR (solid, νCO cm^{-1}): 2028, 1910. UV-Vis (CH_3CN, nm): 318, 340. ^{1}H NMR (400 MHz, acetonitrile-d_3) δ 9.08 (d, *J* = 5.99 Hz, 2H), 8.37 (d, *J* = 1.71 Hz, 2H), 8.12 - 8.19 (m, 2H), 7.86 (s, 1H), 7.77 (dd, *J* = 1.96, 5.99 Hz, 2H), 7.60 - 7.66 (m, 1H), 7.52 - 7.60 (m, 1H), 7.49 (d, *J* = 8.80 Hz, 2H), 7.33 - 7.38 (m, 2H), 7.30 (d, *J* = 6.72 Hz, 2H), 6.53 (d, *J* = 8.80 Hz, 2H), 5.33 - 5.43 (m, 1H), 4.39 (d, *J* = 5.99 Hz, 2H), 3.54 - 3.60 (m, 1H), 1.44 (s, 18H).

***fac*-[Re(CO)$_3$NN3L1]PF$_6$: (ReNN3L1).** Yellow-orange solid, yield 90%, ESI-MS(m/z) calcd. for $C_{42}H_{42}F_6N_6O_5ReP$ (M^+) 897.28, found 897.3. IR (solid, νCO cm^{-1}): 2019, 1893. UV-Vis (CH_3CN, nm): 299, 357. ^{1}H NMR (400 MHz, acetonitrile-d_3) δ 8.49 (d, *J* = 6.85 Hz, 2H), 8.22 (d, *J* = 6.60 Hz, 2H), 7.86 (s, 1H), 7.63 (d, *J* = 8.07 Hz, 1H), 7.56 (s, 1H), 7.50 (d, *J* = 8.68 Hz, 2H), 7.36 (s, 1H), 7.31 - 7.35 (m, 3H), 7.20 (d, *J* = 2.81 Hz, 2H), 6.78 (dd, *J* = 2.81, 6.85 Hz, 2H), 6.56 (d, *J* = 8.68 Hz, 2H), 5.36 - 5.44 (m, 1H), 4.43 (d, *J* = 6.36 Hz, 2H), 3.52 - 3.60 (m, 8H), 1.21 (t, *J* = 7.15 Hz, 12H).

***fac*-[Re(CO)$_3$NN4L1]CF$_3$SO$_3$: (ReNN4L1).** Yellow solid, yield 92%, ESI-MS(m/z) calcd. for $C_{37}H_{28}F_3N_4O_{10}ReS$ (M^+) 815.15, found 815.20. IR (solid, νCO cm^{-1}): 2035, 1916. UV-Vis (CH_3CN, nm): 306, 354. ^{1}H NMR (400 MHz, acetonitrile-d_3) δ 8.96 (d, *J* = 6.48 Hz, 2H), 8.13 - 8.17 (m, 2H), 7.87 (s, 1H), 7.85 (d, *J* = 2.69 Hz, 2H), 7.60 - 7.70 (m, 2H), 7.54 - 7.59 (m, 1H), 7.49 (s, 2H), 7.36 - 7.38 (m, 1H), 7.35 (s, 1H), 7.29 - 7.32 (m, 2H), 7.27 - 7.29 (m, 1H), 7.26 - 7.27 (m,

1H), 6.49 - 6.59 (m, 2H), 5.33 - 5.44 (m, 1H), 4.36 - 4.43 (m, 2H), 4.03 - 4.06 (m, 6H), 3.56 - 3.61 (m, 1H).

***fac*-[Re(CO)$_3$NN6L1]PF$_6$: (ReNN6L1).** Bright yellow solid, yield 90%, ESI-MS(m/z) calcd. for $C_{48}H_{32}F_6N_4O_5ReP$ (M^+) 931.19, found 931.25. IR (solid, νCO cm^{-1}): 2027, 1903. UV-Vis (CH_3CN, nm): 308, 350. ^{1}H NMR (400 MHz, acetonitrile-d$_3$) δ 9.64 (d, *J* = 5.38 Hz, 2H), 8.29 (d, *J* = 6.60 Hz, 2H), 8.11 (s, 2H), 8.07 (s, 1H), 8.06 (s, 1H), 7.81 (s, 1H), 7.67 (d, *J* = 1.96 Hz, 1H), 7.62 - 7.67 (m, 9H), 7.53 - 7.58 (m, 1H), 7.44 (d, *J* = 8.80 Hz, 2H), 7.36 (s, 2H), 7.24 - 7.27 (m, 2H), 6.48 (d, *J* = 8.80 Hz, 2H), 5.31 - 5.38 (m, 1H), 4.31 - 4.37 (m, 2H).

***fac*-[Re(CO)$_3$NN9L1]CF$_3$SO$_3$: (ReNN9L1).** Orange solid, yield 95%, ESI-MS(m/z) calcd. for $C_{37}H_{22}F_9N_4O_8ReS$ (M^+) 891.11, found 891.05. IR (solid, νCO cm^{-1}): 2038, 1923. UV-Vis (CH_3CN, nm): 293, 351. ^{1}H NMR (400 MHz, acetonitrile-d$_3$) δ 8.85 (s, 2H), 8.15 (d, *J* = 6.60 Hz, 2H), 8.09 - 8.13 (m, 2H), 7.86 (s, 1H), 7.61 - 7.66 (m, 1H), 7.53 - 7.59 (m, 1H), 7.49 (d, *J* = 8.80 Hz, 2H), 7.35 (d, *J* = 7.70 Hz, 2H), 7.31 (d, *J* = 6.48 Hz, 2H), 5.37 - 5.43 (m, 1H), 4.39 (d, *J* = 6.36 Hz, 2H).

***fac*-[Re(CO)$_3$NN10L1]PF$_6$: (ReNN10L1).** Pale yellow solid, yield 90%, ESI-MS(m/z) calcd. for $C_{36}H_{28}F_6N_4O_5ReP$ (M^+) 783.16, found 783.10. IR (solid, νCO cm^{-1}): 2026, 1900. UV-Vis (CH_3CN, nm): 260, 361. ^{1}H NMR (400 MHz, acetonitrile-d$_3$) δ 9.02 (d, *J* = 5.75 Hz, 2H), 8.25 (s, 2H), 8.13 - 8.18 (m, 2H), 7.87 (s, 1H), 7.62 - 7.66 (m, 1H), 7.60 (dd, *J* = 0.92, 5.69 Hz, 2H), 7.53 - 7.58 (m, 1H), 7.49 (d, *J* = 8.80 Hz, 2H), 7.35 (d, *J* = 7.58 Hz, 2H), 7.29 (d, *J* = 6.60 Hz, 2H), 6.53 (d, *J* = 8.80 Hz, 2H), 5.31 - 5.39 (m, 1H), 4.39 (d, *J* = 6.36 Hz, 2H), 2.56 (s, 6H).

***fac*-[Re(CO)$_3$NN11L1]PF$_6$: (ReNN11L1).** Orange solid, yield 88%, ESI-MS(m/z) calcd. for $C_{36}H_{22}Br_2F_6N_4O_5ReP$ (M^+) 910.95, found 911.04. IR (solid, νCO cm-1): 2028, 1905. UV-Vis (CH_3CN, nm): 289, 343. ^{1}H NMR (400 MHz, acetonitrile-d$_3$) δ 9.02 (d, *J* = 5.75 Hz, 2H), 8.25 (s, 2H), 8.13 - 8.18 (m, 2H), 7.87 (s, 1H), 7.62 - 7.66 (m, 1H), 7.60 (dd, *J* = 0.92, 5.69 Hz, 2H), 7.53 - 7.58 (m, 1H), 7.49 (d, *J* = 8.80 Hz, 2H), 7.35 (d, *J* = 7.58 Hz, 2H), 7.29 (d, *J* = 6.60 Hz, 2H), 6.53 (d, *J* = 8.80 Hz, 2H), 5.31 - 5.39 (m, 1H), 4.39 (d, *J* = 6.36 Hz, 2H), 2.56 (s, 6H).

***fac*-[Re(CO)$_3$NN12L1]PF$_6$: (ReNN12L1).** Yellow-orangish solid, yield 88%, ESI-MS(m/z) calcd. for $C_{40}H_{32}F_6N_4O_5ReP$ (M^+) 835.19, found 835.2. IR (solid, νCO cm^{-1}): 2027, 1908. UV-Vis (CH_3CN, nm): 281, 342. ^{1}H NMR (400 MHz, acetonitrile-d$_3$) δ 9.22 (s, 2H), 8.17 - 8.20 (m, 2H), 7.68 - 7.73 (m, 1H), 7.49 - 7.53 (m, 1H), 7.41 - 7.47 (m, 1H), 7.29 - 7.35 (m, 2H), 7.21 - 7.25 (m, 2H), 7.04 - 7.09 (m, 2H), 6.32 - 6.38 (m, 2H), 5.25 - 5.30 (m, 1H), 5.15 - 5.23 (m, 1H), 4.16 - 4.23 (m, 2H), 3.48 (s, 6H), 2.71 (s, 6H), 2.57 (s, 6H).

***fac*-[Re(CO)$_3$NN13L1]CF$_3$SO$_3$: (ReNN13L1).** Pale yellow solid, yield 93%, ESI-MS(m/z) calcd. for $C_{37}H_{28}F_3N_4O_8ReS$ (M^+) 783.16, found 783.10. IR (solid, νCO cm^{-1}): 2027, 1905. UV-Vis (CH_3CN, nm): 287, 340. ^{1}H NMR (400 MHz, acetonitrile-d$_3$) δ 7.25 (s, 2H), 7.18 - 7.18 (m, 0H), 7.06 (d, *J* = 6.60 Hz, 2H), 6.39 (d, *J* = 8.80 Hz, 2H), 5.23 - 5.34 (m, 1H), 4.26 (d, *J* = 6.36 Hz, 2H), 3.05 (s, 6H).

***fac*-[Re(CO)$_3$NN1L2]PF$_6$: (ReNN1L2).** Yellow solid, yield 90%, ESI-MS(m/z) calcd. for $C_{46}H_{43}ClF_6N_6O_6PRe$ (M^+) 997.25, found 997.2. IR (solid, νCO cm^{-1}): 2027, 1905. UV-Vis (CH_3CN, nm): 318, 344. ^{1}H NMR (400 MHz, acetonitrile-d$_3$) δ 8.91 (dd, *J* = 0.37, 5.99 Hz, 2H), 8.42 (d, *J* = 5.99 Hz, 2H), 8.38 (d, *J* = 1.83 Hz, 2H), 7.99 (s, 1H), 7.94 (s, 1H), 7.73 (s, 1H), 7.71 (s, 1H), 7.63 (d, *J* = 1.96 Hz, 1H), 7.62 (d, *J* = 1.96 Hz, 1H), 7.57 - 7.61 (m, 1H), 7.49 (s, 1H), 7.47 (s, 1H), 6.88 - 6.93 (m, 2H), 6.61 - 6.66 (m, 2H), 5.20 (s, 2H), 4.34 (s, 2H), 3.37 - 3.46 (m, 2H), 1.39 - 1.45 (m, 18H).

***fac*-[Re(CO)$_3$NN4L2]CF$_3$SO$_3$: (ReNN4L2).** Yellow-greenish solid, yield 85%, ESI-MS(m/z) calcd. for $C_{41}H_{31}ClF_3N_6O_{11}ReS$ (M^+) 945.14, found 945.2. IR (solid, νCO cm^{-1}): 2027, 1900. UV-Vis (CH_3CN, nm): 308, 342. ^{1}H NMR (400 MHz, acetonitrile-d$_3$) δ 8.96 (d, *J* = 6.48 Hz, 1H), 8.75 (d, *J* = 6.48 Hz, 1H), 8.43 - 8.46 (m, 1H), 8.19 - 8.22 (m, 1H), 8.00 (d, *J* = 1.34 Hz, 1H), 7.85 (d, *J* = 2.69 Hz, 1H), 7.79 (d, *J* = 2.57 Hz, 1H), 7.73 - 7.75 (m, 1H), 7.70 - 7.73 (m, 2H), 7.57 - 7.62 (m, 1H), 7.50 - 7.51 (m, 1H), 7.47 - 7.49 (m, 1H), 7.28 (s, 1H), 7.26 (d, *J* = 2.69 Hz, 1H), 7.06 - 7.09 (m, 2H), 6.91 - 6.94 (m, 2H), 6.70 - 6.73 (m, 1H), 5.56 (s, 1H), 5.22 (s, 1H), 4.33 - 4.38 (m, 2H), 4.05 (s, 3H), 4.04 (s, 3H), 3.41 (s, 1H), 3.20 (t, *J* = 6.42 Hz, 1H).

***fac*-[Re(CO)$_3$NN5L2]CF$_3$SO$_3$: (ReNN5L2).** Pale yellow solid, yield 80%, ESI-MS(m/z) calcd. for $C_{40}H_{28}BrClF_3N_6O_9ReS$ (M^+) 977.05, found 977.10. IR (solid, νCO cm^{-1}): 2022, 1899. UV-Vis (CH_3CN, nm): 329, 344. ^{1}H NMR (400 MHz, acetonitrile-d$_3$) δ 9.14 - 9.17 (m, 1H), 8.77 - 8.79 (m, 1H), 8.54 - 8.57 (m, 1H), 8.50 - 8.53 (m, 1H), 8.25 - 8.30 (m, 1H), 8.20 - 8.23 (m, 1H), 7.99 - 8.00 (m, 1H), 7.89 - 7.90 (m, 1H), 7.79 - 7.83 (m, 2H), 7.72 - 7.74 (m, 2H), 7.70 - 7.71 (m, 1H), 7.58 - 7.61 (m, 1H), 7.48 - 7.51 (m, 2H), 7.46 - 7.48 (m, 1H), 7.30 - 7.33 (m, 1H), 6.96 - 6.98 (m, 1H), 6.94 - 6.96 (m, 1H), 6.30 - 6.41 (m, 2H), 5.94 - 5.95 (m, 1H), 5.45 - 5.50 (m, 1H), 4.40 - 4.46 (m, 2H), 3.26 - 3.30 (m, 2H).

***fac*-[Re(CO)$_3$NN6L2]PF$_6$: (ReNN6L2).** Pale yellow solid, yield 95%, ESI-MS(m/z) calcd. For $C_{52}H_{35}ClF_6N_6O_6PRe$ (M^+) 1061.19, found 1061.10. IR (solid, νCO cm^{-1}): 2021, 1891. UV-Vis (CH_3CN, nm): 280, 323. ^{1}H NMR (400 MHz, acetonitrile-d$_3$) δ 9.48 (d, *J* = 5.38 Hz, 2H), 9.42 - 9.54 (m, 2H), 8.19 - 8.29 (m, 2H), 8.08 - 8.10 (m, 2H), 7.97 (s, 1H), 7.90 - 7.91 (m, 2H), 7.89

(s, 1H), 7.72 - 7.74 (m, 1H), 7.70 - 7.72 (m, 1H), 7.66 - 7.68 (m, 6H), 7.58 - 7.61 (m, 3H), 7.58 - 7.61 (m, 4H), 7.56 (d, *J* = 8.56 Hz, 1H), 7.50 - 7.51 (m, 1H), 7.48 - 7.49 (m, 1H), 6.86 (s, 1H), 6.83 (t, *J* = 2.87 Hz, 1H), 6.77 - 6.89 (m, 2H), 6.41 - 6.47 (m, 2H), 6.39 - 6.48 (m, 2H), 5.06 (s, 2H), 4.99 - 5.07 (m, 2H), 4.97 - 5.11 (m, 3H), 4.28 (t, *J* = 6.11 Hz, 3H), 4.22 - 4.33 (m, 2H), 3.49 (s, 2H), 3.42 - 3.52 (m, 2H).

***fac*-[Re(CO)$_3$NN8L2]PF$_6$: (ReNN8L2).** Yellow solid, 85%, ESI-MS(m/z) calcd. for $C_{40}H_{27}ClF_6N_6O_6PRe$ (M^+) 909.12, found 909.2. IR (solid, νCO cm^{-1}): 2029, 1910, UV-Vis (CH_3CN, nm): 298, 384. ^{1}H NMR (400 MHz, acetonitrile-d_3) δ 8.99 - 9.02 (m, 1H), 8.94 - 8.98 (m, 1H), 8.46 (d, *J* = 5.99 Hz, 2H), 8.44 (s, 1H), 8.35 - 8.38 (m, 1H), 8.18 - 8.23 (m, 1H), 8.01 (s, 1H), 7.91 (s, 1H), 7.73 (d, *J* = 8.56 Hz, 2H), 7.62 (s, 2H), 7.59 - 7.61 (m, 1H), 7.50 (d, *J* = 8.56 Hz, 2H), 6.94 (s, 2H), 6.67 (d, *J* = 5.99 Hz, 2H), 5.16 (s, 2H), 4.33 - 4.37 (m, 1H), 4.16 (s, 1H), 3.59 - 3.62 (m, 1H), 3.41 (s, 2H).

***fac*-[Re(CO)$_3$NN9L2]PF$_6$: (ReNN9L2).** Orange solid, yield 90%, ESI-MS(m/z) calcd. for $C_{40}H_{25}ClF_{12}N_6O_6PRe$ (M^+) 1021.10, found 1021.12. IR (solid, νCO cm^{-1}): 2034, 1913. UV-Vis (CH_3CN, nm): 329, 364. ^{1}H NMR (400 MHz, acetonitrile-d_3) δ 9.43 - 9.48 (m, 1H), 9.22 - 9.26 (m, 1H), 8.79 - 8.86 (m, 2H), 8.38 - 8.43 (m, 1H), 8.17 - 8.22 (m, 1H), 8.07 - 8.13 (m, 1H), 7.99 - 8.02 (m, 1H), 7.91 - 7.95 (m, 1H), 7.70 - 7.75 (m, 2H), 7.57 - 7.63 (m, 1H), 7.51 (s, 2H), 7.06 - 7.12 (m, 1H), 6.91 - 6.97 (m, 1H), 6.62 - 6.66 (m, 1H), 5.52 - 5.57 (m, 1H), 5.13 - 5.18 (m, 1H), 4.37 - 4.43 (m, 1H), 4.37 - 4.44 (m, 1H), 4.36 - 4.37 (m, 1H), 3.46 - 3.46 (m, 1H), 3.22 - 3.22 (m, 1H).

***fac*-[Re(CO)$_3$NN11L2]PF$_6$: (ReNN11L2).** Pale yellow solid, yield 95%, ESI-MS(m/z) calcd. for $C_{38}H_{25}Br_2ClF_6N_6O_6PRe$ (M^+) 1040.94, found 1041.0. IR (solid, νCO cm^{-1}): 2031, 1917. UV-Vis (CH_3CN, nm): 330, 346. ^{1}H NMR (400 MHz, acetonitrile-d_3) δ 8.99 - 9.02 (m, 1H), 8.79 (d, *J* = 5.99 Hz, 1H), 8.64 (s, 1H), 8.60 (d, *J* = 1.96 Hz, 1H), 8.48 - 8.51 (m, 1H), 8.17 - 8.20 (m, 1H), 8.01 (s, 2H), 7.92 - 7.94 (m, 1H), 7.79 - 7.83 (m, 1H), 7.74 (s, 1H), 7.72 (s, 1H), 7.58 - 7.63 (m, 1H), 7.50 (d, *J* = 8.68 Hz, 2H), 7.07 - 7.11 (m, 1H), 6.93 (d, *J* = 8.56 Hz, 2H), 6.68 - 6.71 (m, 1H), 5.56 (s, 1H), 5.20 (s, 1H), 4.37 (s, 2H), 3.38 - 3.44 (m, 1H), 3.17 - 3.23 (m, 1H).

***fac*-[Re(CO)$_3$NN13L2]CF$_3$SO$_3$: (ReNN13L2).** Pale yellow solid, yield 90%, ESI-MS(m/z) calcd. for $C_{41}H_{31}ClF_3N_6O_9ReS$ (M^+) 913.16, found 913.0. IR (solid, νCO cm^{-1}): 2025, 1901. UV-Vis (CH_3CN, nm): 320, 334. 1H NMR (400 MHz, acetonitrile-d3) Shift 8.52 - 8.55 (m, 1H), 8.17 (d, J = 8.07 Hz, 1H), 8.03 - 8.08 (m, 2H), 8.01 (d, J = 2.69 Hz, 1H), 8.00 (d, J = 1.59 Hz, 1H), 7.94 (d, J = 7.70 Hz, 1H), 7.89 - 7.92 (m, 1H), 7.74 (d, J = 2.32 Hz, 1H), 7.72 (d, J = 3.06 Hz, 1H), 7.59 (d, J = 4.40 Hz, 1H), 7.57

(d, J = 3.79 Hz, 1H), 7.50 (d, J = 2.08 Hz, 1H), 7.47 - 7.49 (m, 1H), 6.97 (d, J = 6.24 Hz, 1H), 6.91 - 6.94 (m, 1H), 6.86 - 6.89 (m, 1H), 6.81 (d, J = 5.99 Hz, 1H), 5.25 (s, 1H), 4.36 (t, J = 6.42 Hz, 1H), 4.11 (t, J = 6.05 Hz, 1H), 3.18 - 3.22 (m, 1H), 3.14 (s, 2H), 3.08 (s, 3H), 2.93 (s, 3H), 2.76 - 2.80 (m, 1H).

***fac*-[Re(CO)$_3$NN1py]CF$_3$SO$_3$: (ReNN1py).** Yellow solid, yield 90%, ESI-MS(m/z) calcd. for $C_{27}H_{29}F_3N_3O_6ReS$ (M^+) 618.18, found 618.2. IR (solid, νCO cm^{-1}): 2026, 1899. UV-Vis (CH_3CN, nm): 319, 354. ^{1}H NMR (400 MHz, acetonitrile-d_3) δ 9.00 (d, *J* = 5.50 Hz, 2H), 8.51 (br. s., 2H), 8.36 (d, *J* = 8.19 Hz, 2H), 8.20 (dt, *J* = 1.34, 7.95 Hz, 2H), 7.91 - 8.04 (m, 2H), 7.68 - 7.77 (m, 2H), 7.56 - 7.65 (m, 3H), 7.45 - 7.53 (m, 2H), 6.88 - 6.97 (m, 2H), 6.71 (br. s., 2H), 5.15 (s, 2H), 4.36 (t, *J* = 6.05 Hz, 2H), 3.41 (t, *J* = 5.99 Hz, 2H).

***fac*-[Re(CO)$_3$NN3py]CF$_3$SO$_3$: (ReNN3py).** Pale yellow solid, yield 93%, ESI-MS(m/z) calcd. for $C_{27}H_{31}F_3N_5O_6ReS$ (M^+) 648.20, found 648.25. IR (solid, νCO cm^{-1}): 2029, 1912. UV-Vis (CH_3CN, nm): 271, 366. ^{1}H NMR (400 MHz, acetonitrile-d_3) δ 9.00 (d, *J* = 5.50 Hz, 2H), 8.51 (br. s., 2H), 8.36 (d, *J* = 8.19 Hz, 2H), 8.20 (dt, *J* = 1.34, 7.95 Hz, 2H), 7.91 - 8.04 (m, 2H), 7.68 - 7.77 (m, 2H), 7.56 - 7.65 (m, 3H), 7.45 - 7.53 (m, 2H), 6.88 - 6.97 (m, 2H), 6.71 (br. s., 2H), 5.15 (s, 2H), 4.36 (t, *J* = 6.05 Hz, 2H), 3.41 (t, *J* = 5.99 Hz, 2H).

***fac*-[Re(CO)$_3$NN4py]CF$_3$SO$_3$: (ReNN4py).** Pale yellow solid, yield 85%, ESI-MS(m/z) calcd. for $C_{21}H_{17}F_3N_3O_8ReS$ (M^+) 566.07, found 566.1. IR (solid, νCO cm^{-1}): 2023, 1878. UV-Vis (CH_3CN, nm): 255, 350. ^{1}H NMR (400 MHz, acetonitrile-d_3) δ 8.99 (d, *J* = 6.48 Hz, 2H), 8.25 - 8.28 (m, 2H), 7.88 - 7.93 (m, 1H), 7.86 (d, *J* = 2.69 Hz, 2H), 7.33 - 7.37 (m, 2H), 7.30 (dd, *J* = 2.69, 6.60 Hz, 2H), 4.07 (s, 6H).

***fac*-[Re(CO)$_3$NN5py]CF$_3$SO$_3$: (ReNN5py).** Pale yellow solid, yield 73%, ESI-MS(m/z) calcd. for $C_{20}H_{14}BrF_3N_3O_6ReS$ (M^+) 597.98, found 598.0. IR (solid, νCO cm^{-1}): 2027, 1901. UV-Vis (CH_3CN, nm): 274, 345. ^{1}H NMR (400 MHz, acetonitrile-d_3) δ 8.52 - 8.57 (m, 2H), 8.39 - 8.42 (m, 1H), 8.12 (s, 1H), 8.09 (d, *J* = 5.38 Hz, 1H), 7.66 - 7.68 (m, 4H), 7.55 - 7.60 (m, 2H), 7.28 - 7.32 (m, 1H), 1.96 - 1.98 (m, 2H).

***fac*-[Re(CO)$_3$NN6py]CF$_3$SO$_3$: (ReNN6py).** Yellow-brownish solid, yield 90%, ESI-MS(m/z) calcd. for $C_{33}H_{21}F_3N_3O_6ReS$ (M^+) 682.11, found 682.15. IR (solid, νCO cm^{-1}): 2027, 1902. UV-Vis (CH_3CN, nm): 293, 332. ^{1}H NMR (400 MHz, acetonitrile-d_3) δ 9.67 (d, *J* = 5.38 Hz, 2H), 8.39 - 8.42 (m, 2H), 8.11 - 8.13 (m, 2H), 8.09 (d, *J* = 5.38 Hz, 2H), 7.84 (tt, *J* = 1.53, 7.70 Hz, 1H), 7.64 - 7.70 (m, 10H), 7.27 - 7.32 (m, 2H).

***fac*-[Re(CO)$_3$NN8py]CF$_3$SO$_3$: (ReNN8py).** Brown solid, yield 85%, ESI-MS(m/z) calcd. for $C_{21}H_{13}F_3N_3O_6ReS$ (M^+) 530.05, found 530.0. IR (solid, νCO cm^{-1}): 2032, 1916. UV-Vis (CH_3CN,

nm): 315, 380. ^{1}H NMR (400 MHz, acetonitrile-d_3) δ 9.19 - 9.26 (m, 1H), 8.37 - 8.45 (m, 1H), 8.23 - 8.32 (m, 4H), 7.86 - 7.91 (m, 1H), 7.76 - 7.84 (m, 2H), 7.30 - 7.37 (m, 3H), 3.62 - 3.66 (m, 1H).

***fac*-[Re(CO)$_3$NN9py]CF$_3$SO$_3$: (ReNN9py).** Orange solid, yield 90%, ESI-MS(m/z) calcd. for $C_{21}H_{11}F_9N_3O_6ReS$ (M^+) 642.03, found 642.1. IR (solid, νCO cm^{-1}): 2034, 1911. UV-Vis (CH_3CN, nm): 292, 328. ^{1}H NMR (400 MHz, acetonitrile-d_3) δ 9.49 (d, *J* = 5.87 Hz, 2H), 8.83 (d, *J* = 0.73 Hz, 2H), 8.24 - 8.27 (m, 2H), 8.13 (dd, *J* = 1.34, 5.75 Hz, 2H), 7.91 (tt, *J* = 1.51, 7.72 Hz, 1H), 7.33 - 7.38 (m, 2H).

***fac*-[Re(CO)$_3$NN10py]CF$_3$SO$_3$: (ReNN10py).** Pale yellow solid, yield 93%, ESI-MS(m/z) calcd. for $C_{21}H_{17}F_3N_3O_6ReS$ (M^+) 534.09, found 534.1. IR (solid, νCO cm^{-1}): 2028, 1915. UV-Vis (CH_3CN, nm): 308, 355. ^{1}H NMR (400 MHz, acetonitrile-d_3) δ 9.00 (d, *J* = 5.50 Hz, 2H), 8.51 (br. s., 2H), 8.36 (d, *J* = 8.19 Hz, 2H), 8.20 (dt, *J* = 1.34, 7.95 Hz, 2H), 7.91 - 8.04 (m, 2H), 7.68 - 7.77 (m, 2H), 7.56 - 7.65 (m, 3H), 7.45 - 7.53 (m, 2H), 6.88 - 6.97 (m, 2H), 6.71 (br. s., 2H), 5.15 (s, 2H), 4.36 (t, *J* = 6.05 Hz, 2H), 3.41 (t, *J* = 5.99 Hz, 2H).

***fac*-[Re(CO)$_3$NN11py]CF$_3$SO$_3$: (ReNN11py).** Yellow-orangish solid, yield 85%, ESI-MS(m/z) calcd. for $C_{19}H_{11}Br_2F_3N_3O_6ReS$ (M^+) 661.88, found 662.0. IR (solid, νCO cm^{-1}): 2020, 1898. UV-Vis (CH_3CN, nm): 287, 367. ^{1}H NMR (400 MHz, acetonitrile-d_3) δ 9.04 (d, *J* = 5.99 Hz, 2H), 8.64 - 8.67 (m, 2H), 8.23 - 8.26 (m, 2H), 8.03 (d, *J* = 2.08 Hz, 1H), 8.01 (d, *J* = 2.08 Hz, 1H), 7.91 (tt, *J* = 1.53, 7.70 Hz, 1H), 7.34 - 7.38 (m, 2H).

***fac*-[Re(CO)$_3$NN12py]CF$_3$SO$_3$: (ReNN12py).** Pale yellow solid, yield 90%, ESI-MS(m/z) calcd. for $C_{25}H_{21}F_3N_3O_6ReS$ (M^+) 586.11, found 586.09. IR (solid, νCO cm^{-1}): 2027, 1903. UV-Vis (CH_3CN, nm): 283, 375. ^{1}H NMR (400 MHz, acetonitrile-d_3) δ 9.36 (s, 2H), 8.34 (dd, *J* = 1.47, 6.48 Hz, 2H), 8.31 (s, 2H), 7.78 (tt, *J* = 1.53, 7.70 Hz, 1H), 7.19 - 7.26 (m, 2H), 2.84 (s, 6H), 2.70 (s, 6H).

***fac*-[Re(CO)$_3$NN13py]CF$_3$SO$_3$: (ReNN13py).** Yellow solid, yield 85%, ESI-MS(m/z) calcd. for $C_{21}H_{17}F_3N_3O_6ReS$ (M^+) 534.09, found 534.10. IR (solid, νCO cm^{-1}): 2024, 1909. UV-Vis (CH_3CN, nm): 318, 333. ^{1}H NMR (400 MHz, acetonitrile-d_3) δ 8.36 (d, *J* = 7.95 Hz, 2H), 8.11 (t, *J* = 7.82 Hz, 2H), 7.95 (d, *J* = 5.01 Hz, 2H), 7.87 (t, *J* = 7.70 Hz, 1H), 7.82 (d, *J* = 7.70 Hz, 2H), 7.28 (dd, *J* = 6.60, 7.46 Hz, 2H), 3.10 - 3.17 (m, 5H), 3.09 - 3.17 (m, 6H).

***fac*-Re(CO)$_3$NN1Im: (ReNN1Im).** Yellow-greenish solid, yield 95%, ESI-MS(m/z) calcd. for $C_{37}H_{27}ClN_7O_6Re$ 606.1, found 606.15. IR (solid, νCO cm-1): 2013, 1880. UV-Vis (CH_3CN, nm): 291, 362. ^{1}H NMR (400 MHz, acetonitrile-d_3) δ 9.03 (dd, *J* = 0.43, 5.93 Hz, 2H), 8.39 (d, *J* =

1.71 Hz, 2H), 7.71 (dd, *J* = 1.96, 5.87 Hz, 2H), 7.20 (s, 1H), 7.03 (d, *J* = 0.61 Hz, 1H), 6.79 - 6.82 (m, 1H), 6.44 (s, 1H), 1.46 (s, 18H).

***fac*-Re(CO)$_3$NN3Im: (ReNN3Im).** Light green solid, yield 85%, ESI-MS(m/z) calcd. for $C_{24}H_{29}N_6O_3Re$ 636.1, found 636.0. IR (solid, νCO cm^{-1}): 2013, 1878. UV-Vis (CH_3CN, nm): 270, 298. ^{1}H NMR (400 MHz, acetonitrile-d$_3$) δ 8.44 (d, *J* = 6.85 Hz, 2H), 7.37 - 7.39 (m, 1H), 7.38 (s, 1H), 7.26 (d, *J* = 2.81 Hz, 2H), 7.03 (d, *J* = 0.61 Hz, 1H), 6.92 (s, 1H), 6.74 (dd, *J* = 2.81, 6.85 Hz, 2H), 6.58 (t, *J* = 1.22 Hz, 1H).

***fac*-Re(CO)$_3$NN4Im: (ReNN4Im).** Green solid, yield 88%, ESI-MS(m/z) calcd. for $C_{18}H_{15}N_4O_5Re$ 554.0, found 554.1. IR (solid, νCO cm^{-1}): 2015, 1872. UV-Vis (CH_3CN, nm): 264, 305. ^{1}H NMR (400 MHz, acetonitrile-d$_3$) δ 8.91 (d, *J* = 6.48 Hz, 2H), 7.86 (d, *J* = 2.69 Hz, 2H), 7.19 (d, *J* = 2.69 Hz, 1H), 7.18 (d, *J* = 2.69 Hz, 1H), 6.81 (s, 1H), 6.60 (s, 1H), 6.32 (s, 1H), 4.05 (s, 6H).

***fac*-Re(CO)$_3$NN5Im: (ReNN5Im).** Pale green solid, yield 80%, ESI-MS(m/z) calcd. for $C_{17}H_{12}BrN_4O_5$ Re 586.5, found 586.6. IR (solid, νCO cm^{-1}): 2025, 1901. UV-Vis (CH_3CN, nm): 318, 327.5. ^{1}H NMR (400 MHz, acetonitrile-d$_3$) δ 9.21 - 9.24 (m, 1H), 8.36 (d, *J* = 8.31 Hz, 1H), 8.27 (s, 1H), 8.18 - 8.23 (m, 2H), 7.95 (s, 1H), 7.67 - 7.71 (m, 1H), 6.64 (s, 1H), 6.55 (s, 1H), 6.16 (s, 1H), 3.61 (s, 2H).

***fac*-Re(CO)$_3$NN6Im: (ReNN6Im).** Light green solid, yield 88%, ESI-MS(m/z) calcd. for $C_{30}H_{19}N_4O_3Re$ 670.10, found 670.05. IR (solid, νCO cm^{-1}): 2018, 1890. UV-Vis (CH_3CN, nm): 290.5. ^{1}H NMR (400 MHz, acetonitrile-d$_3$) δ 9.49 (d, *J* = 5.38 Hz, 2H), 7.99 (s, 2H), 7.87 (d, *J* = 5.38 Hz, 2H), 7.56 (s, 10H), 6.85 (s, 1H), 6.48 (s, 1H), 6.29 (s, 1H).

***fac*-Re(CO)$_3$NN10Im: (ReNN10Im).** Green solid, yield 93%, ESI-MS(m/z) calcd. for $C_{18}H_{15}N_4O_3Re$ 522.07, found 522.10. IR (solid, νCO cm^{-1}): 2014, 1889. UV-Vis (CH_3CN, nm): 288, 371. ^{1}H NMR (400 MHz, acetonitrile-d$_3$) δ 8.98 (d, *J* = 5.75 Hz, 2H), 8.20 - 8.26 (m, 2H), 7.45 - 7.56 (m, 2H), 6.74 (s, 1H), 6.55 (t, *J* = 0.79 Hz, 1H), 6.27 (t, *J* = 0.92 Hz, 1H), 2.52 - 2.58 (m, 6H).

***fac*-Re(CO)$_3$NN12Im: (ReNN12Im).** Light green solid, yield 90%, ESI-MS(m/z) calcd. for $C_{37}H_{27}ClN_7O_6Re$ 574.10, found 573.90. IR (solid, νCO cm^{-1}): 2012, 1893. UV-Vis (CH_3CN, nm): 322.5. ^{1}H NMR (400 MHz, acetonitrile-d$_3$) δ 9.28 (s, 2H), 8.28 (s, 2H), 6.78 (s, 1H), 6.46 (s, 1H), 6.25 (t, *J* = 0.98 Hz, 1H), 2.82 (s, 6H), 2.63 - 2.66 (m, 6H).

***fac*-Re(CO)$_3$NN13Im: (ReNN13Im).** Pale yellow-greenish solid, yield 90%, ESI-MS(m/z) calcd. for $C_{18}H_{15}N_4O_3Re$ 522.0, found 522.09. IR (solid, νCO cm^{-1}): 2014, 1877. UV-Vis (CH_3CN, nm): 298,

384. ^{1}H NMR (400 MHz, acetonitrile-d_3) δ 8.00 - 8.08 (m, 4H), 7.67 (dd, *J* = 1.71, 7.09 Hz, 2H), 6.84 (d, *J* = 0.49 Hz, 1H), 6.72 (s, 1H), 6.15 (s, 1H), 3.11 (s, 6H).

***fac*-Re(CO)$_3$NN1BzIm: (ReNN1BzIm).** Bright yellow solid, yield 90%, ESI-MS(m/z) calcd. for $C_{28}H_{29}N_4O_3Re$ 656.1, found 657.0. IR (solid, νCO cm^{-1}): 2018, 1887. UV-Vis (CH_3CN, nm): 279. ^{1}H NMR (400 MHz, acetonitrile-d_3) δ 9.14 (d, *J* = 5.99 Hz, 2H), 8.38 (d, *J* = 1.59 Hz, 2H), 7.69 (d, *J* = 1.96 Hz, 1H), 7.68 (d, *J* = 1.83 Hz, 1H), 7.60 - 7.64 (m, 1H), 7.39 - 7.43 (m, 1H), 7.24 - 7.27 (m, 1H), 7.01 - 7.06 (m, 1H), 6.94 - 6.99 (m, 1H), 6.92 (s, 1H), 1.43 (s, 18H).

***fac*-Re(CO)$_3$NN6BzIm: (ReNN6BzIm).** Yellow-greenish solid, yield 95%, ESI-MS(m/z) calcd. for $C_{34}H_{21}N_4O_3Re$ 719.2, found 719.0. IR (solid, νCO cm^{-1}): 2018, 1894. UV-Vis (CH_3CN, nm): 283. ^{1}H NMR (400 MHz, acetonitrile-d_3) δ 9.00 (d, *J* = 5.50 Hz, 2H), 8.51 (br. s., 2H), 8.36 (d, *J* = 8.19 Hz, 2H), 8.20 (dt, *J* = 1.34, 7.95 Hz, 2H), 7.91 - 8.04 (m, 2H), 7.68 - 7.77 (m, 2H), 7.56 - 7.65 (m, 3H), 7.45 - 7.53 (m, 2H), 6.88 - 6.97 (m, 2H), 6.71 (br. s., 2H), 5.15 (s, 2H), 4.36 (t, *J* = 6.05 Hz, 2H), 3.41 (t, *J* = 5.99 Hz, 2H).

***fac*-Re(CO)$_3$NN10BzIm: (ReNN10BzIm).** Dark green solid, yield 90%, ESI-MS(m/z) calcd. for $C_{22}H_{17}N_4O_3Re$ 571.6, found 571.5. IR (solid, νCO cm^{-1}): 2016, 1892. UV-Vis (CH_3CN, nm): 274. ^{1}H NMR (400 MHz, acetonitrile-d_3) δ 9.11 (d, *J* = 5.62 Hz, 2H), 8.19 (s, 2H), 8.16 (s, 1H), 8.03 (s, 1H), 7.66 (dd, *J* = 0.67, 7.64 Hz, 1H), 7.59 - 7.62 (m, 1H), 7.50 - 7.53 (m, 1H), 7.48 (dd, *J* = 0.92, 5.69 Hz, 2H), 7.36 (s, 0H), 7.35 - 7.39 (m, 1H), 7.23 - 7.26 (m, 1H), 7.00 (dt, *J* = 1.28, 7.55 Hz, 1H), 6.94 (dd, *J* = 1.10, 7.82 Hz, 1H), 6.92 (s, 1H), 2.46 - 2.54 (m, 6H).

***fac*-Re(CO)$_3$NN12BzIm: (ReNN12BzIm).** Bright yellow solid, yield 85%, ESI-MS(m/z) calcd. for $C_{28}H_{21}N_4O_3Re$ 624.12, found 624.05. IR (solid, νCO cm^{-1}): 2013, 1895**.** UV-Vis (CH_3CN, nm): 281.5. ^{1}H NMR (400 MHz, DMSO-d_6) δ 9.44 - 9.46 (m, 2H), 8.38 - 8.40 (m, 2H), 7.68 - 7.72 (m, 1H), 7.23 - 7.25 (m, 1H), 6.91 - 6.98 (m, 1H), 6.79 - 6.84 (m, 1H), 6.59 - 6.61 (m, 1H), 2.80 - 2.82 (m, 6H), 2.64 - 2.66 (m, 6H).

***fac*-Re(CO)$_3$NN13BzIm: (ReNN13BzIm).** Yellow-greenish solid, yield 88%, ESI-MS(m/z) calcd. for $C_{22}H_{17}N_4O_3Re$ 572.09, found 572.0. IR (solid, νCO cm^{-1}): 2016, 1891. UV-Vis (CH_3CN, nm): 270.5, 322. ^{1}H NMR (400 MHz, methanol-d_4) δ 7.91 - 7.95 (m, 2H), 7.83 - 7.89 (m, 2H), 7.56 - 7.60 (m, 2H), 7.23 - 7.27 (m, 1H), 6.87 - 6.90 (m, 1H), 6.79 - 6.84 (m, 1H), 6.72 - 6.78 (m, 1H), 6.62 - 6.64 (m, 1H), 3.07 (s, 5H), 3.06 - 3.08 (m, 6H).

Strains and culture conditions. *Staphylococcus aureus* MRSA43300 (methicillin-resistant), *S. aureus* ATCC25923 (methicillin-sensitive), *Candida albicans* SC5314, *C. glabrata, C. kruzei* and *C. parapsilosis* were obtained from the American Type Culture Collection (ATCC).

Prior to each experiment, frozen stocks in 20% glycerol at -80 °C were thawed and inoculated onto solid Yeast-Potato Dextose (YPD) plates (fungi) or Brain-Heart Infusion (BHI) agar plates (bacteria), and cultured at 37 °C for 24-48 h.

***In vitro* antimicrobial activity determination.** Antimicrobial activity was addressed by determining the minimum inhibitory concentration (MIC) of the tested complexes according to the standard broth microdilution assays, recommended by CLSI (the Clinical and Laboratory Standards Institute; M07-A10. CLSI) and EUCAST (European Committee on Antimicrobial Susceptibility Testing; EUCAST antifungal MIC method for yeasts, v 7.3.1). The test strains grown in YPD (fungi) and BHI (bacteria) agar media were diluted in RPMI 1640 medium with 2% glucose (Gibco) and Luria-Bertani broth (Biolife Italiana S.r.l., Milano, Italy) to give the concentration of $5x10^5$ CFU/mL (for bacteria) and $1x10^5$ CFU/mL cells (for fungi), respectively. The MIC assay was performed in 96-well microtiter plates by making serial twofold dilutions of the tested substances in appropriate liquid media to give the volume of 100 µL. The media solution with microorganisms was dispensed to each well to make the final volume of 200 µL. All complexes were tested in the concentrations range from 0.78 to 50 µM. After incubation at 37 C for 18-24 h without shaking, the growth of tested microorganisms was determined measuring absorbance at 530 nm (*Candida*) and 600 nm (*Staphylococcus*) using a Tecan Infinite 200 Pro multiplate reader (Tecan Group Ltd., Männedorf, Switzerland). The negative control (media only) and positive control (only microorganisms) on the same plate were used as references to determine the growth inhibition. Samples with inhibition values above 90% were classified as active agents.

***In vivo* toxicity assessment.** Toxicity evaluation of Re(I) tricarbonyl complexes was carried in the zebrafish (*Danio rerio*) model according to previously published procedure following the general rules of the OECD Guidelines for the Testing of Chemicals (OECD, 2013, Test No. 236). All experiments involving zebrafish were performed in compliance with the European directive 2010/63/EU and the ethical guidelines of the Guide for Care and Use of Laboratory Animals of the Institute of Molecular Genetics and Genetic Engineering, University of Belgrade. Wild type (AB) zebrafish were kindly provided by Dr Ana Cvejić (Wellcome Trust Sanger Institute, Cambridge, UK), raised to adult stage in a temperature- and light-controlled zebrafish facility at 28 °C and standard 14:10-hour light-dark photoperiod, and regularly fed with commercially dry food (SDS300 granular food; Special Diet Services, Essex; UK and TetraMin^{TM} flakes; Tetra Melle, Germany) twice a day and A*rtemia nauplii* once daily. Embryos produced by pair-wise mating were collected and distributed into 24-well plates

containing 10 embryos per well and 1 mL E3 medium (5 mM NaCl, 0.17 mM KCl, 0.33 mM $CaCl_2$ and 0.33 mM $MgSO_4$ in distilled water) and raised at 28 °C. For assessing acute (lethality) and developmental (teratogenicity) toxicity, the embryos at 6 hours post fertilization (hpf) stage were treated with eight different concentrations of the tested compounds (50, 40, 25, 12.5, 6.25, 3.12, 1.56 and 0.78 μM), and inspected for apical endpoints (Table S1) every day by 120 hpf upon an steremicroscope (Carl Zeiss™ Stemi 508 doc Stereomicroscope, Germany). Dead embryos were recorded and discarded every 24 h DMSO (0.25%) was used as negative control. Experiments were performed three times using 20 embryos per concentration. At 120 hpf, embryos have been inspected for the heartbeat rate, anesthetized by addition of 0.1% (w/v) tricaine solution (Sigma-Aldrich, St. Louis, MO), photographed and killed by freezing at -20 °C for ≥ 24 h.

In addition to developmental toxicity, antimicrobial Re(I) tricarbonyl complexes with the best therapeutic profile, ReNN1Py, ReNN3Py, ReNN6Py, ReNN1L1, ReNN9L2 and ReNN6BzIm, have been selected and evaluated for the hepatoxicity in transgenic *Tg(-2.8fabp10a*:EGFP) zebrafish embryos with the fluorescently labeled liver.[2] Embryos were exposed to the non-toxic doses of each selected complex from 72 hpf (a stage when the liver is fully functional, vascularized and started metabolic transformation of absorbed compounds) to 120 hpf, and evaluated for the hepatotoxicity endpoints by fluorescent microscopy. The liver toxicity was assessed in relation to the control group according to the liver area index (the ration between liver area and embryonic lateral area x 100%), the liver color and the yolk retention,[3] that proved to accurately represent the liver damages. Experiment was performed two times using 10 embryos per concentration. The liver area index was determined by ImageJ program. In all mentioned toxicity assays, itraconazole and erythromycin (Sigma Aldrich), clinically approved antifungal and antibiotic, respectively, were used as the control.

***In vitro* toxicity assessment – blood hemolysis evaluation.**

In order evaluate the potential cytotoxicity of the tested Re tricarbonyl complexes towards the blood erythrocytes, we determined their hemolytic activity on the sheep erythrocytes. Hemolysis assays were performed following previously reported protocols with some minor modifications.[4] Briefly, sheep blood erythrocytes (RBCs) were collected by centrifugation at 2200 x g for 5 min and washed with sterile PBS (pH 7.4) at least three times until clear supernatant was obtained. The hemolytic activity was tested in 96-well plates containing 100 μL of 8% RBCs suspension in PBS (4% final) and 100 μL of 12.5 μM complexes in PBS (6.25

μM final). Plates were incubated at 37 °C for 3 h. Amphotericin B and PBS (RPMI) were used as a positive and a negative control, respectively. Plates were then centrifuged at 2200 rpm for 5 min, and 100 μL of the supernatant was transferred into a new plate. Absorbance was measured at 490 nm using a Tecan Infinite 200 Promultiplate reader (Tecan Group Ltd., Männedorf, Switzerland). The percentage of hemolysis was determined in relation to the hemolysis rate of negative control.

Antimicrobial efficacy of Re complexes *in vivo.*

To examine the selected rhenium complexes for antimicrobial efficacy *in vivo*, wild type zebrafish embryos were challenged to *C. albicans* and *S. aureus* infections. Anti-staphylococcal activity was evaluated using the zebrafish - *S. aureus* MRSA43300 model of systemic infection following the protocol of Prajsnar,[1, 5] while the efficacy against *C. albicans* infection was assayed using the zebrafish model of lethal disseminated candidiasis, according to the previously established procedure.[6, 7]

The *S. aureus*-zebrafish model of systemic infection

S. aureus culture and preparation of the cells for microinjection. Briefly, the overnight bacterial culture grown in BHI broth were diluted at 1:500 ration and incubated at 37 °C with shaking to reach a mid of exponential phase (OD_{600} 0.6-0.7). After centrifugation at 4500 × *g* for 10 min (Centrifuge 5415D, Eppendorf, Hamburg, Germany), bacterial pellet was washed three times in sterile PBS. Bacterial cells were than labelled with 2 μM CellTracker™ RedCMTPX (Thermofisher Scientific) according to the manufacturer's instructions. To prepare bacterial inoculum for injection, the bacterial pellet was centrifuged 4500 × *g* for 10 min, washed three times in PBS and resuspended in 3% polyvinyl-pyrrolidone (PVP) to achieve a final concentration of 5×10^8 cells/mL.

Infection of zebrafish embryos. Prior to infection, embryos were manually dechorionated at 24 hpf stage and keep at 28 °C. Aiming to establish a fast systemic infection, 30-hpf dechorionated embryos were anesthetized with 200 μg/mL of tricaine (MS-222) solution and microinjected with 5 nL containing 1500-1600 labelled-MRSA cells into the circulation valley by a pneumatic picopump (PV820, World Precision Instruments, USA). To confirm the number of injected bacteria, a few infected embryos was crashed and the viable counts was determined on BHI agar plates after incubation at 37 °C for 2 days. Injected embryos were allowed to recover for 2 h at 28 °C, dead embryos were discarded, and then alive embryos were transferred

into 24-well plates containing 1 mL of E3 medium and 10 embryos per well. The infected embryos were treated with three doses (½ × MIC, 1 × MIC and 2× MIC) of the selected complex, and maintained at 31 °C by 120 hpf. Linezolid was used as a positive control. The embryos injected with 3% PVP and non-injected embryos served as the negative control groups. Twenty embryos were used per concentration, and experiment was performed two times. The survival and development of MRSA-infected embryos was recorded every day until 120 hpf (corresponding to fourth days post infection). Anti-staphylococcal efficacy of applied complexes was determined according to the survival rate of treated embryos in relation to those in the untreated group, while the effect on infection eradication was followed in real time by fluorescence microscopy.

The zebrafish model of lethal disseminated candidiasis

C. albicans culture and preparation of the cells for microinjection. For the infection experiments, the GFP (green fluorescent protein) expressing strain M137 of *C. albicans* CS5314 (provided by Prof. Bernhard Hube, Department of Microbial Pathogenicity Mechanisms, Hans Knöll Institute, Jena, Germany) was used.[8] Briefly, the overnight fungal culture grown in YPD broth on the rotary shaker (180 rpm) and 30 °C were subcultered at 1:100 ratio upon the same conditions to reach a mid of exponential phase (OD_{530} 0.7-0.8). After centrifugation at 2200 × *g* for 5 min (Centrifuge 5415D, Eppendorf, Hamburg, Germany) and washing three times with sterile PBS, fungal cells were resuspended in 3% PVP to achieve a final concentration of 2×10^7 cells/mL.

Infection of zebrafish embryos

The infection experiments were performed using wild type AB zebrafish embryos generated on the previously described manner. At 34 hpf, manually dechorionated embryos were anesthetized by tricaine (200 μg/mL) and microinjected with 5 nL of fungal cells suspension in 3% PVP through otic vesicle into the hindbrain to achieve a dose of 55-70 fungal cell. After recovery for 2 h at 28 °C, alive embryos were distributed into 24-well plate (10 embryos per well) and treated with different doses (½ × MIC, 1 × MIC and 2× MIC) of each of the selected complexes. The embryos injected only with 3% PVP were used as the control group. The inhibitory effect of applied complexes on *C. albicans* cells filamentation and the survival of infected embryos were monitored every day by 4 days post infection (dpi).

Statistical analysis. Survival experiments were evaluated using the Kaplan–Meier method. Comparisons between curves were made using the log rank test. Analysis was performed using GraphPad Prism version 6.0 and statistical significance was assumed at P-value below 0.05.

Table S1. Crystallographic details of L2 and selected ReNN#X complexes

	L2	**ReNN10L1**	**ReNN10Py**	**ReNN9Py**
Formula	$C_{25}H_{19}ClN_4O_3$	$C_{38}Cl_4F_6H_{32}N_4O_5PRe$	$C_{43}H_{35}Cl_3F_6N_6O_{12}Re_2S_2$	$C_{20}H_{11}F_{12}N_3O_3PRe$
M_W	458.89	1097.64	1484.64	786.49
T [K]	200(2)	200(2)	200(2)	200(2)
Lattice	triclinic	monoclinic	triclinic	orthorhombic
Space group	*P*-1	*C2*/c	*P*-1	*Pna21*
Z	2	8	2	4
a [Å]	6.1224(2)	42.6175(10)	11.6260(2)	13.4247(2)
b [Å]	11.0201(4)	11.0183(2)	12.8511(2)	14.4465(2)
c [Å]	16.7545(6)	18.2031(4)	17.5011(2)	12.5141(3)
α [°]	80.586(3)	90	99.3080(10)	90
β [°]	82.205(3)	102.780(2)	93.0250(10)	90
γ [°]	75.513(3)	90	91.8590(10)	90
V [Å^3]	1074.41(7)	8335.9(3)	2574.53(7)	2426.98(8)
d_{calcd} [g/cm^3]	1.418	1.749	1.915	2.152
R_1, wR_2	0.0561, 0.1216	0.0688, 0.1527	0.0232, 0.0540	0.0271, 0.0795

	ReNN12Py	**ReNN13Py**	**ReNN10BzIm**	**ReNN13BzIm**
Formula	$C_{25}H_{21}F_3N_3O_6ReS$	$C_{21}H_{17}F_3N_3O_6ReS$	$C_{22}H_{17}N_4O_3Re$	$C_{23}H_{18}Cl_3N_4O_3Re$
M_W	734.71	682.64	571.59	690.96
T [K]	250(2)	200(2)	250(2)	293(2)
Lattice	Monoclinic	monoclinic	monoclinic	monoclinic
Space group	*P2$_1$/n*	*P2$_1$/n*	*P2$_1$/n*	*P2$_1$/n*
Z	4	4	4	4
a [Å]	11.9135(5)	11.7416(2)	8.5099(11)	11.2305(3)
b [Å]	13.2125(4)	13.7067(2)	16.2690(14)	14.0386(3)
c [Å]	16.9994(6)	14.3137(3)	15.5858(19)	16.3604(5)
α [°]	90	90	90	90
β [°]	98.545(3)	100.757(2)	103.137(10)	98.171(2)
γ [°]	90	90	90	90
V [Å^3]	2646.12(17)	2263.15(7)	2101.3(4)	2553.20(12)
d_{calcd} [g/cm^3]	1.844	1.635	1.807	1.798
R_1, wR_2	0.0363, 0.0842	0.0174, 0.0409	0.0571, 0.1137	0.0238, 0.0609

Table S2. Complete list of the minimum inhibitory concentrations (MIC, μM) of tested molecules.

Comp.	Zebrafish LC_{50}	*C. albicans* SC5314	*C. parapsilosis* ATCC22019	*C. krusei* ATCC6258	*C. glabrata* ATCC2001	*C. auris* strain *8*	*S. aureus* MRSA43300	*S. aureus* ATCC25923
ReNN#Br where # = 1-13	>25	-	-	-	-	-	-	-
ReNN1Im	>60	-	-	-	-	-	25	25
ReNN3Im	7.1	**3.1 (2.3)**	12.5	25	50	25	**3.1**	**3.1**
ReNN4Im	>60	-	-	-	-	-	25	50
ReNN5Im	27.4	50	25	12.5 **(2.2)**	25	50	12.5	12.5
ReNN6Im	7.1	6.2	-	-	-	25	**3.1**	**3.1**
ReNN10Im	>60	-	-	-	-	-	25	25
ReNN12Im	>25	50	-	-	-	50	12.5	12.5
ReNN13Im	>60	-	-	-	-	-	25	25
ReNN1BzIm	17.9	25	12.5	25	-	25	12.5	12.5
ReNN6BzIm	>60	12.5 **(4.8)**	12.5 **(4.8)**	25 **(2.4)**	-	12.5 **(4.8)**	6.2 **(9.7)**	12.5 **(4.8)**
ReNN10BzIm	>60	50	25 **(2.4)**	25 **(2.4)**	50	50	6.2 **(9.7)**	6.2 **(9.7)**
ReNN12BzIm	17.9	20	-	-	-	-	12.5	25
ReNN13BzIm	17.9	50	-	-	-	-	50	50
ReNN1Py	>60	25	25		-	-	12.5 **(4.8)**	12.5 **(4.8)**
ReNN2Py	>25	>50	-	-	-	-	-	-
ReNN3Py	18.7	**6.2 (3)**	**3.1 (6)**	25	-	-	**0.8 (23.9)**	**0.8 (23.9)**
ReNN4Py	>60	-			-	-	25	12.5 **(4.8)**
ReNN5Py	38.9	12.5 **(3)**	12.5 **(3)**	25	25	-	**3.1 (12.6)**	**3.1 (12.6)**
ReNN6Py	18.7	6.2 **(3)**	12.5	12.5	25	50	**0.4 (47.4)**	**0.6 (31.2)**
ReNN#Py where # = 7-11	>25	-	-	-	-	-	-	-
ReNN12Py	41.5	50	25	-	50	-	12.5 **(3.3)**	12.5 **(3.3)**
ReNN13Py	>25	-	-	-	-	-	>50	-
ReNN1L1	7.1	**3.1 (2.3)**	6.2	-	-	-	0.8 (9.1)	3.1
ReNN3L1	48.6	-	-	-	-	-	25	12.5
ReNN4L1	30.3	50	50	-	-	-	6.2 **(4.9)**	6.2 **(4.9)**
ReNN6L1	>60	-	-	-	-	-	50	6.2 **(9.7)**
ReNN7L1	>60	-	-	-	-	-	-	-
ReNN9L1	56.2	-	50	-	-	-	12.5 **(4.5)**	6.2 **(9)**
ReNN10L1	>60	-	25	-	-	-	3.12 **(19.2)**	6.2 **(9.6)**
ReNN11L1	>60	-	-	-	-	-	25	12.5 **(4.8)**
ReNN12L1	14.1	6.2 **(2.3)**	-	-	-	-	3.12 **(4.5)**	6.2
ReNN13L1	7.1	6.2	**3.1 (2.3)**	12.5	25		1.56 **(4.6)**	**3.1**
ReNN1L2	7.1	6.2	-	-	-	12.5	12.5	25
ReNN4L2	7.1	12.5	12.5	12.5	25	-	6.2	12.5
ReNN5L2	>25	-	-	-	-	-	-	-
ReNN6L2	>25	-	-	-	-	-	-	-
ReNN8L2	>25	-	-	-	-	-	-	-
ReNN9L2	>60	-	-	-	-	-	**1.56 (38.6)**	6.2 **(9.7)**
ReNN11L2	>60	-	-	-	12.5	-	6.2 **(4.8)**	25
ReNN13L2	7.1	50	25	50	50	50	**12.5**	12.5
NN1	3.6	-	-	-	-	-	-	-
NN2	>25	-	-	-	-	-	-	-
NN3	18.2	25	25	50	>50 (50)	50	50	-
NN4	>25	50	25	25	50	50	-	-
NN5	>25	-	-	-	50	-	-	-
NN6	<1.8	6.2	12.5	6.2	**3.1**	>50 (12.5)	**3.1 (1.6)**	**3.1 (1.6)**
NN7-9	>25	-	-	-	-	-	-	-
NN10	17.8	25	25	25	-	25	-	-
NN11	>25	-	-	-	-	-	-	-
NN12*	6.3	**0.8**	**0.8**	**0.8**	**0.8**	**0.8**	25	25
NN13	17.8	-	-	12.5	-	12.5	-	-

*NN12 is cardiotoxic, hepatotoxic and teratogenic at the doses ≥ 1.56 uM.

NMR spectra of most active and non-toxic compounds

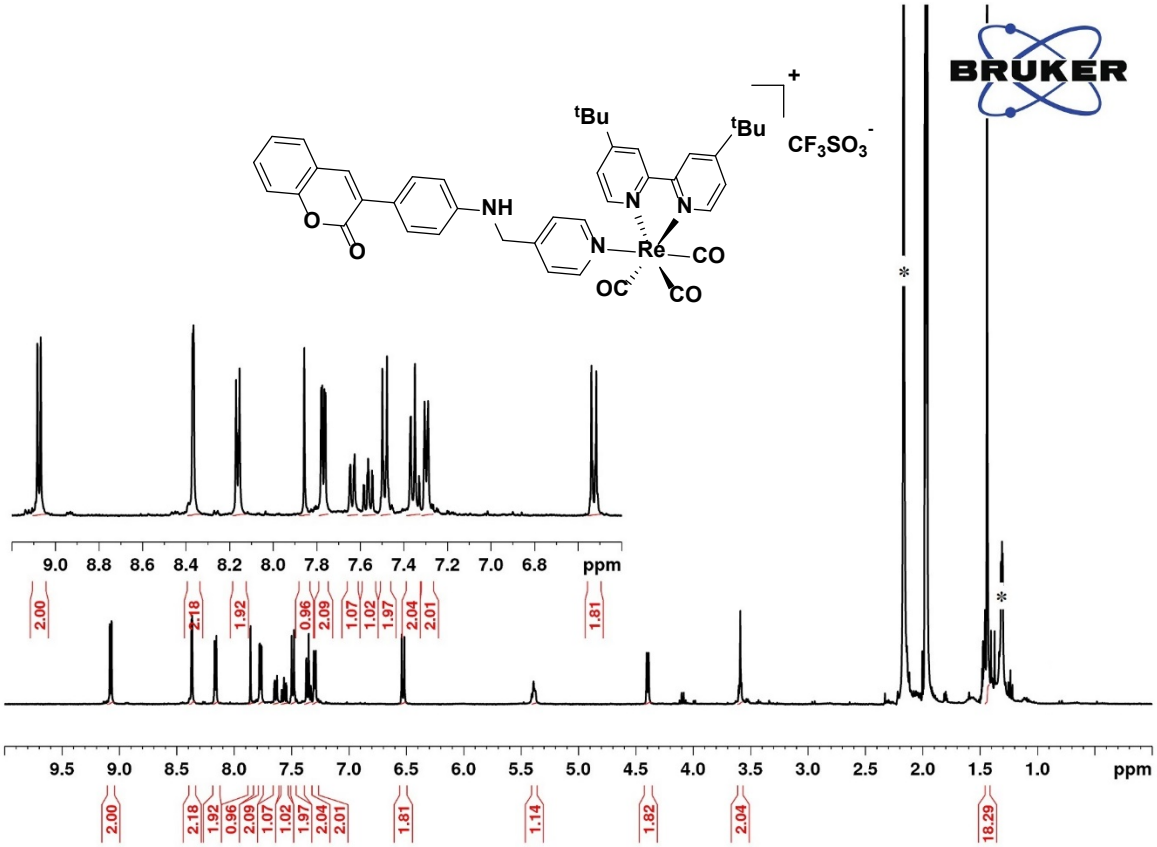

Figure S1. 400 MHz ^{1}H-NMR of ReNN1L1 (in Acetonitrile, ✻= solvent residual peak).

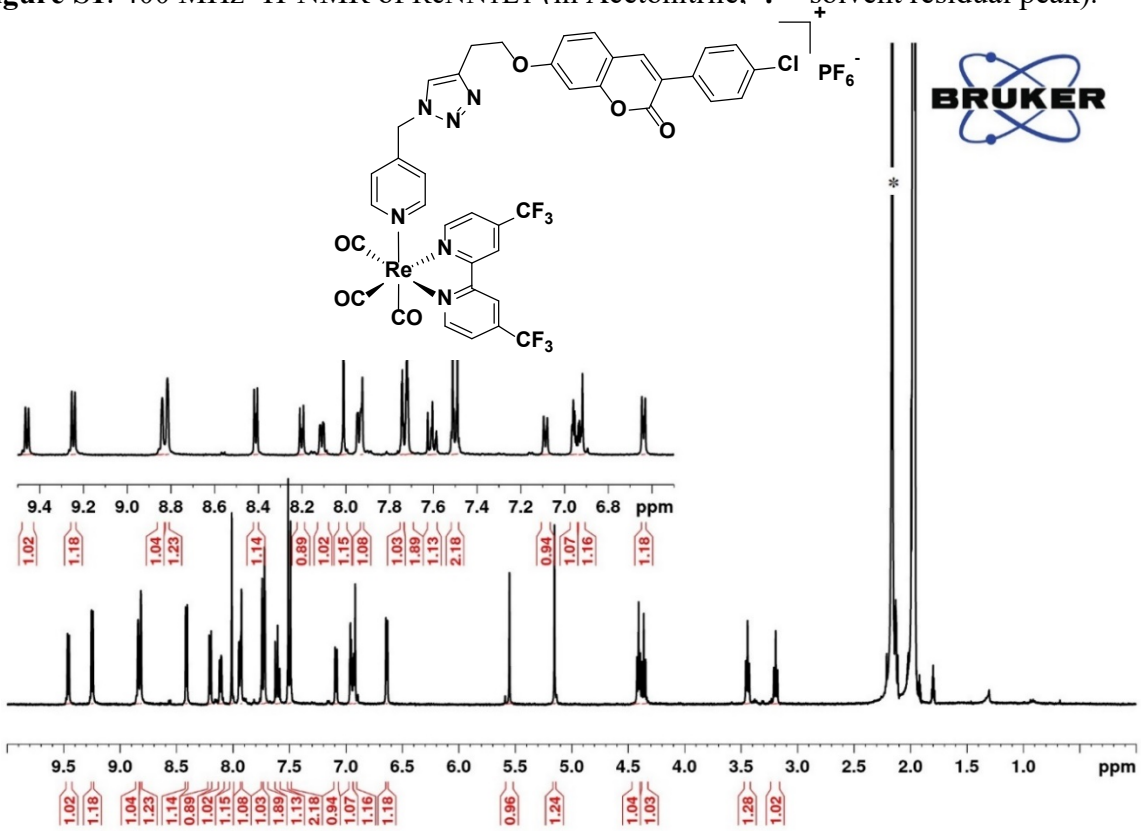

Figure S2. 400 MHz ^{1}H-NMR of ReNN9L2 (in Acetonitrile, ✻= solvent residual peak).

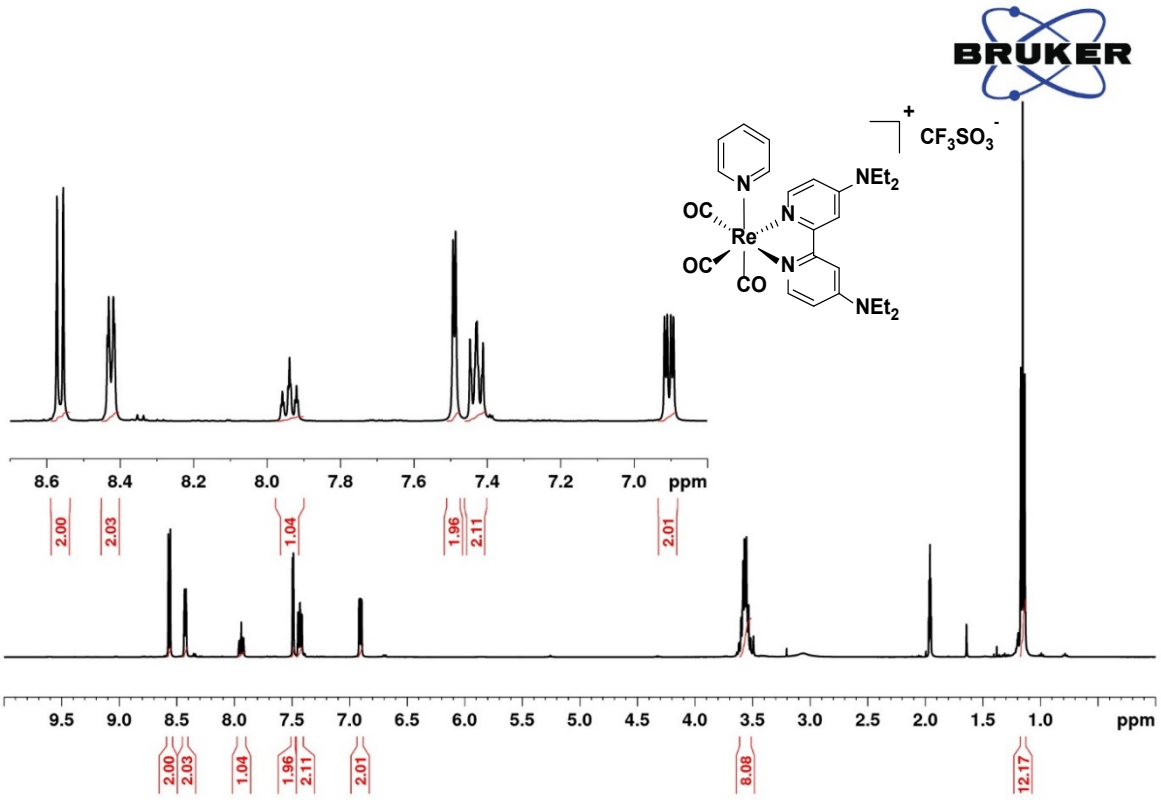

Figure S3. 400 MHz ^{1}H-NMR of ReNN3Py (in Acetonitrile, ✻= solvent residual peak).

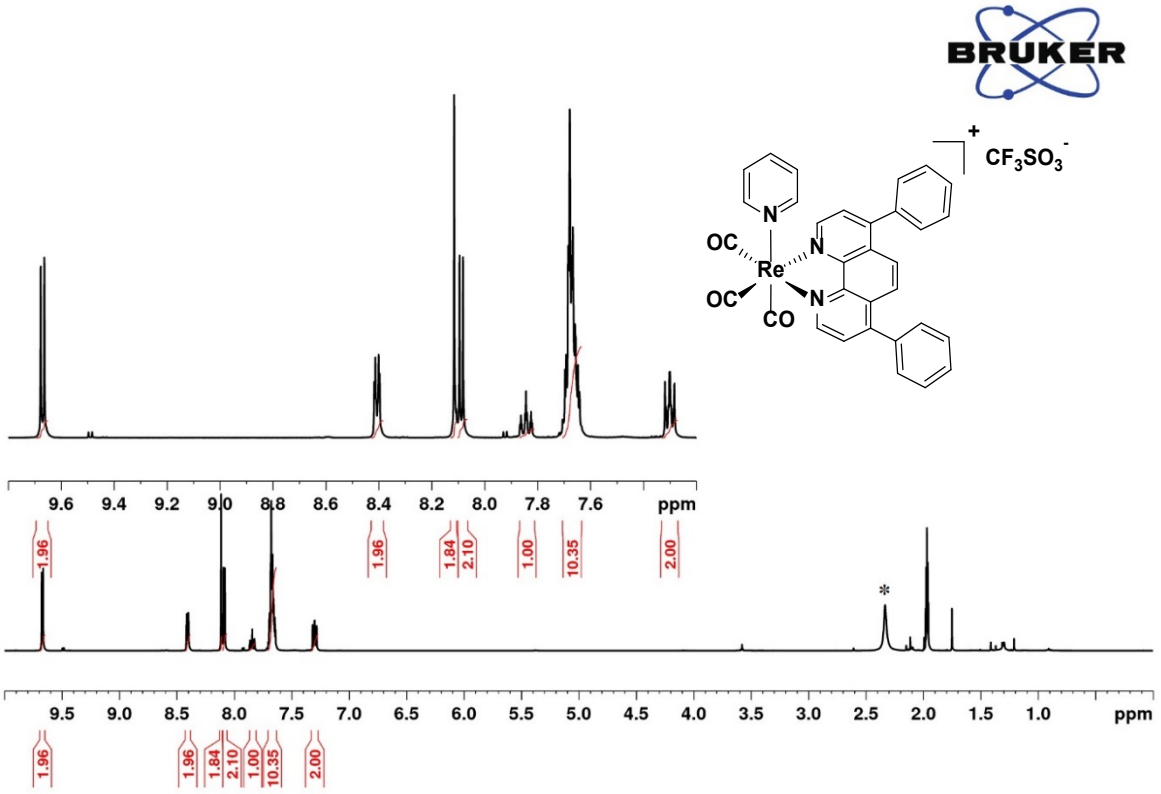

Figure S4. 400 MHz ^{1}H-NMR of ReNN6Py (in Acetonitrile, ✻= solvent residual peak).

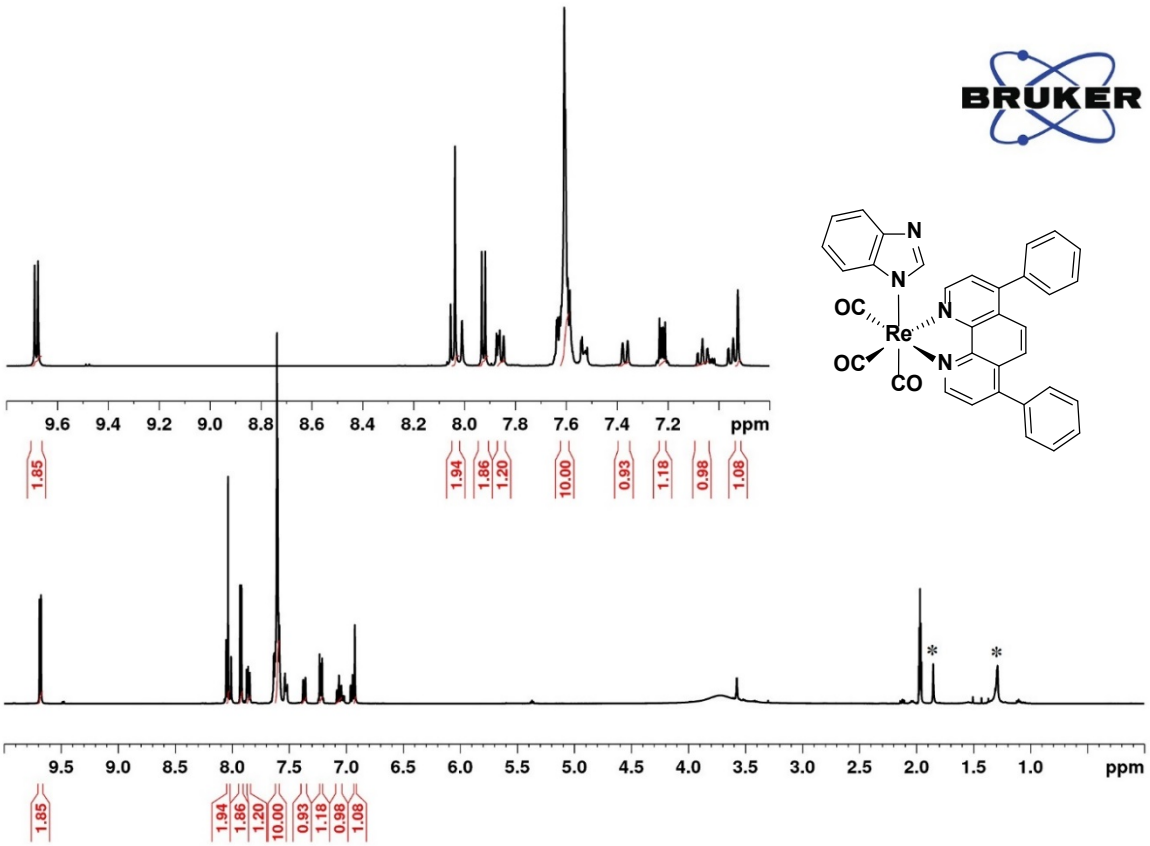

Figure S5. 400 MHz ^{1}H-NMR of ReNN6BzIm (in Acetonitrile, ✻= solvent residual peak).

IR Spectra of most active and non-toxic compounds

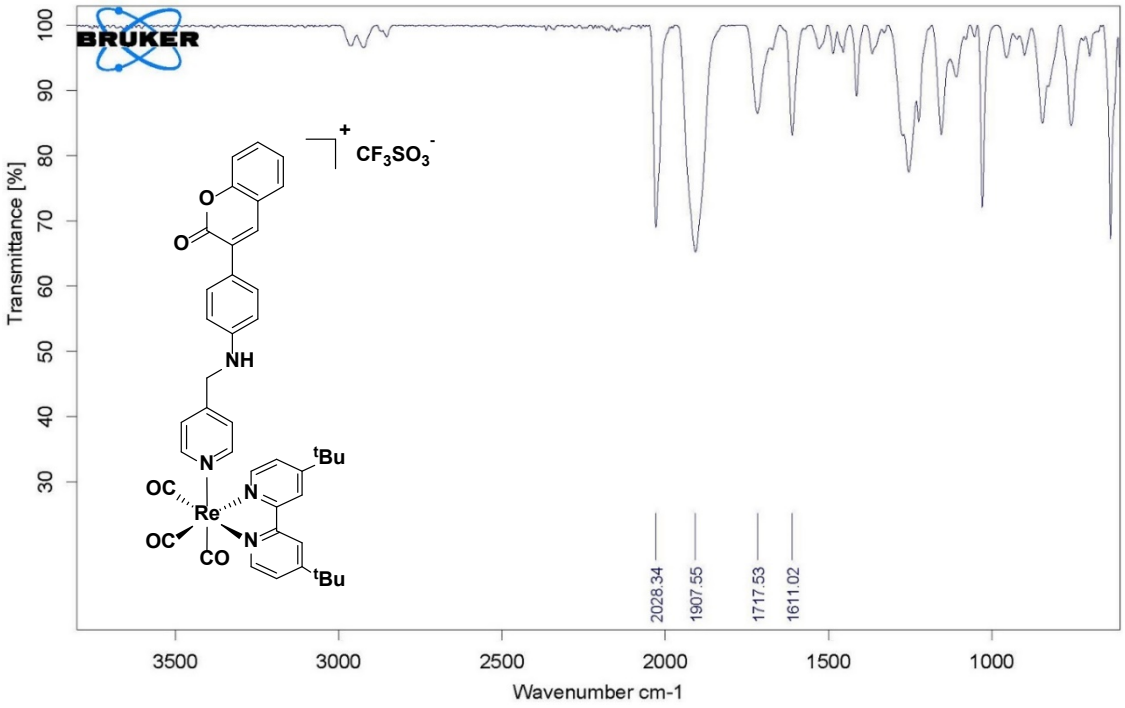

Figure S6. IR spectrum of ReNN1L1

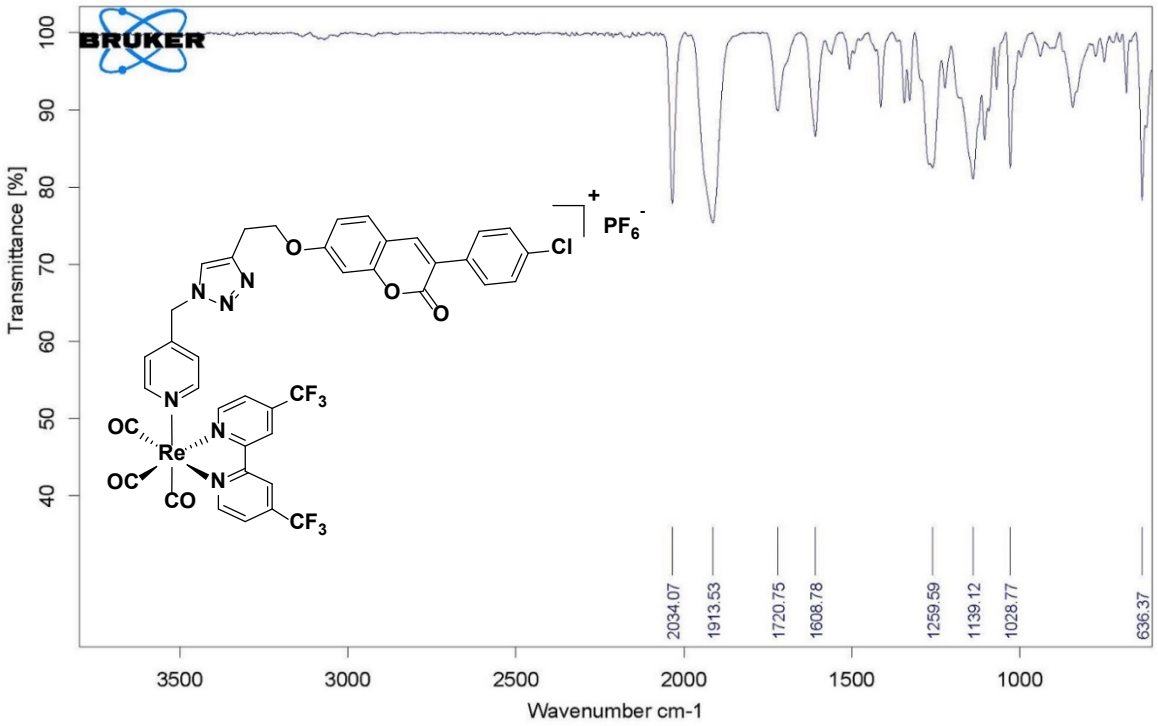

Figure S7. IR spectrum of ReNN9L2

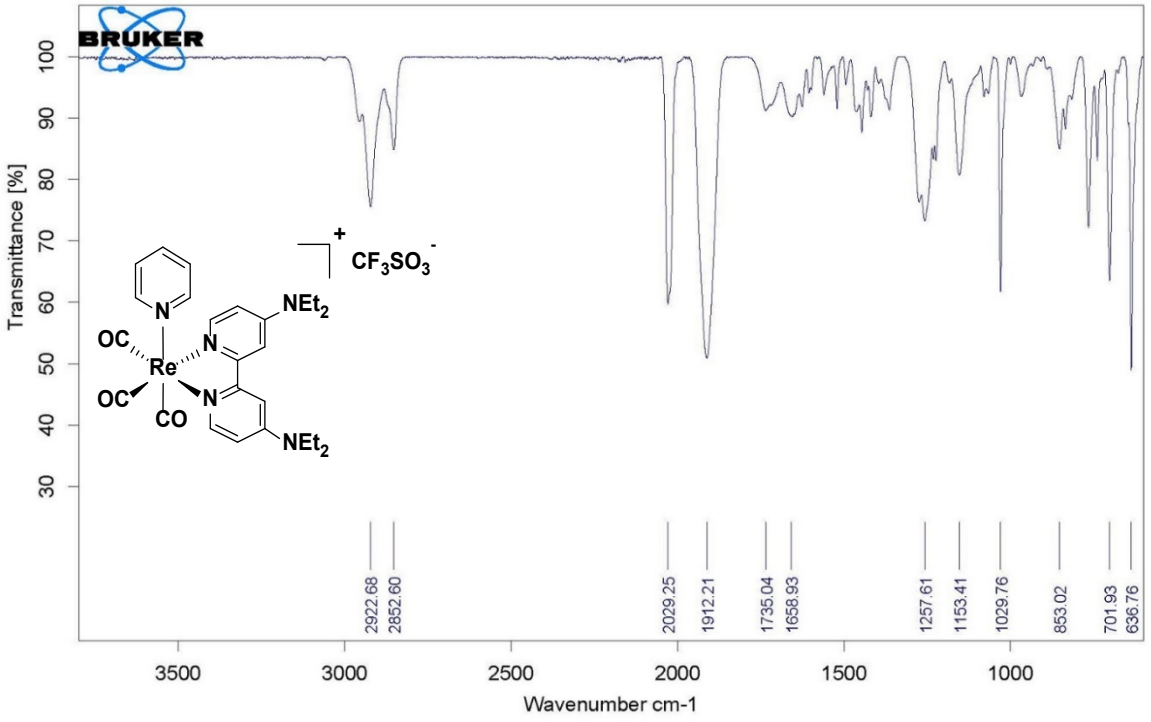

Figure S8. IR spectrum of ReNN3Py

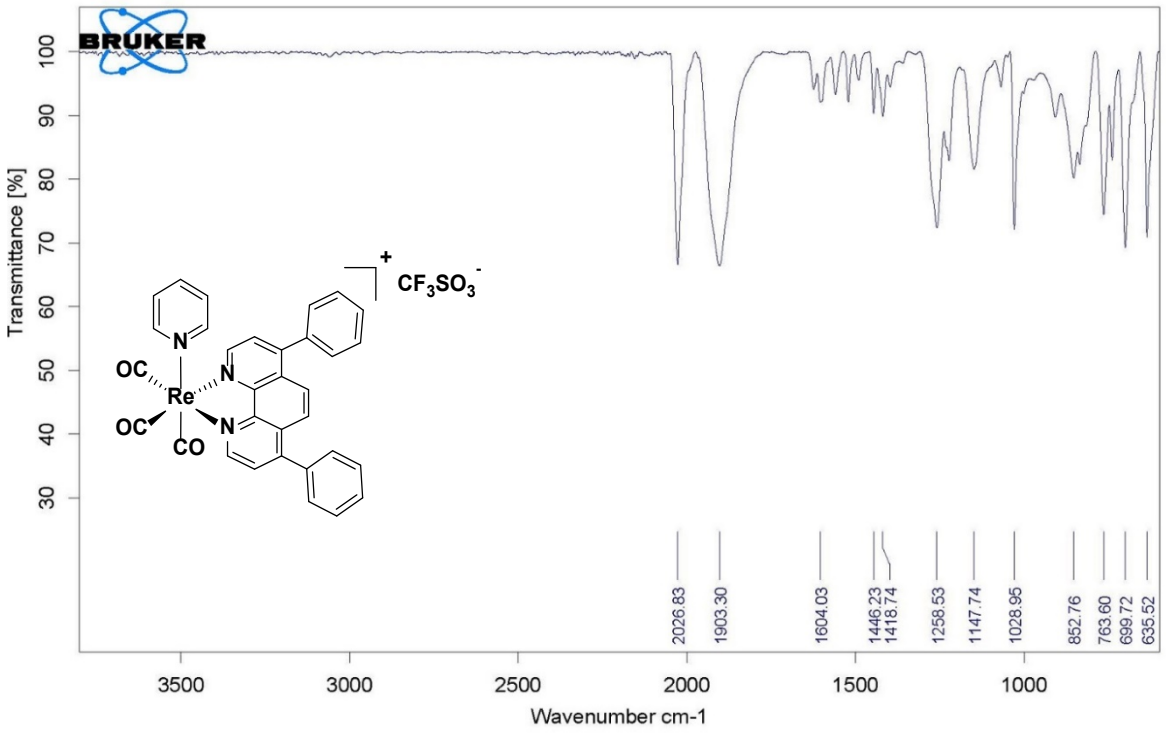

Figure S9. IR spectrum of ReNN6Py

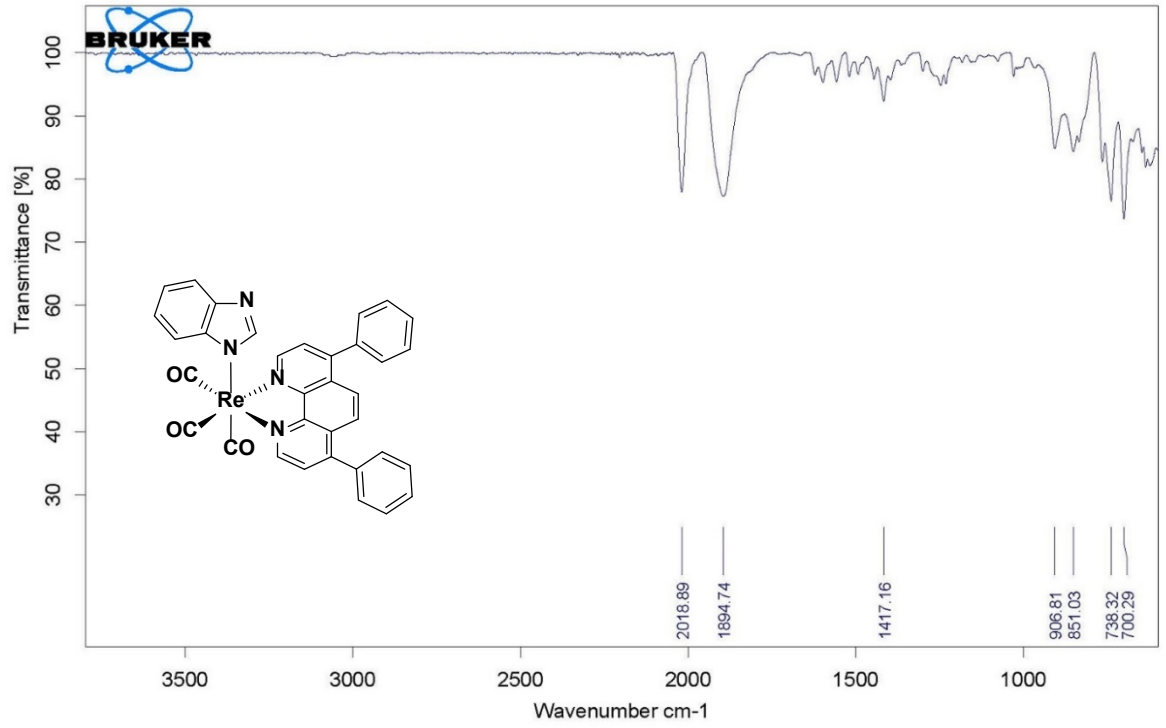

Figure S10. IR spectrum of ReNN6BzIm

UV-Vis spectra of most active and non-toxic compounds

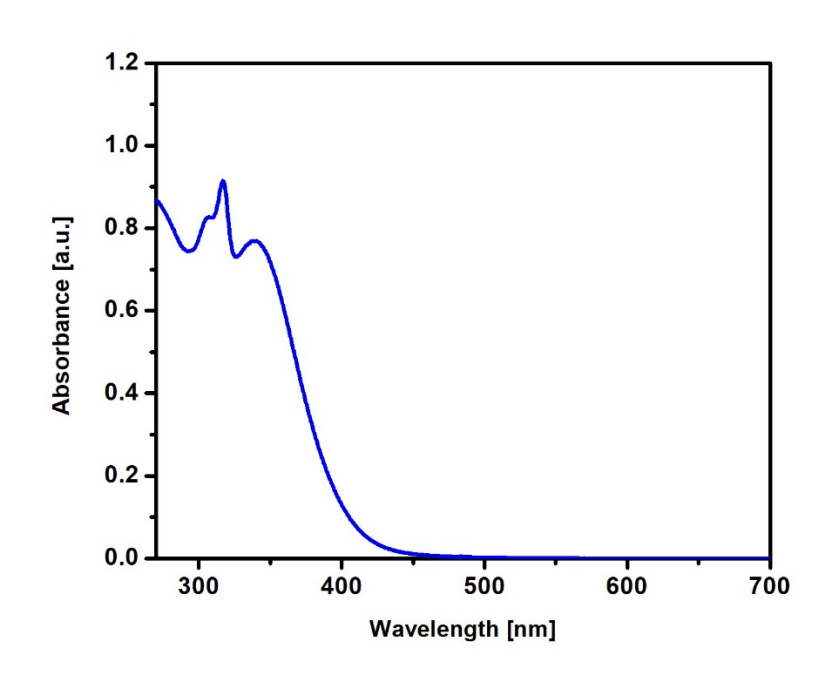

Figure S11. UV-Vis spectrum of ReNN1L1 in Acetonitrile.

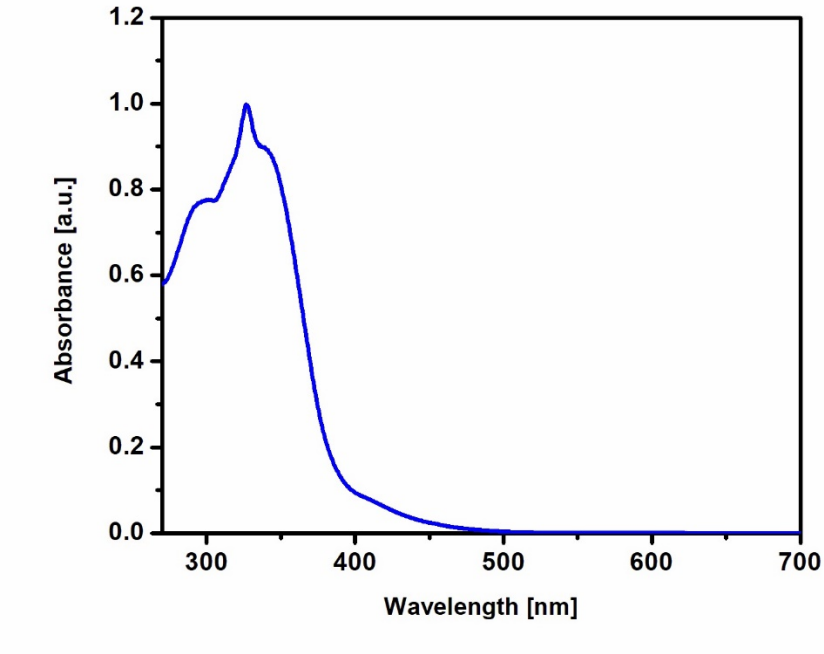

Figure S12. UV-Vis spectrum of ReNN9L2 in Acetonitrile.

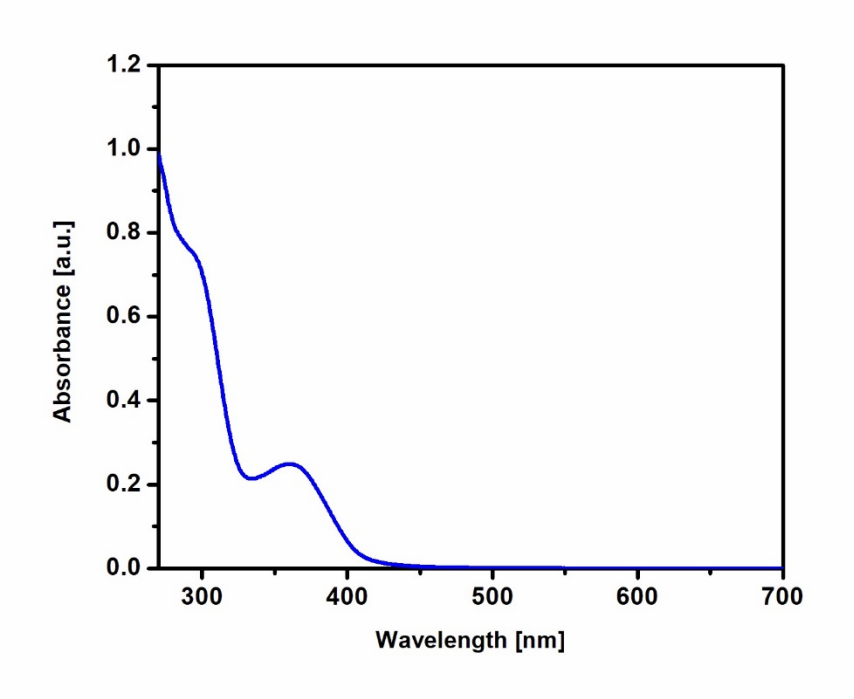

Figure S13. UV-Vis spectrum of ReNN3Py in Acetonitrile.

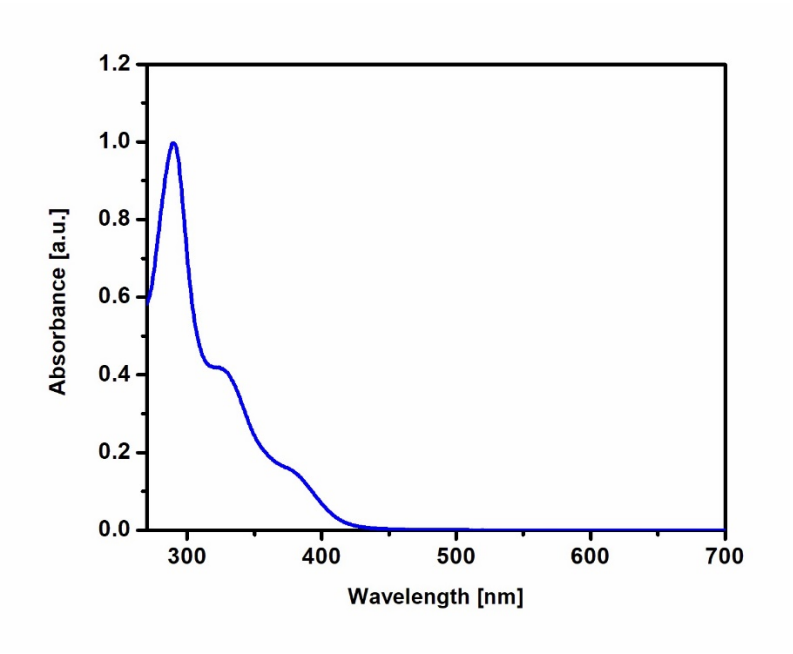

Figure S14. UV-Vis spectrum of ReNN6Py in Acetonitrile.

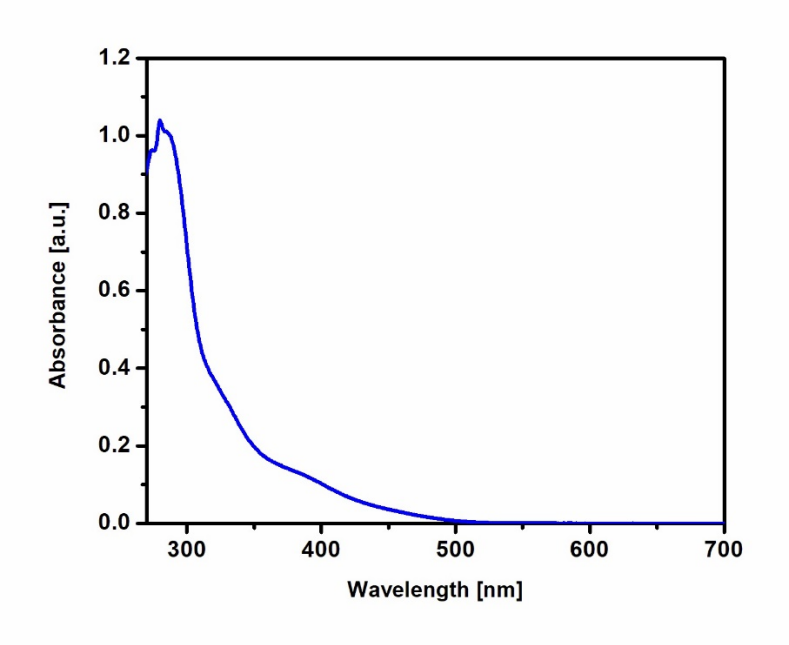

Figure S15. UV-Vis spectrum of ReNN6BzIm in Acetonitrile.

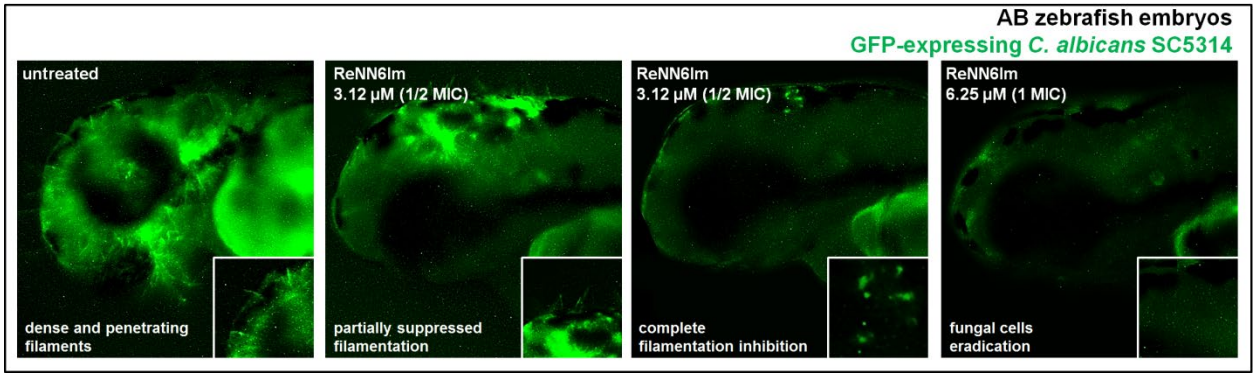

Figure S16. Non-homogenous embryos response against *Candida* filamentation at sub-MIC doses of ReNN6Im complex.

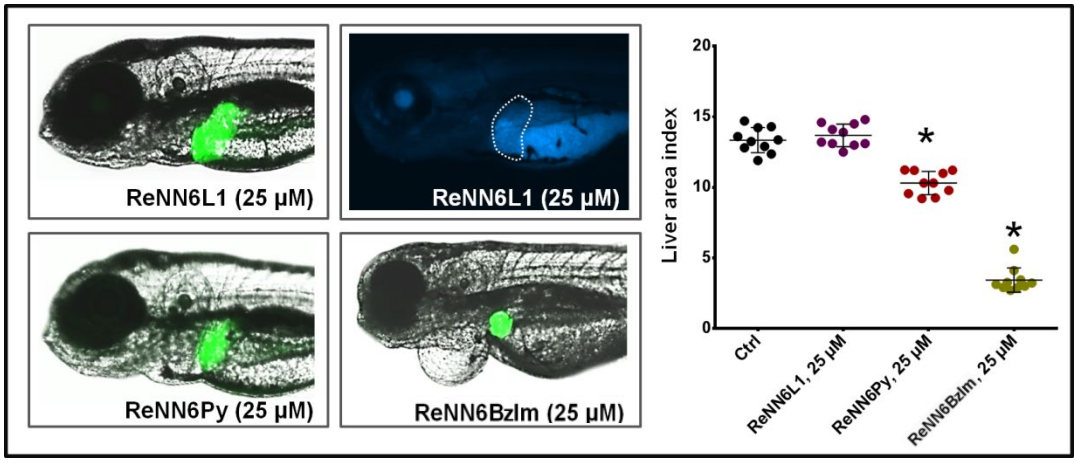

Figure S17. Modulation of the liver toxicity in relation to the X ligand type. Note a remarkable hepatotoxicity and decreased liver size and area index in the embryos exposed to ReNN6BzIm compared to less pronounced effect upon ReNN6Py and no detrimental effect upon ReNN6L1. Owing to the complex fluorescence (blue) which originates from the coumarin L1 ligand, we detected ReNN6L1 accumulation in the liver (dashed area) of a treated embryo.

References

1. Sovari, S. N.; Vojnovic, S.; Bogojevic, S. S.; Crochet, A.; Pavic, A.; Nikodinovic-Runic, J.; Zobi, F., Design, synthesis and in vivo evaluation of 3-arylcoumarin derivatives of rhenium(I) tricarbonyl complexes as potent antibacterial agents against methicillin-resistant Staphylococcus aureus (MRSA). *Eur. J. Med. Chem.* **2020,** *205*, 112533.
2. Zhang, Y.; Han, L. W.; He, Q. X.; Chen, W. Y.; Sun, C.; Wang, X.; Chen, X. Q.; Wang, R. C.; Hsiao, C. D.; Liu, K. C., A rapid assessment for predicting drug-induced hepatotoxicity using zebrafish. *J. Pharmacol. Toxicol. Met.* **2017,** *84*, 102-110.
3. He, J. H.; Guo, S. Y.; Zhu, F.; Zhu, J. J.; Chen, Y. X.; Huang, C. J.; Gao, J. M.; Dong, Q. X.; Xuan, Y. X.; Li, C. Q., A zebrafish phenotypic assay for assessing drug-induced hepatotoxicity. *J. Pharmacol. Toxicol. Met.* **2013,** *67* (1), 25-32.
4. Rojas-Mancilla, E.; Oyarce, A.; Verdugo, V.; Zheng, Z.; Ramírez-Tagle, R., The Cluster [Re6Se8I6]3− Induces Low Hemolysis of Human Erythrocytes in Vitro: Protective Effect of Albumin. *Int. J. Mol. Sci.* **2015,** *16* (1), 1728-1735.
5. Prajsnar, T. K.; Cunliffe, V. T.; Foster, S. J.; Renshaw, S. A., A novel vertebrate model of Staphylococcus aureus infection reveals phagocyte-dependent resistance of zebrafish to non-host specialized pathogens. *Cell Microbiol.* **2008,** *10* (11), 2312-25.
6. Pavic, A.; Savic, N. D.; Glisic, B. D.; Crochet, A.; Vojnovic, S.; Kurutos, A.; Stankovic, D. M.; Fromm, K. M.; Nikodinovic-Runic, J.; Djuran, M. I., Silver(I) complexes with 4,7-phenanthroline efficient in rescuing the zebrafish embryos of lethal Candida albicans infection. *J. Inorg. Biochem.* **2019,** *195*, 149-163.
7. Brothers, K. M.; Wheeler, R. T., Non-invasive imaging of disseminated candidiasis in zebrafish larvae. *J. Vis. Exp.* **2012,** (65).
8. Fradin, C.; De Groot, P.; MacCallum, D.; Schaller, M.; Klis, F.; Odds, F. C.; Hube, B., Granulocytes govern the transcriptional response, morphology and proliferation of Candida albicans in human blood. *Mol. Microbiol.* **2005,** *56* (2), 397-415.

checkCIF/PLATON report

Structure factors have been supplied for datablock(s) l11-2

THIS REPORT IS FOR GUIDANCE ONLY. IF USED AS PART OF A REVIEW PROCEDURE FOR PUBLICATION, IT SHOULD NOT REPLACE THE EXPERTISE OF AN EXPERIENCED CRYSTALLOGRAPHIC REFEREE.

No syntax errors found. CIF dictionary Interpreting this report

Datablock: l11-2

```
Bond precision:  C-C = 0.0030 A          Wavelength=1.54186

Cell:          a=6.1224(2)       b=11.0201(4)     c=16.7545(6)
               alpha=80.586(3)   beta=82.205(3)   gamma=75.513(3)
Temperature:   200 K
```

	Calculated	Reported
Volume	1074.41(7)	1074.41(7)
Space group	P -1	P -1
Hall group	-P 1	-P 1
Moiety formula	C25 H19 Cl N4 O3	C25 H19 Cl N4 O3
Sum formula	C25 H19 Cl N4 O3	C25 H19 Cl N4 O3
Mr	458.89	458.89
Dx,g cm-3	1.418	1.418
Z	2	2
Mu (mm-1)	1.881	1.881
F000	476.0	476.0
F000’	478.09	
h,k,lmax	7,12,19	6,12,19
Nref	3638	3490
Tmin,Tmax	0.873,0.910	0.009,0.732
Tmin’	0.637	

```
Correction method= # Reported T Limits: Tmin=0.009 Tmax=0.732
AbsCorr = MULTI-SCAN

Data completeness= 0.959          Theta(max)= 64.893

R(reflections)= 0.0439( 2856)     wR2(reflections)= 0.1216( 3490)

S = 1.026                 Npar= 298
```

The following ALERTS were generated. Each ALERT has the format
test-name_ALERT_alert-type_alert-level.
Click on the hyperlinks for more details of the test.

Alert level B

PLAT029_ALERT_3_B _diffrn_measured_fraction_theta_full value Low . 0.959 Why?

Author Response: Poor diffraction intensities in high angles.

Alert level C

THETM01_ALERT_3_C The value of sine(theta_max)/wavelength is less than 0.590
Calculated sin(theta_max)/wavelength = 0.5873
PLAT911_ALERT_3_C Missing FCF Refl Between Thmin & STh/L= 0.587 109 Report

---

Alert level G

PLAT154_ALERT_1_G The s.u.’s on the Cell Angles are Equal ..(Note) 0.003 Degree
PLAT909_ALERT_3_G Percentage of I>2sig(I) Data at Theta(Max) Still 49% Note
PLAT910_ALERT_3_G Missing # of FCF Reflection(s) Below Theta(Min). 1 Note
PLAT978_ALERT_2_G Number C-C Bonds with Positive Residual Density. 9 Info
PLAT992_ALERT_5_G Repd & Actual _reflns_number_gt Values Differ by 1 Check

---

0 **ALERT level A** = Most likely a serious problem - resolve or explain
1 **ALERT level B** = A potentially serious problem, consider carefully
2 **ALERT level C** = Check. Ensure it is not caused by an omission or oversight
5 **ALERT level G** = General information/check it is not something unexpected

1 ALERT type 1 CIF construction/syntax error, inconsistent or missing data
1 ALERT type 2 Indicator that the structure model may be wrong or deficient
5 ALERT type 3 Indicator that the structure quality may be low
0 ALERT type 4 Improvement, methodology, query or suggestion
1 ALERT type 5 Informative message, check

It is advisable to attempt to resolve as many as possible of the alerts in all categories. Often the minor alerts point to easily fixed oversights, errors and omissions in your CIF or refinement strategy, so attention to these fine details can be worthwhile. In order to resolve some of the more serious problems it may be necessary to carry out additional measurements or structure refinements. However, the purpose of your study may justify the reported deviations and the more serious of these should normally be commented upon in the discussion or experimental section of a paper or in the "special_details" fields of the CIF. checkCIF was carefully designed to identify outliers and unusual parameters, but every test has its limitations and alerts that are not important in a particular case may appear. Conversely, the absence of alerts does not guarantee there are no aspects of the results needing attention. It is up to the individual to critically assess their own results and, if necessary, seek expert advice.

Publication of your CIF in IUCr journals

A basic structural check has been run on your CIF. These basic checks will be run on all CIFs submitted for publication in IUCr journals (*Acta Crystallographica, Journal of Applied Crystallography, Journal of Synchrotron Radiation*); however, if you intend to submit to *Acta Crystallographica Section C* or *E* or *IUCrData*, you should make sure that full publication checks are run on the final version of your CIF prior to submission.

Publication of your CIF in other journals

Please refer to the *Notes for Authors* of the relevant journal for any special instructions relating to CIF submission.

PLATON version of 08/07/2020; check.def file version of 17/06/2020

Datablock l11-2 - ellipsoid plot

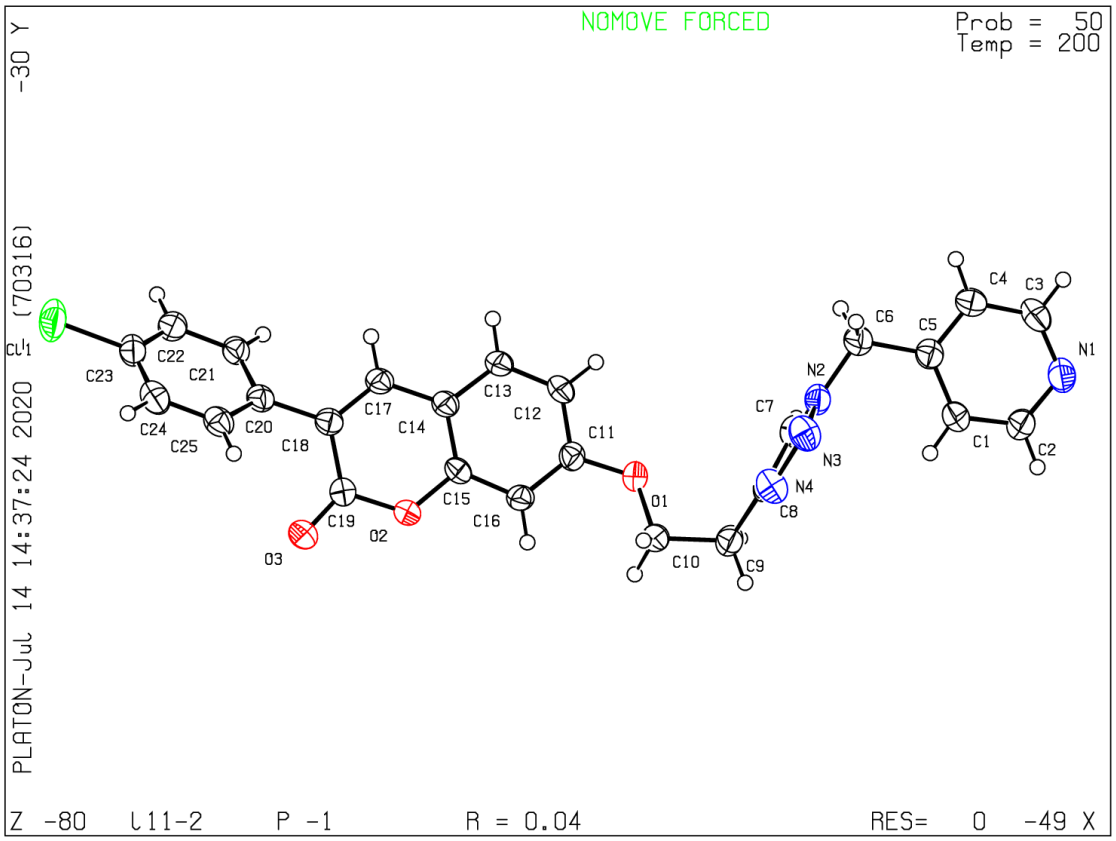

checkCIF/PLATON report

Structure factors have been supplied for datablock(s) renn9py

THIS REPORT IS FOR GUIDANCE ONLY. IF USED AS PART OF A REVIEW PROCEDURE FOR PUBLICATION, IT SHOULD NOT REPLACE THE EXPERTISE OF AN EXPERIENCED CRYSTALLOGRAPHIC REFEREE.

No syntax errors found. CIF dictionary Interpreting this report

Datablock: renn9py

```
Bond precision:  C-C = 0.0097 A          Wavelength=1.54186

Cell:            a=13.4247(2)     b=14.4465(2)     c=12.5141(3)
                 alpha=90         beta=90          gamma=90
Temperature:     200 K
```

	Calculated	Reported
Volume	2426.98(8)	2426.98(8)
Space group	P n a 21	P n a 21
Hall group	P 2c -2n	P 2c -2n
Moiety formula	C20 H11 F6 N3 O3 Re, F6 P	C20 H11 F6 N3 O3 Re, F6 P
Sum formula	C20 H11 F12 N3 O3 P Re	C20 H11 F12 N3 O3 P Re
Mr	786.50	786.49
Dx,g cm-3	2.152	2.152
Z	4	4
Mu (mm-1)	11.585	11.585
F000	1496.0	1496.0
F000’	1482.17	
h,k,lmax	16,17,15	16,16,14
Nref	4387[2304]	3365
Tmin,Tmax	0.107,0.314	0.226,1.000
Tmin’	0.018	

```
Correction method= # Reported T Limits: Tmin=0.226 Tmax=1.000
AbsCorr = MULTI-SCAN

Data completeness= 1.46/0.77      Theta(max)= 67.745

R(reflections)= 0.0269( 3323)     wR2(reflections)= 0.0795( 3365)

S = 1.079                 Npar= 363
```

The following ALERTS were generated. Each ALERT has the format
test-name_ALERT_alert-type_alert-level.
Click on the hyperlinks for more details of the test.

Alert level C

```
STRVA01_ALERT_4_C           Flack test results are ambiguous.
           From the CIF: _refine_ls_abs_structure_Flack    0.513
           From the CIF: _refine_ls_abs_structure_Flack_su    0.019
PLAT090_ALERT_3_C Poor Data / Parameter Ratio (Zmax > 18) ........       6.23 Note
PLAT342_ALERT_3_C Low Bond Precision on  C-C Bonds ..............    0.00973 Ang.
PLAT907_ALERT_2_C Flack x > 0.5, Structure Needs to be Inverted? .       0.51 Check
PLAT911_ALERT_3_C Missing FCF Refl Between Thmin & STh/L=    0.600         33 Report
```

Alert level G

```
PLAT242_ALERT_2_G Low    'MainMol' Ueq as Compared to Neighbors of        C19 Check
PLAT242_ALERT_2_G Low    'MainMol' Ueq as Compared to Neighbors of        C20 Check
PLAT244_ALERT_4_G Low    'Solvent' Ueq as Compared to Neighbors of         P1 Check
PLAT870_ALERT_4_G ALERTS Related to Twinning Effects Suppressed ..          ! Info
PLAT909_ALERT_3_G Percentage of I>2sig(I) Data at Theta(Max) Still        94% Note
PLAT912_ALERT_4_G Missing # of FCF Reflections Above STh/L=  0.600          2 Note
PLAT933_ALERT_2_G Number of OMIT Records in Embedded .res File ...          3 Note
PLAT961_ALERT_5_G Dataset Contains no Negative Intensities .......     Please Check
```

---

0 **ALERT level A** = Most likely a serious problem - resolve or explain
0 **ALERT level B** = A potentially serious problem, consider carefully
5 **ALERT level C** = Check. Ensure it is not caused by an omission or oversight
8 **ALERT level G** = General information/check it is not something unexpected

0 ALERT type 1 CIF construction/syntax error, inconsistent or missing data
4 ALERT type 2 Indicator that the structure model may be wrong or deficient
4 ALERT type 3 Indicator that the structure quality may be low
4 ALERT type 4 Improvement, methodology, query or suggestion
1 ALERT type 5 Informative message, check

It is advisable to attempt to resolve as many as possible of the alerts in all categories. Often the minor alerts point to easily fixed oversights, errors and omissions in your CIF or refinement strategy, so attention to these fine details can be worthwhile. In order to resolve some of the more serious problems it may be necessary to carry out additional measurements or structure refinements. However, the purpose of your study may justify the reported deviations and the more serious of these should normally be commented upon in the discussion or experimental section of a paper or in the "special_details" fields of the CIF. checkCIF was carefully designed to identify outliers and unusual parameters, but every test has its limitations and alerts that are not important in a particular case may appear. Conversely, the absence of alerts does not guarantee there are no aspects of the results needing attention. It is up to the individual to critically assess their own results and, if necessary, seek expert advice.

Publication of your CIF in IUCr journals

A basic structural check has been run on your CIF. These basic checks will be run on all CIFs submitted for publication in IUCr journals (*Acta Crystallographica, Journal of Applied Crystallography, Journal of Synchrotron Radiation*); however, if you intend to submit to *Acta Crystallographica Section C* or *E* or *IUCrData*, you should make sure that full publication checks are run on the final version of your CIF prior to submission.

Publication of your CIF in other journals

Please refer to the *Notes for Authors* of the relevant journal for any special instructions relating to CIF submission.

PLATON version of 05/12/2020; check.def file version of 05/12/2020

Datablock renn9py - ellipsoid plot

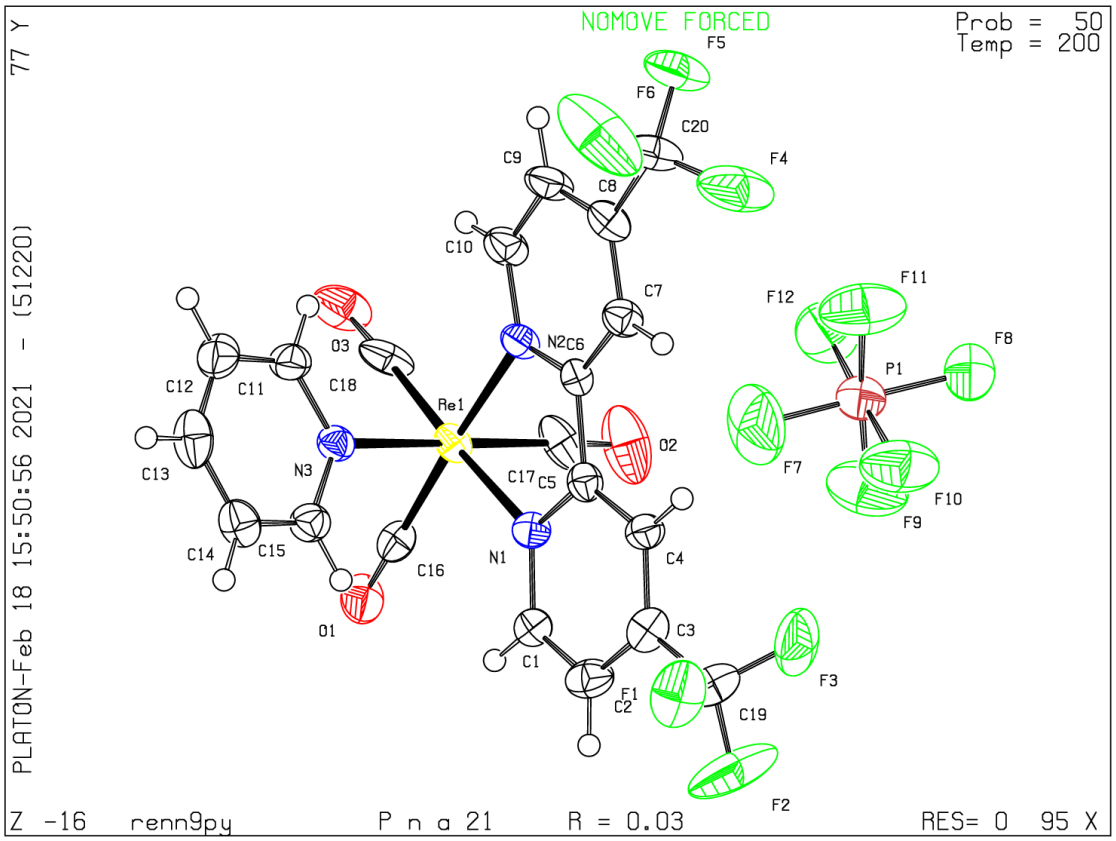

checkCIF/PLATON report

Structure factors have been supplied for datablock(s) renn10py

THIS REPORT IS FOR GUIDANCE ONLY. IF USED AS PART OF A REVIEW PROCEDURE FOR PUBLICATION, IT SHOULD NOT REPLACE THE EXPERTISE OF AN EXPERIENCED CRYSTALLOGRAPHIC REFEREE.

No syntax errors found. CIF dictionary Interpreting this report

Datablock: renn10py

Bond precision: C-C = 0.0053 A Wavelength=1.54186

Cell: a=11.6260(2) b=12.8511(2) c=17.5011(2)
alpha=99.308(1) beta=93.025(1) gamma=91.859(1)
Temperature: 200 K

	Calculated	Reported
Volume	2574.53(7)	2574.53(7)
Space group	P -1	P -1
Hall group	-P 1	-P 1
Moiety formula	2(C20 H17 N3 O3 Re), 2(C F3 O3 S), C H Cl3	2(C20 H17 N3 O3 Re), C H Cl3, 2(C F3 O3 S)
Sum formula	C43 H35 Cl3 F6 N6 O12 Re2 S2	C43 H35 Cl3 F6 N6 O12 Re2 S2
Mr	1484.66	1484.64
Dx,g cm-3	1.915	1.915
Z	2	2
Mu (mm-1)	12.012	12.012
F000	1436.0	1436.0
F000’	1422.68	
h,k,lmax	13,15,21	13,15,20
Nref	9334	8750
Tmin,Tmax	0.080,0.237	0.098,0.305
Tmin’	0.008	

Correction method= # Reported T Limits: Tmin=0.098 Tmax=0.305
AbsCorr = MULTI-SCAN

Data completeness= 0.937 Theta(max)= 67.847

R(reflections)= 0.0229(8647) wR2(reflections)= 0.0540(8750)

S = 1.150 Npar= 672

The following ALERTS were generated. Each ALERT has the format
test-name_ALERT_alert-type_alert-level.
Click on the hyperlinks for more details of the test.

Alert level B

PLAT029_ALERT_3_B _diffrn_measured_fraction_theta_full value Low . 0.940 Why?

Author Response: Low diffraction intensities in high angles

PLAT911_ALERT_3_B Missing FCF Refl Between Thmin & STh/L= 0.600 556 Report

Author Response: Low diffraction intensities in high angles

Alert level C

PLAT244_ALERT_4_C Low 'Solvent' Ueq as Compared to Neighbors of S1 Check
PLAT244_ALERT_4_C Low 'Solvent' Ueq as Compared to Neighbors of S2 Check
PLAT244_ALERT_4_C Low 'Solvent' Ueq as Compared to Neighbors of C43 Check
PLAT906_ALERT_3_C Large K Value in the Analysis of Variance ..... 2.036 Check

---

Alert level G

PLAT003_ALERT_2_G Number of Uiso or Uij Restrained non-H Atoms ... 2 Report
PLAT042_ALERT_1_G Calc. and Reported MoietyFormula Strings Differ Please Check
PLAT153_ALERT_1_G The s.u.'s on the Cell Axes are Equal ..(Note) 0.0002 Ang.
PLAT154_ALERT_1_G The s.u.'s on the Cell Angles are Equal ..(Note) 0.001 Degree
PLAT177_ALERT_4_G The CIF-Embedded .res File Contains DELU Records 1 Report
PLAT232_ALERT_2_G Hirshfeld Test Diff (M-X) Re1 --C18 . 5.5 s.u.
PLAT232_ALERT_2_G Hirshfeld Test Diff (M-X) Re1 --C19 . 5.5 s.u.
PLAT232_ALERT_2_G Hirshfeld Test Diff (M-X) Re2 --C38 . 6.7 s.u.
PLAT232_ALERT_2_G Hirshfeld Test Diff (M-X) Re2 --C40 . 5.6 s.u.
PLAT244_ALERT_4_G Low 'Solvent' Ueq as Compared to Neighbors of C41 Check
PLAT244_ALERT_4_G Low 'Solvent' Ueq as Compared to Neighbors of C42 Check
PLAT432_ALERT_2_G Short Inter X...Y Contact O12 ..C29 2.99 Ang.
1+x,y,z = 1_655 Check
PLAT860_ALERT_3_G Number of Least-Squares Restraints ..... 1 Note
PLAT909_ALERT_3_G Percentage of I>2sig(I) Data at Theta(Max) Still 95% Note
PLAT910_ALERT_3_G Missing # of FCF Reflection(s) Below Theta(Min). 1 Note
PLAT912_ALERT_4_G Missing # of FCF Reflections Above STh/L= 0.600 26 Note
PLAT933_ALERT_2_G Number of OMIT Records in Embedded .res File ... 4 Note
PLAT978_ALERT_2_G Number C-C Bonds with Positive Residual Density. 1 Info

---

0 **ALERT level A** = Most likely a serious problem - resolve or explain
2 **ALERT level B** = A potentially serious problem, consider carefully
4 **ALERT level C** = Check. Ensure it is not caused by an omission or oversight
18 **ALERT level G** = General information/check it is not something unexpected

3 ALERT type 1 CIF construction/syntax error, inconsistent or missing data
8 ALERT type 2 Indicator that the structure model may be wrong or deficient
6 ALERT type 3 Indicator that the structure quality may be low
7 ALERT type 4 Improvement, methodology, query or suggestion
0 ALERT type 5 Informative message, check

It is advisable to attempt to resolve as many as possible of the alerts in all categories. Often the minor alerts point to easily fixed oversights, errors and omissions in your CIF or refinement strategy, so attention to these fine details can be worthwhile. In order to resolve some of the more serious problems it may be necessary to carry out additional measurements or structure refinements. However, the purpose of your study may justify the reported deviations and the more serious of these should normally be commented upon in the discussion or experimental section of a paper or in the "special_details" fields of the CIF. checkCIF was carefully designed to identify outliers and unusual parameters, but every test has its limitations and alerts that are not important in a particular case may appear. Conversely, the absence of alerts does not guarantee there are no aspects of the results needing attention. It is up to the individual to critically assess their own results and, if necessary, seek expert advice.

Publication of your CIF in IUCr journals

A basic structural check has been run on your CIF. These basic checks will be run on all CIFs submitted for publication in IUCr journals (*Acta Crystallographica, Journal of Applied Crystallography, Journal of Synchrotron Radiation*); however, if you intend to submit to *Acta Crystallographica Section C* or *E* or *IUCrData*, you should make sure that full publication checks are run on the final version of your CIF prior to submission.

Publication of your CIF in other journals

Please refer to the *Notes for Authors* of the relevant journal for any special instructions relating to CIF submission.

PLATON version of 08/07/2020; check.def file version of 17/06/2020

checkCIF/PLATON report

Structure factors have been supplied for datablock(s) renn12py

THIS REPORT IS FOR GUIDANCE ONLY. IF USED AS PART OF A REVIEW PROCEDURE FOR PUBLICATION, IT SHOULD NOT REPLACE THE EXPERTISE OF AN EXPERIENCED CRYSTALLOGRAPHIC REFEREE.

No syntax errors found. CIF dictionary Interpreting this report

Datablock: renn12py

```
Bond precision:  C-C = 0.0075 A          Wavelength=0.71073

Cell:            a=11.9135(5)    b=13.2125(4)       c=16.9994(6)
                 alpha=90        beta=98.545(3)     gamma=90
Temperature:     250 K
```

	Calculated	Reported
Volume	2646.12(17)	2646.12(17)
Space group	P 21/n	P 1 21/n 1
Hall group	-P 2yn	-P 2yn
Moiety formula	C24 H21 N3 O3 Re, C F3 O3 S	C24 H21 N3 O3 Re, C F3 O3 S
Sum formula	C25 H21 F3 N3 O6 Re S	C25 H21 F3 N3 O6 Re S
Mr	734.72	734.71
Dx,g cm-3	1.844	1.844
Z	4	4
Mu (mm-1)	4.738	4.738
F000	1432.0	1432.0
F000’	1429.23	
h,k,lmax	14,16,21	14,16,21
Nref	5329	5289
Tmin,Tmax	0.198,0.388	0.474,0.804
Tmin’	0.152	

```
Correction method= # Reported T Limits: Tmin=0.474 Tmax=0.804
AbsCorr = MULTI-SCAN

Data completeness= 0.992          Theta(max)= 26.249

R(reflections)= 0.0301( 4521)     wR2(reflections)= 0.0842( 5289)

S = 1.032                 Npar= 334
```

The following ALERTS were generated. Each ALERT has the format
test-name_ALERT_alert-type_alert-level.
Click on the hyperlinks for more details of the test.

Alert level C

```
PLAT260_ALERT_2_C Large Average Ueq of Residue Including       S1A      0.145 Check
PLAT260_ALERT_2_C Large Average Ueq of Residue Including        S1      0.145 Check
```

Alert level G

```
PLAT002_ALERT_2_G Number of Distance or Angle Restraints on AtSite         16 Note
PLAT171_ALERT_4_G The CIF-Embedded .res File Contains EADP Records          3 Report
PLAT176_ALERT_4_G The CIF-Embedded .res File Contains SADI Records         19 Report
PLAT230_ALERT_2_G Hirshfeld Test Diff for    O1       --C22      .        6.0 s.u.
PLAT231_ALERT_4_G Hirshfeld Test (Solvent)   S1A      --O4A      .       14.5 s.u.
PLAT231_ALERT_4_G Hirshfeld Test (Solvent)   S1A      --O6A      .       15.7 s.u.
PLAT231_ALERT_4_G Hirshfeld Test (Solvent)   F1A      --C25A     .       11.4 s.u.
PLAT231_ALERT_4_G Hirshfeld Test (Solvent)   F2A      --C25A     .       25.8 s.u.
PLAT232_ALERT_2_G Hirshfeld Test Diff (M-X)  Re1      --C22      .        7.0 s.u.
PLAT232_ALERT_2_G Hirshfeld Test Diff (M-X)  Re1      --C23      .        5.7 s.u.
PLAT232_ALERT_2_G Hirshfeld Test Diff (M-X)  Re1      --C24      .        6.0 s.u.
PLAT302_ALERT_4_G Anion/Solvent/Minor-Residue Disorder (Resd  2  )       100% Note
PLAT302_ALERT_4_G Anion/Solvent/Minor-Residue Disorder (Resd  3  )       100% Note
PLAT304_ALERT_4_G Non-Integer Number of Atoms in ..... (Resd  2  )       4.45 Check
PLAT304_ALERT_4_G Non-Integer Number of Atoms in ..... (Resd  3  )       3.55 Check
PLAT432_ALERT_2_G Short Inter X...Y Contact  O5       ..C12            2.91 Ang.
                                                      x,y,z  =      1_555 Check
PLAT802_ALERT_4_G CIF Input Record(s) with more than 80 Characters          1 Info
PLAT860_ALERT_3_G Number of Least-Squares Restraints .............        19 Note
PLAT912_ALERT_4_G Missing # of FCF Reflections Above STh/L=  0.600         39 Note
PLAT933_ALERT_2_G Number of OMIT Records in Embedded .res File ...          1 Note
PLAT978_ALERT_2_G Number C-C Bonds with Positive Residual Density.          1 Info
```

```
   0 ALERT level A = Most likely a serious problem - resolve or explain
   0 ALERT level B = A potentially serious problem, consider carefully
   2 ALERT level C = Check. Ensure it is not caused by an omission or oversight
  21 ALERT level G = General information/check it is not something unexpected

   0 ALERT type 1 CIF construction/syntax error, inconsistent or missing data
  10 ALERT type 2 Indicator that the structure model may be wrong or deficient
   1 ALERT type 3 Indicator that the structure quality may be low
  12 ALERT type 4 Improvement, methodology, query or suggestion
   0 ALERT type 5 Informative message, check
```

It is advisable to attempt to resolve as many as possible of the alerts in all categories. Often the minor alerts point to easily fixed oversights, errors and omissions in your CIF or refinement strategy, so attention to these fine details can be worthwhile. In order to resolve some of the more serious problems it may be necessary to carry out additional measurements or structure refinements. However, the purpose of your study may justify the reported deviations and the more serious of these should normally be commented upon in the discussion or experimental section of a paper or in the "special_details" fields of the CIF. checkCIF was carefully designed to identify outliers and unusual parameters, but every test has its limitations and alerts that are not important in a particular case may appear. Conversely, the absence of alerts does not guarantee there are no aspects of the results needing attention. It is up to the individual to critically assess their own results and, if necessary, seek expert advice.

Publication of your CIF in IUCr journals

A basic structural check has been run on your CIF. These basic checks will be run on all CIFs submitted for publication in IUCr journals (*Acta Crystallographica, Journal of Applied Crystallography, Journal of Synchrotron Radiation*); however, if you intend to submit to *Acta Crystallographica Section C* or *E* or *IUCrData*, you should make sure that full publication checks are run on the final version of your CIF prior to submission.

Publication of your CIF in other journals

Please refer to the *Notes for Authors* of the relevant journal for any special instructions relating to CIF submission.

PLATON version of 16/07/2020; check.def file version of 12/07/2020

Datablock renn12py - ellipsoid plot

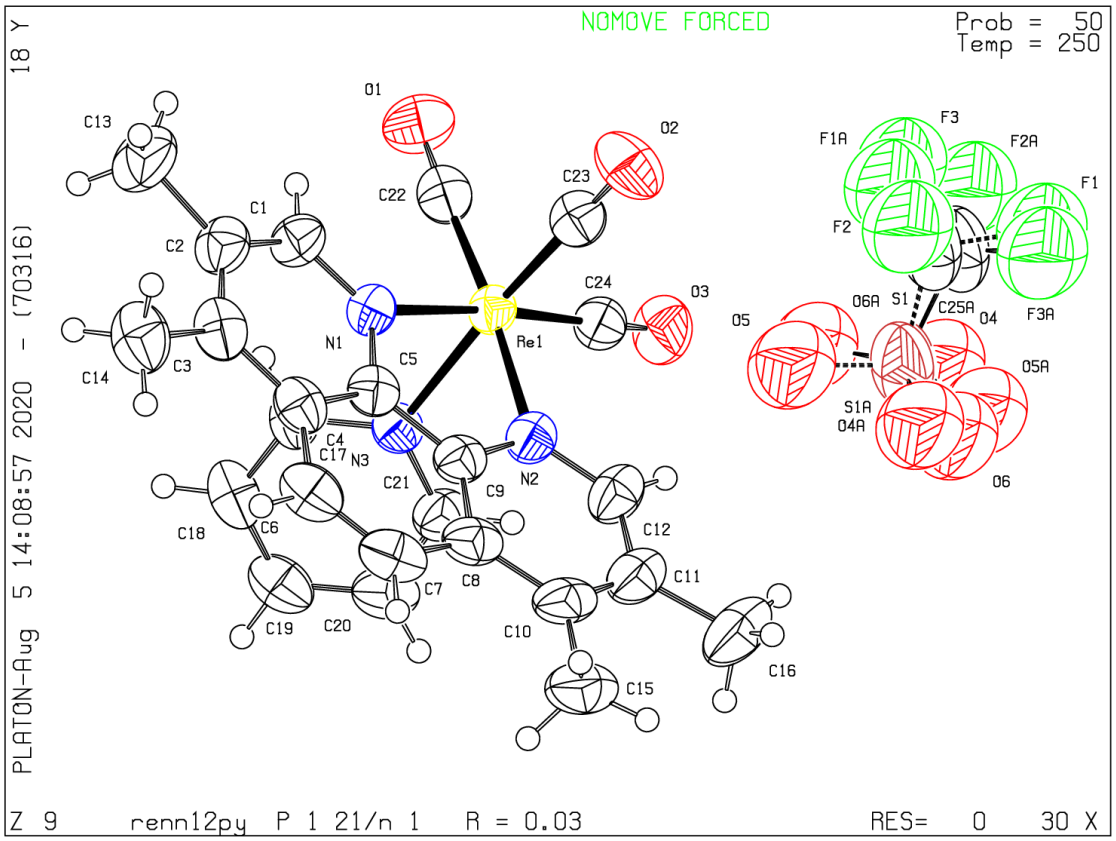

checkCIF/PLATON report

Structure factors have been supplied for datablock(s) renn13py

THIS REPORT IS FOR GUIDANCE ONLY. IF USED AS PART OF A REVIEW PROCEDURE FOR PUBLICATION, IT SHOULD NOT REPLACE THE EXPERTISE OF AN EXPERIENCED CRYSTALLOGRAPHIC REFEREE.

No syntax errors found. CIF dictionary Interpreting this report

Datablock: renn13py

```
Bond precision:  C-C = 0.0035 A          Wavelength=1.54186

Cell:           a=11.7416(2)    b=13.7067(2)        c=14.3137(3)
                alpha=90        beta=100.757(2)     gamma=90
Temperature:    200 K
```

	Calculated	Reported
Volume	2263.15(7)	2263.15(7)
Space group	P 21/n	P 1 21/n 1
Hall group	-P 2yn	-P 2yn
Moiety formula	C20 H17 N3 O3 Re, C F3 O3 S	C20 H17 N3 O3 Re, C F3 O3 S
Sum formula	C21 H17 F3 N3 O6 Re S	C21 H17 F3 N3 O6 Re S
Mr	682.65	682.64
Dx,g cm-3	2.003	2.003
Z	4	4
Mu (mm-1)	12.002	12.002
F000	1320.0	1320.0
F000’	1304.40	
h,k,lmax	14,16,17	13,15,16
Nref	4116	3975
Tmin,Tmax	0.150,0.887	0.082,0.259
Tmin’	0.004	

```
Correction method= # Reported T Limits: Tmin=0.082 Tmax=0.259
AbsCorr = MULTI-SCAN

Data completeness= 0.966          Theta(max)= 67.840

R(reflections)= 0.0156( 3679)     wR2(reflections)= 0.0409( 3975)

S = 1.069                 Npar= 319
```

The following ALERTS were generated. Each ALERT has the format
test-name_ALERT_alert-type_alert-level.
Click on the hyperlinks for more details of the test.

Alert level C

PLAT029_ALERT_3_C _diffrn_measured_fraction_theta_full value Low . 0.968 Why?
PLAT244_ALERT_4_C Low ’Solvent’ Ueq as Compared to Neighbors of S1 Check
PLAT911_ALERT_3_C Missing FCF Refl Between Thmin & STh/L= 0.600 97 Report

---

Alert level G

PLAT230_ALERT_2_G Hirshfeld Test Diff for O1 --C18 . 8.3 s.u.
PLAT230_ALERT_2_G Hirshfeld Test Diff for O2 --C19 . 5.3 s.u.
PLAT231_ALERT_4_G Hirshfeld Test (Solvent) S1 --C21 . 5.6 s.u.
PLAT232_ALERT_2_G Hirshfeld Test Diff (M-X) Re1 --C18 . 11.2 s.u.
PLAT232_ALERT_2_G Hirshfeld Test Diff (M-X) Re1 --C19 . 9.2 s.u.
PLAT232_ALERT_2_G Hirshfeld Test Diff (M-X) Re1 --C20 . 5.8 s.u.
PLAT244_ALERT_4_G Low ’Solvent’ Ueq as Compared to Neighbors of C21 Check
PLAT909_ALERT_3_G Percentage of I>2sig(I) Data at Theta(Max) Still 84% Note
PLAT912_ALERT_4_G Missing # of FCF Reflections Above STh/L= 0.600 8 Note
PLAT933_ALERT_2_G Number of OMIT Records in Embedded .res File ... 1 Note
PLAT978_ALERT_2_G Number C-C Bonds with Positive Residual Density. 1 Info

---

0 **ALERT level A** = Most likely a serious problem - resolve or explain
0 **ALERT level B** = A potentially serious problem, consider carefully
3 **ALERT level C** = Check. Ensure it is not caused by an omission or oversight
11 **ALERT level G** = General information/check it is not something unexpected

0 ALERT type 1 CIF construction/syntax error, inconsistent or missing data
7 ALERT type 2 Indicator that the structure model may be wrong or deficient
3 ALERT type 3 Indicator that the structure quality may be low
4 ALERT type 4 Improvement, methodology, query or suggestion
0 ALERT type 5 Informative message, check

It is advisable to attempt to resolve as many as possible of the alerts in all categories. Often the minor alerts point to easily fixed oversights, errors and omissions in your CIF or refinement strategy, so attention to these fine details can be worthwhile. In order to resolve some of the more serious problems it may be necessary to carry out additional measurements or structure refinements. However, the purpose of your study may justify the reported deviations and the more serious of these should normally be commented upon in the discussion or experimental section of a paper or in the "special_details" fields of the CIF. checkCIF was carefully designed to identify outliers and unusual parameters, but every test has its limitations and alerts that are not important in a particular case may appear. Conversely, the absence of alerts does not guarantee there are no aspects of the results needing attention. It is up to the individual to critically assess their own results and, if necessary, seek expert advice.

Publication of your CIF in IUCr journals

A basic structural check has been run on your CIF. These basic checks will be run on all CIFs submitted for publication in IUCr journals (*Acta Crystallographica, Journal of Applied Crystallography, Journal of Synchrotron Radiation*); however, if you intend to submit to *Acta Crystallographica Section C* or *E* or *IUCrData*, you should make sure that full publication checks are run on the final version of your CIF prior to submission.

Publication of your CIF in other journals

Please refer to the *Notes for Authors* of the relevant journal for any special instructions relating to CIF submission.

PLATON version of 16/07/2020; check.def file version of 12/07/2020

Datablock renn13py - ellipsoid plot

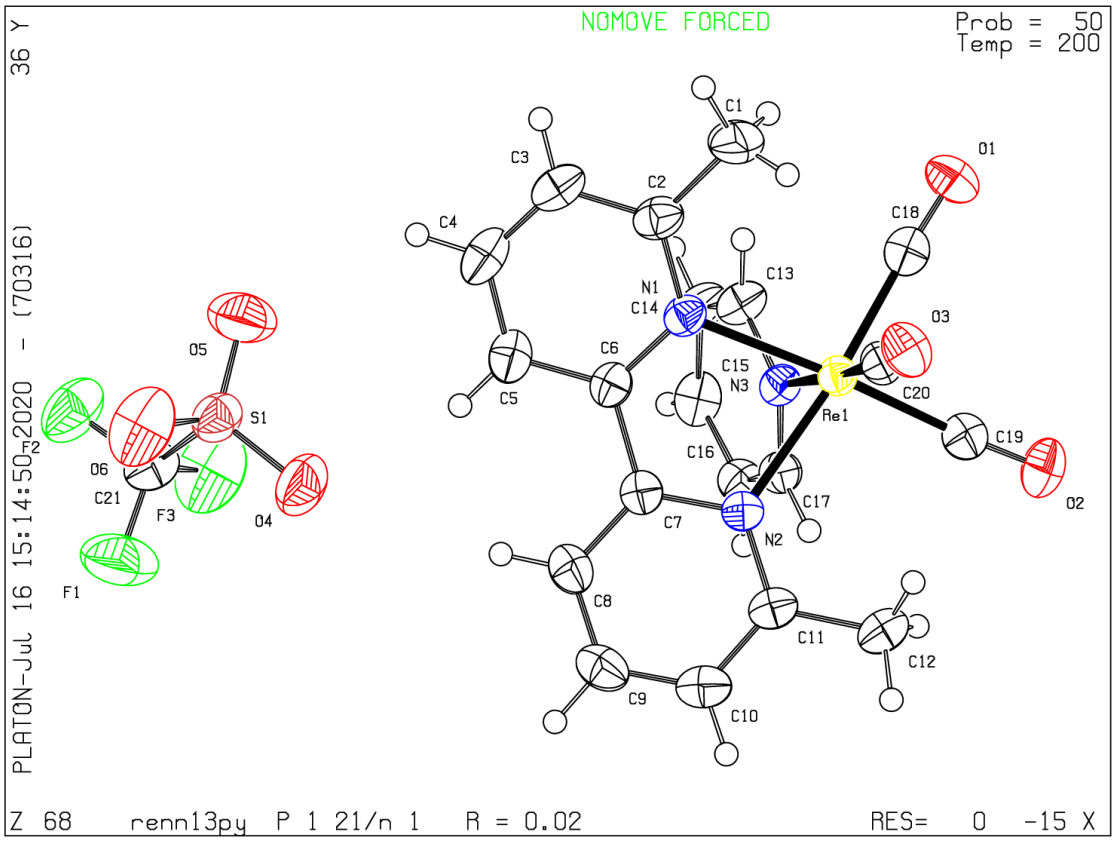

checkCIF/PLATON report

Structure factors have been supplied for datablock(s) renn10bpy

THIS REPORT IS FOR GUIDANCE ONLY. IF USED AS PART OF A REVIEW PROCEDURE FOR PUBLICATION, IT SHOULD NOT REPLACE THE EXPERTISE OF AN EXPERIENCED CRYSTALLOGRAPHIC REFEREE.

No syntax errors found. CIF dictionary Interpreting this report

Datablock: renn10bpy

```
Bond precision:  C-C = 0.0093 A          Wavelength=0.71073

Cell:           a=8.5099(11)    b=16.2690(14)       c=15.5858(19)
                alpha=90        beta=103.137(10)    gamma=90
Temperature:    250 K

                Calculated                Reported
Volume          2101.3(4)                 2101.3(4)
Space group     P 21/n                    P 1 21/n 1
Hall group      -P 2yn                    -P 2yn
Moiety formula  C22 H17 N4 O3 Re          C22 H17 N4 O3 Re
Sum formula     C22 H17 N4 O3 Re          C22 H17 N4 O3 Re
Mr              571.61                    571.59
Dx,g cm-3       1.807                     1.807
Z               4                         4
Mu (mm-1)       5.813                     5.813
F000            1104.0                    1104.0
F000'           1100.47
h,k,lmax        10,20,19                  10,20,19
Nref            4273                      4219
Tmin,Tmax       0.080,0.313               0.125,0.422
Tmin'           0.053

Correction method= # Reported T Limits: Tmin=0.125 Tmax=0.422
AbsCorr = MULTI-SCAN

Data completeness= 0.987          Theta(max)= 26.298

R(reflections)= 0.0428( 3262)     wR2(reflections)= 0.1137( 4219)

S = 0.985                 Npar= 274
```

The following ALERTS were generated. Each ALERT has the format
test-name_ALERT_alert-type_alert-level.
Click on the hyperlinks for more details of the test.

Alert level B

PLAT971_ALERT_2_B Check Calcd Resid. Dens. 1.01A   From Re1 2.53 eA-3

Alert level C

RINTA01_ALERT_3_C The value of Rint is greater than 0.12
Rint given 0.127
PLAT234_ALERT_4_C Large Hirshfeld Difference O1 --C20 . 0.16 Ang.
PLAT342_ALERT_3_C Low Bond Precision on C-C Bonds ..... 0.00929 Ang.
PLAT911_ALERT_3_C Missing FCF Refl Between Thmin & STh/L= 0.600 2 Report
PLAT971_ALERT_2_C Check Calcd Resid. Dens. 1.04A From Re1 2.36 eA-3
PLAT972_ALERT_2_C Check Calcd Resid. Dens. 0.96A From C21 -1.73 eA-3
PLAT972_ALERT_2_C Check Calcd Resid. Dens. 0.85A From Re1 -1.63 eA-3

Alert level G

PLAT020_ALERT_3_G The Value of Rint is Greater Than 0.12 ..... 0.127 Report
PLAT230_ALERT_2_G Hirshfeld Test Diff for O2 --C21 . 8.0 s.u.
PLAT232_ALERT_2_G Hirshfeld Test Diff (M-X) Re1 --C21 . 8.8 s.u.
PLAT802_ALERT_4_G CIF Input Record(s) with more than 80 Characters 1 Info
PLAT912_ALERT_4_G Missing # of FCF Reflections Above STh/L= 0.600 52 Note
PLAT933_ALERT_2_G Number of OMIT Records in Embedded .res File ... 7 Note
PLAT978_ALERT_2_G Number C-C Bonds with Positive Residual Density. 0 Info

0 **ALERT level A** = Most likely a serious problem - resolve or explain
1 **ALERT level B** = A potentially serious problem, consider carefully
7 **ALERT level C** = Check. Ensure it is not caused by an omission or oversight
7 **ALERT level G** = General information/check it is not something unexpected

0 ALERT type 1 CIF construction/syntax error, inconsistent or missing data
8 ALERT type 2 Indicator that the structure model may be wrong or deficient
4 ALERT type 3 Indicator that the structure quality may be low
3 ALERT type 4 Improvement, methodology, query or suggestion
0 ALERT type 5 Informative message, check

It is advisable to attempt to resolve as many as possible of the alerts in all categories. Often the minor alerts point to easily fixed oversights, errors and omissions in your CIF or refinement strategy, so attention to these fine details can be worthwhile. In order to resolve some of the more serious problems it may be necessary to carry out additional measurements or structure refinements. However, the purpose of your study may justify the reported deviations and the more serious of these should normally be commented upon in the discussion or experimental section of a paper or in the "special_details" fields of the CIF. checkCIF was carefully designed to identify outliers and unusual parameters, but every test has its limitations and alerts that are not important in a particular case may appear. Conversely, the absence of alerts does not guarantee there are no aspects of the results needing attention. It is up to the individual to critically assess their own results and, if necessary, seek expert advice.

Publication of your CIF in IUCr journals

A basic structural check has been run on your CIF. These basic checks will be run on all CIFs submitted for publication in IUCr journals (*Acta Crystallographica, Journal of Applied Crystallography, Journal of Synchrotron Radiation*); however, if you intend to submit to *Acta Crystallographica Section C* or *E* or *IUCrData*, you should make sure that full publication checks are run on the final version of your CIF prior to submission.

Publication of your CIF in other journals

Please refer to the *Notes for Authors* of the relevant journal for any special instructions relating to CIF submission.

PLATON version of 16/07/2020; check.def file version of 12/07/2020

Datablock renn10bpy - ellipsoid plot

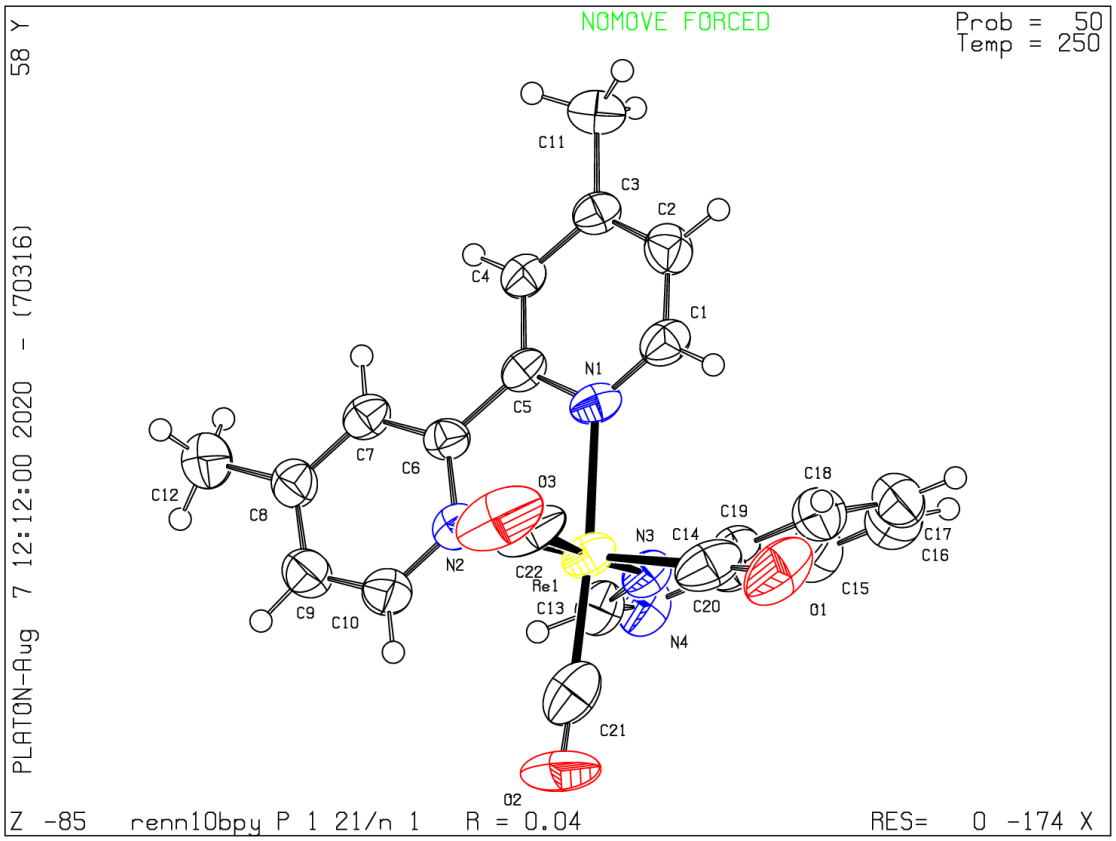

checkCIF/PLATON report

Structure factors have been supplied for datablock(s) ren13bim

THIS REPORT IS FOR GUIDANCE ONLY. IF USED AS PART OF A REVIEW PROCEDURE FOR PUBLICATION, IT SHOULD NOT REPLACE THE EXPERTISE OF AN EXPERIENCED CRYSTALLOGRAPHIC REFEREE.

No syntax errors found. CIF dictionary Interpreting this report

Datablock: ren13bim

```
Bond precision:  C-C = 0.0056 A          Wavelength=1.54186

Cell:            a=11.2305(3)    b=14.0386(3)       c=16.3604(5)
                 alpha=90        beta=98.171(2)     gamma=90
Temperature:     250 K

                 Calculated                Reported
Volume           2553.20(12)               2553.20(12)
Space group      P 21/n                    P 1 21/n 1
Hall group       -P 2yn                    -P 2yn
Moiety formula   C22 H17 N4 O3 Re, C H Cl3 C22 H17 N4 O3 Re, C H Cl3
Sum formula      C23 H18 Cl3 N4 O3 Re      C23 H18 Cl3 N4 O3 Re
Mr               690.97                    690.96
Dx,g cm-3        1.798                     1.798
Z                4                         4
Mu (mm-1)        12.471                    12.471
F000             1336.0                    1336.0
F000'            1322.35
h,k,lmax         12,15,17                  12,15,17
Nref             3439                      3385
Tmin,Tmax        0.080,0.174               0.103,0.270
Tmin'            0.008

Correction method= # Reported T Limits: Tmin=0.103 Tmax=0.270
AbsCorr = MULTI-SCAN

Data completeness= 0.984          Theta(max)= 56.983

R(reflections)= 0.0225( 3246)     wR2(reflections)= 0.0609( 3385)

S = 1.118                 Npar= 391
```

The following ALERTS were generated. Each ALERT has the format
test-name_ALERT_alert-type_alert-level.
Click on the hyperlinks for more details of the test.

Alert level A

THETM01_ALERT_3_A The value of sine(theta_max)/wavelength is less than 0.550
Calculated sin(theta_max)/wavelength = 0.5438

Author Response: Too low diffraction intensities in high angles.

Alert level C

PLAT088_ALERT_3_C Poor Data / Parameter Ratio ..... 8.66 Note
PLAT234_ALERT_4_C Large Hirshfeld Difference Cl3 --C23 . 0.16 Ang.
PLAT244_ALERT_4_C Low 'Solvent' Ueq as Compared to Neighbors of C23 Check
PLAT260_ALERT_2_C Large Average Ueq of Residue Including Cl1 0.119 Check
PLAT336_ALERT_2_C Long Bond Distance for ..... C23 -Cl2 1.870 Ang.
PLAT910_ALERT_3_C Missing # of FCF Reflection(s) Below Theta(Min). 9 Note
PLAT911_ALERT_3_C Missing FCF Refl Between Thmin & STh/L= 0.544 45 Report
PLAT918_ALERT_3_C Reflection(s) with I(obs) much Smaller I(calc) . 2 Check

---

Alert level G

PLAT177_ALERT_4_G The CIF-Embedded .res File Contains DELU Records 1 Report
PLAT187_ALERT_4_G The CIF-Embedded .res File Contains RIGU Records 1 Report
PLAT230_ALERT_2_G Hirshfeld Test Diff for O2 --C21 . 6.0 s.u.
PLAT232_ALERT_2_G Hirshfeld Test Diff (M-X) Re1 --C21 . 6.7 s.u.
PLAT300_ALERT_4_G Atom Site Occupancy of Cl1 Constrained at 0.25 Check
PLAT300_ALERT_4_G Atom Site Occupancy of Cl1A Constrained at 0.25 Check
PLAT300_ALERT_4_G Atom Site Occupancy of Cl1B Constrained at 0.25 Check
PLAT300_ALERT_4_G Atom Site Occupancy of Cl1C Constrained at 0.25 Check
PLAT300_ALERT_4_G Atom Site Occupancy of Cl2 Constrained at 0.25 Check
PLAT300_ALERT_4_G Atom Site Occupancy of Cl2A Constrained at 0.25 Check
PLAT300_ALERT_4_G Atom Site Occupancy of Cl2B Constrained at 0.25 Check
PLAT300_ALERT_4_G Atom Site Occupancy of Cl2C Constrained at 0.25 Check
PLAT300_ALERT_4_G Atom Site Occupancy of Cl3 Constrained at 0.25 Check
PLAT300_ALERT_4_G Atom Site Occupancy of Cl3A Constrained at 0.25 Check
PLAT300_ALERT_4_G Atom Site Occupancy of Cl3B Constrained at 0.25 Check
PLAT300_ALERT_4_G Atom Site Occupancy of Cl3C Constrained at 0.25 Check
PLAT300_ALERT_4_G Atom Site Occupancy of H23 Constrained at 0.25 Check
PLAT300_ALERT_4_G Atom Site Occupancy of H23A Constrained at 0.25 Check
PLAT300_ALERT_4_G Atom Site Occupancy of H23B Constrained at 0.25 Check
PLAT300_ALERT_4_G Atom Site Occupancy of H23C Constrained at 0.25 Check
PLAT302_ALERT_4_G Anion/Solvent/Minor-Residue Disorder (Resd 2) 75% Note
PLAT790_ALERT_4_G Centre of Gravity not Within Unit Cell: Resd. # 2 Note
C H Cl3
PLAT909_ALERT_3_G Percentage of I>2sig(I) Data at Theta(Max) Still 94% Note
PLAT933_ALERT_2_G Number of OMIT Records in Embedded .res File ... 2 Note
PLAT978_ALERT_2_G Number C-C Bonds with Positive Residual Density. 0 Info

---

1 **ALERT level A** = Most likely a serious problem - resolve or explain
0 **ALERT level B** = A potentially serious problem, consider carefully
8 **ALERT level C** = Check. Ensure it is not caused by an omission or oversight
25 **ALERT level G** = General information/check it is not something unexpected

0 ALERT type 1 CIF construction/syntax error, inconsistent or missing data

```
  6 ALERT type 2 Indicator that the structure model may be wrong or deficient
  6 ALERT type 3 Indicator that the structure quality may be low
 22 ALERT type 4 Improvement, methodology, query or suggestion
  0 ALERT type 5 Informative message, check
```

It is advisable to attempt to resolve as many as possible of the alerts in all categories. Often the minor alerts point to easily fixed oversights, errors and omissions in your CIF or refinement strategy, so attention to these fine details can be worthwhile. In order to resolve some of the more serious problems it may be necessary to carry out additional measurements or structure refinements. However, the purpose of your study may justify the reported deviations and the more serious of these should normally be commented upon in the discussion or experimental section of a paper or in the "special_details" fields of the CIF. checkCIF was carefully designed to identify outliers and unusual parameters, but every test has its limitations and alerts that are not important in a particular case may appear. Conversely, the absence of alerts does not guarantee there are no aspects of the results needing attention. It is up to the individual to critically assess their own results and, if necessary, seek expert advice.

Publication of your CIF in IUCr journals

A basic structural check has been run on your CIF. These basic checks will be run on all CIFs submitted for publication in IUCr journals (*Acta Crystallographica, Journal of Applied Crystallography, Journal of Synchrotron Radiation*); however, if you intend to submit to *Acta Crystallographica Section C* or *E* or *IUCrData*, you should make sure that full publication checks are run on the final version of your CIF prior to submission.

Publication of your CIF in other journals

Please refer to the *Notes for Authors* of the relevant journal for any special instructions relating to CIF submission.

PLATON version of 16/05/2021; check.def file version of 13/05/2021

Datablock ren13bim - ellipsoid plot

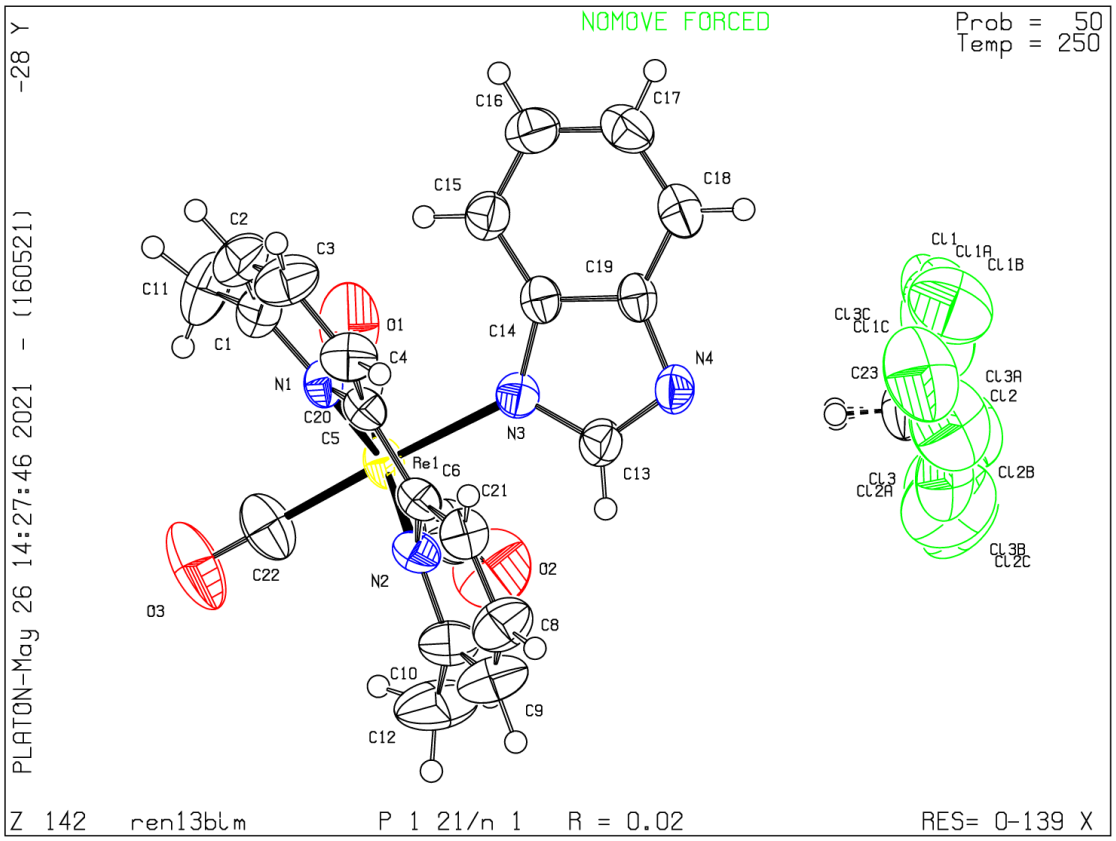

checkCIF/PLATON report

Structure factors have been supplied for datablock(s) n10l1

THIS REPORT IS FOR GUIDANCE ONLY. IF USED AS PART OF A REVIEW PROCEDURE FOR PUBLICATION, IT SHOULD NOT REPLACE THE EXPERTISE OF AN EXPERIENCED CRYSTALLOGRAPHIC REFEREE.

No syntax errors found. CIF dictionary Interpreting this report

Datablock: n10l1

Bond precision: C-C = 0.0105 A Wavelength=1.54186

Cell:	a=42.6175(10)	b=11.0183(2)	c=18.2031(4)
	alpha=90	beta=102.780(2)	gamma=90
Temperature:	200 K		

	Calculated	Reported
Volume	8335.9(3)	8335.9(3)
Space group	C 2/c	C 1 2/c 1
Hall group	-C 2yc	-C 2yc
Moiety formula	C36 H28 N4 O5 Re, F6 P [+ solvent]	C36 H28 N4 O5 Re, F6 P, 1[CH2CL2], 1[CH2CL2]
Sum formula	C36 H28 F6 N4 O5 P Re [+ solvent]	C38 H32 Cl4 F6 N4 O5 P Re
Mr	927.80	1097.64
Dx,g cm-3	1.479	1.749
Z	8	8
Mu (mm-1)	6.673	9.086
F000	3648.0	4320.0
F000’	3619.95	
h,k,lmax	51,13,21	50,13,21
Nref	7619	7456
Tmin,Tmax	0.311,0.695	0.106,0.557
Tmin’	0.098	

Correction method= # Reported T Limits: Tmin=0.106 Tmax=0.557
AbsCorr = MULTI-SCAN

Data completeness= 0.979 Theta(max)= 68.107

R(reflections)= 0.0526(5237) wR2(reflections)= 0.1527(7456)

S = 0.964 Npar= 451

The following ALERTS were generated. Each ALERT has the format
test-name_ALERT_alert-type_alert-level.
Click on the hyperlinks for more details of the test.

Alert level C

ABSTY02_ALERT_1_C An _exptl_absorpt_correction_type has been given without a literature citation. This should be contained in the _exptl_absorpt_process_details field.
Absorption correction given as multi-scan

PLAT234_ALERT_4_C	Large Hirshfeld Difference O2	--C14	.	0.16 Ang.
PLAT241_ALERT_2_C	High 'MainMol' Ueq as Compared to Neighbors of			C2 Check
PLAT260_ALERT_2_C	Large Average Ueq of Residue Including	P2A		0.124 Check
PLAT260_ALERT_2_C	Large Average Ueq of Residue Including	P2		0.124 Check
PLAT342_ALERT_3_C	Low Bond Precision on C-C Bonds			0.0105 Ang.
PLAT910_ALERT_3_C	Missing # of FCF Reflection(s) Below Theta(Min).			5 Note
PLAT911_ALERT_3_C	Missing FCF Refl Between Thmin & STh/L=	0.600		111 Report

---

Alert level G

FORMU01_ALERT_1_G There is a discrepancy between the atom counts in the _chemical_formula_sum and _chemical_formula_moiety. This is usually due to the moiety formula being in the wrong format.
Atom count from _chemical_formula_sum: C38 H32 Cl4 F6 N4 O5 P1 Re1
Atom count from _chemical_formula_moiety:C37 H30 Cl2 F6 N4 O5 P1 Re1

FORMU01_ALERT_2_G There is a discrepancy between the atom counts in the _chemical_formula_sum and the formula from the _atom_site* data.
Atom count from _chemical_formula_sum:C38 H32 Cl4 F6 N4 O5 P1 Re1
Atom count from the _atom_site data: C36 H28 F6 N4 O5 P1 Re1

CELLZ01_ALERT_1_G Difference between formula and atom_site contents detected.

CELLZ01_ALERT_1_G ALERT: Large difference may be due to a symmetry error - see SYMMG tests
From the CIF: _cell_formula_units_Z 8
From the CIF: _chemical_formula_sum C38 H32 Cl4 F6 N4 O5 P Re
TEST: Compare cell contents of formula and atom_site data

atom	Z*formula	cif sites	diff
C	304.00	288.00	16.00
H	256.00	224.00	32.00
Cl	32.00	0.00	32.00
F	48.00	48.00	0.00
N	32.00	32.00	0.00
O	40.00	40.00	0.00
P	8.00	8.00	0.00
Re	8.00	8.00	0.00

PLAT002_ALERT_2_G	Number of Distance or Angle Restraints on AtSite			14 Note
PLAT007_ALERT_5_G	Number of Unrefined Donor-H Atoms			1 Report
PLAT041_ALERT_1_G	Calc. and Reported SumFormula Strings	Differ		Please Check
PLAT051_ALERT_1_G	Mu(calc) and Mu(CIF) Ratio Differs from 1.0 by .			26.55 %
PLAT068_ALERT_1_G	Reported F000 Differs from Calcd (or Missing)...			Please Check
PLAT072_ALERT_2_G	SHELXL First Parameter in WGHT Unusually Large			0.11 Report
PLAT128_ALERT_4_G	Alternate Setting for Input Space Group	C2/c		I2/a Note
PLAT171_ALERT_4_G	The CIF-Embedded .res File Contains EADP Records			1 Report
PLAT176_ALERT_4_G	The CIF-Embedded .res File Contains SADI Records			21 Report
PLAT177_ALERT_4_G	The CIF-Embedded .res File Contains DELU Records			2 Report
PLAT231_ALERT_4_G	Hirshfeld Test (Solvent)	P2A	--F3A .	9.5 s.u.
PLAT231_ALERT_4_G	Hirshfeld Test (Solvent)	P2A	--F4A .	15.5 s.u.
PLAT231_ALERT_4_G	Hirshfeld Test (Solvent)	P2A	--F5A .	9.5 s.u.
PLAT231_ALERT_4_G	Hirshfeld Test (Solvent)	P2A	--F6A .	15.5 s.u.
PLAT231_ALERT_4_G	Hirshfeld Test (Solvent)	P2A	--F7A .	25.7 s.u.
PLAT231_ALERT_4_G	Hirshfeld Test (Solvent)	P2A	--F8A .	25.3 s.u.

```
PLAT302_ALERT_4_G Anion/Solvent/Minor-Residue Disorder (Resd  2  )       100% Note
PLAT302_ALERT_4_G Anion/Solvent/Minor-Residue Disorder (Resd  3  )       100% Note
PLAT304_ALERT_4_G Non-Integer Number of Atoms in ..... (Resd  2  )      4.69 Check
PLAT304_ALERT_4_G Non-Integer Number of Atoms in ..... (Resd  3  )      2.31 Check
PLAT606_ALERT_4_G VERY LARGE Solvent Accessible VOID(S) in Structure        ! Info
PLAT860_ALERT_3_G Number of Least-Squares Restraints .............         21 Note
PLAT868_ALERT_4_G ALERTS Due to the Use of _smtbx_masks Suppressed          ! Info
PLAT909_ALERT_3_G Percentage of I>2sig(I) Data at Theta(Max) Still        37% Note
PLAT912_ALERT_4_G Missing # of FCF Reflections Above STh/L=  0.600         44 Note
PLAT933_ALERT_2_G Number of OMIT Records in Embedded .res File ...          1 Note
PLAT978_ALERT_2_G Number C-C Bonds with Positive Residual Density.          1 Info
```

```
   0 ALERT level A = Most likely a serious problem - resolve or explain
   0 ALERT level B = A potentially serious problem, consider carefully
   8 ALERT level C = Check. Ensure it is not caused by an omission or oversight
  31 ALERT level G = General information/check it is not something unexpected

   7 ALERT type 1 CIF construction/syntax error, inconsistent or missing data
   8 ALERT type 2 Indicator that the structure model may be wrong or deficient
   5 ALERT type 3 Indicator that the structure quality may be low
  18 ALERT type 4 Improvement, methodology, query or suggestion
   1 ALERT type 5 Informative message, check
```

It is advisable to attempt to resolve as many as possible of the alerts in all categories. Often the minor alerts point to easily fixed oversights, errors and omissions in your CIF or refinement strategy, so attention to these fine details can be worthwhile. In order to resolve some of the more serious problems it may be necessary to carry out additional measurements or structure refinements. However, the purpose of your study may justify the reported deviations and the more serious of these should normally be commented upon in the discussion or experimental section of a paper or in the "special_details" fields of the CIF. checkCIF was carefully designed to identify outliers and unusual parameters, but every test has its limitations and alerts that are not important in a particular case may appear. Conversely, the absence of alerts does not guarantee there are no aspects of the results needing attention. It is up to the individual to critically assess their own results and, if necessary, seek expert advice.

Publication of your CIF in IUCr journals

A basic structural check has been run on your CIF. These basic checks will be run on all CIFs submitted for publication in IUCr journals (*Acta Crystallographica*, *Journal of Applied Crystallography*, *Journal of Synchrotron Radiation*); however, if you intend to submit to *Acta Crystallographica Section C* or *E* or *IUCrData*, you should make sure that full publication checks are run on the final version of your CIF prior to submission.

Publication of your CIF in other journals

Please refer to the *Notes for Authors* of the relevant journal for any special instructions relating to CIF submission.

PLATON version of 08/07/2020; check.def file version of 17/06/2020

Datablock n10l1 - ellipsoid plot